

RADIO ASTRONOMY

Journal of the Society of Amateur Radio Astronomers
March - April 2025



SARA 2025 Western Conference



Dr. Richard A. Russel
*SARA President and
Editor*

Bogdan Vacaliuc
Contributing Editor

Radio Astronomy is published bimonthly as the official journal of the Society of Amateur Radio Astronomers. Duplication of uncopyrighted material for educational purposes is permitted but credit shall be given to SARA and to the specific author. Copyrighted materials may not be copied without written permission from the copyright owner.

Radio Astronomy is available for download only by SARA members from the SARA web site and may not be posted anywhere else.

It is the mission of the Society of Amateur Radio Astronomers (SARA) to: Facilitate the flow of information pertinent to the field of Radio Astronomy among our members; Promote members to mentor newcomers to our hobby and share the excitement of radio astronomy with other interested persons and organizations; Promote individual and multi station observing programs; Encourage programs that enhance the technical abilities of our members to monitor cosmic radio signals, as well as to share and analyze such signals; Encourage educational programs within SARA and educational outreach initiatives. Founded in 1981, the Society of Amateur Radio Astronomers, Inc. is a membership supported, non-profit [501(c) (3)], educational and scientific corporation.

Copyright © 2025 by the Society of Amateur Radio Astronomers, Inc. All rights reserved.

Cover Photo:
SARA

Contents

President's Page	2
Editor's Notes	3
SARA NOTES	4
British Astronomical Association – Radio Astronomy Section Programs	8
THE BYTE - Marcus Fisher	10
Announcing Radio JOVE 2.0.....	18
John Cook's VLF Report.....	23
Featured Articles	43
Operation & Comparison of Total Power, Dicke and Correlation Radiometers – Peter East.....	43
HAARP Riometer Observations ~ 17 March 2025 – Whitham D. Reeve	62
Does adding WTMicrowave Chinese Hydrogen Cavity Filter improve hydrogen signal detection over Nooelec SAWBird H1 Low Noise Amplifier Alone? – Dr. Andrew Thornett...66	
Plotting of interpolated velocity against galactic longitude in 3D for large data set at Lichfield Radio Astronomy (LRO-H1 Data from Second Lichfield Radio Astronomy Milky way Map) using new functionality in Easy Radio Astronomy SoftwSuite (ezRA). – Dr. Andrew Thornett.....	72
The 6.7 GHz maser telescope parameters by solar measurements - <i>Dimitry Fedorov</i>	77
H1 Mosaic (Raster Scan) Study - Paul Gochin.....	82
Journal Archives and Other Promotions	101
What is Radio Astronomy?	102
Administrative	103
Officers, directors, and additional SARA contacts	103
Resources	104
Great Projects to Get Started in Radio Astronomy	104
Radio Astronomy Online Resources	106
SARA Brochure.....	110

President's Page



Congratulations!

Ken Redcap, Jason Burnfield, and Tom Jacobs

Ken, Jason, and Tom did an outstanding job organizing and running the 2025 Western Conference at Socorro, N.M.!

Thanks also to the outstanding authors and presenters who provided high quality content to the conference.

The presentations are posted on the SARA YouTube channel:

https://www.youtube.com/playlist?list=PLCEbOD5_znsIB33p_InLLonYLCorleIZU

The presentation slides and papers can be obtained from the SARA Store:

[Proceedings of Western Annual Conference](#)

Nominations are open for 2 officers and 4 board members!

SARA Eastern Conference Planning

The SARA Eastern Conference will be held at Green Bank, W.V. from 7-11 June 2025.

Sign up for the conference at the SARA Store:

[Registration for On Site 2025 Eastern / National SARA Conference](#)

Get your SARA Eastern Conference shirts, mugs, etc... at the SARA Gift store. Note - expect at least 3 weeks for delivery, so order soon!

[2025 Eastern Conference – Society of Amateur Radio Astronomers Gift Shop](#)



Editor's Notes

We are always looking for basic radio astronomy articles, radio astronomy tutorials, theoretical articles, application and construction articles, news pertinent to radio astronomy, profiles and interviews with amateur and professional radio astronomers, book reviews, puzzles (including word challenges, riddles, and crossword puzzles), anecdotes, expository on "bad astronomy," articles on radio astronomy observations, suggestions for reprint of articles from past journals and other publications, and announcements of radio astronomy star parties, meetings, and outreach activities.

Subscribe to the SARA YouTube Channel

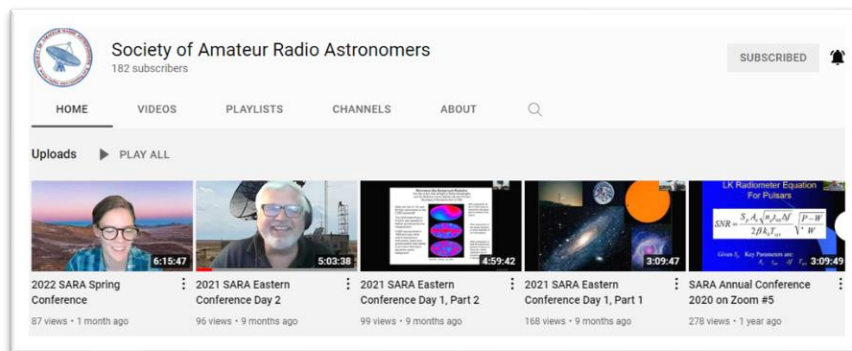
SARA has a YouTube channel at: <https://www.youtube.com/@radio-astronomy>

Don't forget to LIKE



the videos! It helps with the YouTube distribution algorithm.

We are also looking to add content to the site. Anyone who wants to help produce a series of 5 - minute videos relating to radio astronomy technology or observations please contact me. (drrichrussel@netscape.net)



Observation Reports

We are now accepting 1-2 page observation reports. These reports should include the astronomical object's RA/DEC plus UTC of the observation. Also include the telescope configuration, process used to observe the object and results. Picture of the setup and plots of the observation are a plus to the report.

If you would like to write an article for Radio Astronomy, please follow **the newly updated Author's Guide** on the SARA web site:

http://www.radio-astronomy.org/publicat/RA-JSARA_Author's_Guide.pdf.

Let us know if you have questions; we are glad to assist authors with their articles and papers and will not hesitate to work with you. You may contact your editors any time via email here: edit@radio-astronomy.org.

The editor(s) will acknowledge that they have received your submission within two days. If they do not reply, assume they did not receive it and please try again.

Please consider submitting your radio astronomy observations for publication: any object, any wavelength. Strip charts, spectrograms, magnetograms, meteor scatter records, space radar records, photographs; examples of radio frequency interference (RFI) are also welcome.

Guidelines for submitting observations may be found here: http://www.radio-astronomy.org/publicat/RA-JSARA_Observation_Submission_Guide.pdf

SARA NOTES

Society of Amateur Radio Astronomers (SARA)

2025 SARA & Radio Jove Eastern Conference
June 7 (Sat) – June 11 (Wed) 2025
Green Bank Observatory (GBO) West Virginia (WV)



Block your calendars and plan your trip for this summer. We have teamed up with the Radio Jove group and are holding a joint conference this summer!

- 2025 SARA and Radio Jove Eastern Conference
- June 7 (Sat) – June 11 (Wed) 2025
- Green Bank Observatory (GBO) West Virginia (WV)

Abstracts and presentations will be accepted up until end of April so if you want to get some of your work published send me an email ASAP.

The general plan for this year follows similar formats as years past with two additions. We have teamed up with Radio Jove this year and we have added one day of hands-on learning where attendees will assemble and operate the telescopes that SARA offers. For example:

- Saturday (6/7): Guided tours of public exhibits, Dave Lacko and Jay Wilson discussion on “What is Radio Astronomy Anyhow?”, hands on workshop assembling Scope in a Box and eZRA software
- Sunday (6/8): hands on workshop for 40’ telescope and 20-meter telescopes, with attendees able to plan and make observations
- Monday – Tuesday: SARA and Radio Jove technical discussions
- Evenings: Drake lounge discussions, flea market, and observations using Scope in a Box, Radio Jove, Super SID, 40’, 20m telescopes
- Wednesday (6/11): technical tours of GBO

Any comments and/or suggestions please reach out to the committee chair Marcus Fisher (vicepresident@radio-astronomy.org)

Officer and Board Member Nominations for 2026-2027 Terms

The following Officer and Board member positions are open for nominations:

Officers: Secretary

Asst Treasurer

Board: 4 positions open for nominations

If you want to nominate someone or yourself for any of these positions, send a note to Bruce Randall and myself. (Note – check with the person who you are nominating first)

Ballots will be sent out in June in conjunction with the SARA Eastern Conference.

President: Rich Russel: <https://www.radio-astronomy.org/contact/President>

Secretary: Bruce Randall, NT4RT, <https://www.radio-astronomy.org/contact/Secretary>

NEW The BYTE

A new section is being added to the bimonthly SARA journal focused on system software applicable for amateur radio astronomy (RA).

<p>Society of Amateur Radio Astronomers (SARA)</p> <p>2025 SARA Eastern Conference</p>	
---	--

Block off your calendars and start thinking about your travels for next summer! We have teamed up with the Radio Jove group and are holding a combined conference next year!

- 2025 SARA Eastern Conference and Radio Jove
- June 7 (Sat) – June 11 (Wed) 2025
- Green Bank Observatory (GBO) West Virginia (WV)

Planning is underway and more information will be coming as it develops. Any comments and/or suggestions please reach out to the committee chair Marcus Fisher (vicepresident@radio-astronomy.org)

2025 EU Conference on Amateur Radio Astronomy (EUCARA25)

We are pleased to announce the date of the 2025 EU Conference on Amateur Radio Astronomy (EUCARA25) - Friday September 5th - Sunday 7th.

This will be held at the Visitor Center on the Harwell Campus. Further details will be published soon on our website – www.eucara.org .

We are honored that **Professor Jocelyn Bell Burnell** will be our keynote speaker.

When registration is open, we will let you know via the forums.

SARA Student & Teacher Grant Program

All, SARA has a grant program that is, sad to say, very underutilized. We will provide kits or money for students and teachers, including college students, to help them with a radio telescope project. SARA can supply any of the following kits:

- [1] SuperSID
- [2] Scope in a Box
- [3] IBT (Itty Bitty Telescope)
- [4] Radio Jove kit
- [5] Inspire
- [6] Sky Scan

We can also provide up to five hundred dollars (\$500.00 USD) for an approved radio telescope project.

We have on occasion provided more money based on the merits of the project and the SARA Grant Committee approval.

More information on the grant program can be found at the URL below.

[SARA Student and Teacher Project Grants | Society of Amateur Radio Astronomers \(radio-astronomy.org\)](https://www.radio-astronomy.org/SARA-Student-and-Teacher-Project-Grants)

All that is required is the SARA grant request form to be filled out and sent in. If it needs more work for approval, we will work with the students to help ensure their success.

Please pass the word that SARA will fund any legitimate radio telescope project anywhere in the world.

If you have a question, contact me at crowleytj@hotmail.com .

Tom Crowley - SARA Grant Program Administrator

Drake's Lounge Australia

This new zoom forum is geared to the Melbourne, Australia time zone (UTC+10) in order to improve coordination with our Australia, New Zealand, and Japanese members. The meetings are scheduled for the 4th Friday of every month, 9 AM Melbourne time. A zoom announcement will be sent out to all SARA members before the meeting.

Radio Telescope Observation Party (RTOP)

RTOP is designed to demonstrate how to take observations using various radio telescopes. It will also cover how to record and analyze data.

RTOP is every month on the 1st Sunday at 2 pm Eastern time (1800 UTC). ZOOM email notifications will be sent to all members.

Drake's Lounge

Join the SARA community as we discuss the latest astronomy and radio astronomy news. The lounge also provides a forum to share and get advice on your radio astronomy projects from very experienced amateur radio astronomers.

Drake's Lounge is every month on the 3rd Sunday at 2 pm Eastern time (1800 UTC). ZOOM email notifications will be sent to all members.



British Astronomical Association
Supporting amateur astronomers since 1890
Radio Astronomy Section



Director: Paul Hearn

The Radio Astronomy Section aspires to encourage and support the construction of radio telescopes by amateurs, their use for observing programmes, and the development of a deeper understanding of the science underlying what is being observed. Programmes can be aimed at any radio astronomical phenomenon, at any radio frequency. This encouragement will be through the operation of continuing group programmes, and through building communication and information exchange between individuals and groups pursuing their own projects. The main purpose of the Group is to act as a reservoir and clearing house for information on radio telescope design, construction and debugging, and how to use these instruments effectively. This will include the discussion of observing techniques and data analysis. Members should be able to exchange ideas, give advice and help each other. Establishing a pool of design information and software suitable for use in observing and data processing is a priority.

BAA Radio Astronomy Section Seminar programme.

These seminars are on Zoom, if you are not on the BAA RA Section email list please contact Paul Hearn – Section Director – paul@hearn.org.uk

Friday 2nd May 19:30 (18:30 UTC)

Binary Stars and Stellar Cannibalism

Dr. Noel Castro-Segura University of Warwick [Astronomy and Astrophysics Group](#)

Stars are the building blocks of the universe. The majority of the stars in our galaxy spend their lives associated with a stellar companion, bound by the gravitational pull between them. The population of so-called binary stars encompasses up to 80% of the stars in the galaxy, and approximately half of these systems have an orbital period short enough to induce mass transfer between the two celestial objects at some point in their evolution.

Many of these interacting binaries contain a compact stellar remnant, which accretes material stripped from the surface of its companion star, thus providing an ideal laboratory to study physical bodies with extreme gravity such as white dwarfs and neutron stars. Furthermore, they offer a unique opportunity to infer the presence of one of the most exotic objects in the universe: black holes. This allows us to learn how they interact with their environment while shaping the universe we observe.

Here, I will review the basics of binary evolution and provide an overview of the phenomena observed in these systems. Additionally, I will highlight how amateur astronomers and citizen scientists can contribute to advancing science.

Friday 6th June 19:30 (18:30 UTC)

Observing Magnetic Fields in space, using Micro-wave Radio Observations

Prof. Derek Waed-Thompson

Director of the Jeremiah Horrocks Institute [School of Engineering and Computing](#) Lancaster University

Friday 4th July 19:30 BST (18:30 UTC)

The detection of ultra-high-energy cosmic rays and neutrinos through their radio signals

Dr Katharine Mulrey Associate professor - Astrophysics (Radboud University, the Netherlands)

Cosmic rays have been observed for over a century, and yet the sources of the highest energy particles still remain a mystery. We can detect these cosmic rays, and the associated high energy neutrinos, through the particle cascades they initiate when they interact in the atmosphere or the earth. In this talk, I will present an overview of modern efforts to measure these cascades using the radio signals they generate, in particular, using radio telescopes like LOFAR and the SKA.

And...

If any SARA members are planning a trip to Europe, then they would be very welcome to attend EuCARA – Eu Conference on Radio Astronomy.

Visit: <https://eucara.org>

Best wishes,

Paul.

Paul Hearn

BAA Radio Astronomy Section Director

UKRAA Trustee

British Astronomical Association !!

https://britastro.org/section_front/24

<https://www.youtube.com/user/britishastronomical/playlists>

The BYTE Society of Amateur Radio Astronomers Bimonthly Journal Marcus Fisher	01010011 01101111 01100011 01101001 01100101 01110100 01111001 00100000 01101111 01100110 00100000 01000001 01101101 01100001 01110100 01100101 01110101 01110010 00100000 01010010 01100001 01100100 01101001 01101111 00100000 01000001 01110011 01110100 01110010 01101111 01101110 01101111 01101101 01100101 01110010 01110011
---	--

The Byte, software section of SARA’s bimonthly journal, is focused on system software applicable to amateur radio astronomy (RA). Given that it is SARA’s mission to facilitate the flow of information, promote observing programs, enhance the technical abilities of its members, to name just a few, we feel it is pertinent to dedicate a section of the journal around software articles that enables our members and pushes us forward as a group.

- Learn Astro.py
 - o <https://learn.astropy.org/>
 - o The Astropy Project is a community effort to develop a single package for Astronomy in Python. It contains core functionality and common tools needed for performing astronomy and astrophysics research with Python.
- A List, not an exhaustive list, but a list of software supporting the entire life cycle of Radio Astronomy. I am not a spokesperson for any of these packages, I am simply trying to collect a list of potential software that could be used by an amateur in making his or her observations. As a note, I tried to stay with only open source applications / packages.
 - o Planning and Scheduling Observations
 - Skyfield (<https://rhodesmill.org/skyfield/>)
 - python library for computes positions for the stars, planets, and satellites in orbit around the Earth. Its results should agree with the positions generated by the United States Naval Observatory and their Astronomical Almanac to within 0.0005 arcseconds (half a “mas” or milliarcsecond).
 - Stellarium (<https://stellarium.org/>)
 - Stellarium is a software project that allows people to use their home computer as a virtual planetarium. It calculates the positions of the Sun and Moon, planets and stars, and draws how the sky would look to an observer depending on their location and the time.
 - Astroplanner (<https://www.astroplanner.net/index.html>)
 - AstroPlanner is a stand-alone application that allows the user to plan and execute an observing session. The user can enter objects to be viewed manually, import them from text files, look them up in several supplied catalogues, or use observing plans previously created by others. These objects can be both deep-sky and solar system objects (planets, sun, moon, asteroids, comets, etc.).
 - SkyChart (<https://www.ap-i.net/skychart//en/start>)
 - This program enables you to draw sky charts, making use of the data in many catalogs of stars and nebulae. In addition, the position of planets, asteroids and comets are shown. The purpose of this program is to prepare different sky maps for a particular observation.
 -
 - Kstars (<https://kstars.kde.org>)
 - KStars caters to a wide variety of use cases. Whether you are a student, an educator, an amateur astronomer or an astronomy enthusiast, you will find

tools in KStars that are useful to you. Have a look at the Features page for a full listing of features, organized by use case

- Radio Sky (radiosky.com)
 - Does cost money and seem to cover the entire life cycle of an observation
- Control Systems
 - ASCOM compliant mount in which you could then use Stellarium to control the mount (<https://ascom-standards.org/>)
 - Indi All Sky (<https://www.indilib.org/>)
- Data Acquisition and Data Processing
 - CASA (<https://casa.nrao.edu/index.shtml>)
 - CASA, the Common Astronomy Software Applications package, is the primary data processing software for the Atacama Large Millimeter/submillimeter Array (ALMA) and NSF's Karl G. Jansky Very Large Array (VLA) and is frequently used also for other radio telescopes. The CASA software can process data from both single-dish and aperture-synthesis telescopes, and one of its core functionalities is to support the data reduction and imaging pipelines for ALMA, VLA and the VLA Sky Survey (VLASS).
 - Plot Digitizer (<https://plotdigitizer.com/>)
 - Plotdigitizer is an online data extraction tool that allows users to extract data from images in numerical format. In short, it reverse-engineers your visual graphs into numbers
 - ezRA (<https://github.com/tedcline/ezRA>)
 - The ezRA Easy Radio Astronomy set of programs are free PC tools to help folks begin to explore Radio Astronomy, with 1420 MHz Galactic hydrogen data collection and analysis.
 - Obit (<https://www.cv.nrao.edu/~bcotton/Obit.html>)
 - Obit is a group of software packages for handling radio astronomy data, especially interferometric imaging.
 - AIPS (<http://www.aips.nrao.edu/index.shtml>)
 - The NRAO Astronomical Image Processing System (AIPS) is a software package for interactive (and, optionally, batch) calibration and editing of radio interferometric data and for the calibration, construction, display and analysis of astronomical images made from those data using Fourier synthesis methods
 - Astropy (<https://www.astropy.org/>)
 - The Astropy Project is a community effort to develop a core package for astronomy using the Python programming language and improve usability, interoperability, and collaboration between astronomy Python packages. The core astropy package contains functionality aimed at professional astronomers and astrophysicists but may be useful to anyone developing astronomy software.
 - GNU Radio (<https://www.gnuradio.org/>)
 - GNU Radio is a free & open-source software development toolkit that provides signal processing blocks to implement software radios. A software radio is a radio system which performs the required signal processing in software instead of using dedicated integrated circuits in hardware. The benefit is that since software can be easily replaced in the radio system, the same hardware can be

used to create many kinds of radios for many different communications standards; thus, one software radio can be used for a variety of applications!

- VIRGO (<https://github.com/OxCoto/Virgo?tab=readme-ov-file>)
 - Virgo is an easy-to-use open-source spectrometer and radiometer based on Python and GNU Radio (GR) that is conveniently applicable to any radio telescope working with a GR-supported software-defined radio (SDR). In addition to data acquisition, Virgo also carries out automated analysis of the recorded samples, producing an averaged spectrum, a calibrated spectrum, a dynamic spectrum (waterfall), a time series (power vs time) and a total power distribution plot.
- SDR# (<https://airspy.com/>)
 - SDRSharp is a customizable and integrated program for RTL-SDR dongles and AIRSPY devices. It can be used for signal acquisition, analysis, navigation, and demodulation
- Kern (<https://kernsuite.info/>)
 - set of radio astronomical software packages. It should contain most of the tools that a radio astronomer needs to work with radio telescope data. KERN is based on the latest Ubuntu LTS.
- High Definition Software Defined Radio (<https://www.hdsdr.de/>)
 - HDSDR is a freeware Software Defined Radio (SDR) program for Microsoft Windows 2000/XP/Vista/7/8/10/11. Typical applications are Radio listening, Ham Radio, SWL, Radio Astronomy, NDB-hunting and Spectrum analysis. HDSDR (former WinradHD) is an advanced version of Winrad, written by Alberto di Bene
- SDR Console (<https://www.sdr-radio.com/console>)
 - Did not check out web site, seems buggy
- GNU Octave (octave.org)
 - Numerical analysis
- Software News
 - Microsoft founder Bill Gates reflects upon a 50-year-old computer code that reshaped technology (https://techxplore.com/news/2025-04-microsoft-founder-bill-gates-year.html#google_vignette)
 - Bill Gates reflected on the 50th anniversary of Microsoft, recalling the pivotal code he wrote with Paul Allen in 1975 that launched the company and revolutionized personal computing. Inspired by an article about the Altair 8800, they developed software using BASIC without even having access to the computer itself. Gates called it the "coolest" code he ever wrote, as it laid the foundation for Microsoft's success and the rise of personal computers.
 - Supercomputing memory management tool makes data storage more efficient (<https://techxplore.com/news/2025-03-supercomputing-memory-tool-storage-efficient.html>)
 - Researchers at Oak Ridge National Laboratory developed a new system called SICM to optimize memory use in supercomputers by automatically placing frequently used data in faster memory and less-used data in slower memory. This approach outperforms traditional "first touch" methods, improving performance and efficiency in handling massive data loads. The technology also enables dynamic memory sharing between multiple programs within a supercomputing rack, enhancing flexibility and resource management.

- How NASA's 'autonomy choreography' will impact advanced technologies (<https://techxplore.com/news/2025-03-nasa-autonomy-choreography-impact-advanced.html>)
 - NASA's Ames Research Center developed the Data & Reasoning Fabric (DRF), a software framework that enables safe, secure, real-time data sharing and coordination between autonomous systems from different companies and industries. Originally designed for drones, DRF helps autonomous vehicles, traffic systems, and other technologies work together efficiently, improving safety and performance. Its potential applications range from smart transportation and medical supply delivery to mining operations and even future lunar exploration.
- Software is increasingly being built by AI, so it's vital to know if it can be trusted (<https://techxplore.com/news/2025-03-software-built-ai-vital.html>)
 - AI agents are rapidly transforming software development by autonomously building applications from simple user descriptions, potentially enabling anyone to create software without coding skills. While this technology could greatly increase productivity and accessibility, it also raises concerns about security, bias, and ethical behavior. Researchers are developing safeguards, like transparent blueprints and rigorous testing of AI models, to ensure these systems are safe, fair, and trustworthy.
- Spectroscope App Review (<https://scopetrader.com/spectroscope-app-review/>)
- AI, Data Science, and the Transformation of Scientific Research: A Primer (<https://www.technology.org/2025/04/06/ai-data-science-and-the-transformation-of-scientific-research-a-primer/>)
- 3D radio data visualization in open science platforms for next-generation observatories (<https://arxiv.org/abs/2503.16237>)
 - Next-generation telescopes will bring groundbreaking discoveries, but they will also present new technological challenges. The Square Kilometre Array Observatory (SKAO) will be one of the most demanding scientific infrastructures, with a projected data output of 700 PB per year to be distributed to a network of SKA Regional Centres. Current tools are not fully suited to manage such massive data volumes, therefore, new research is required to transform science archives from data providers into service providers. In this paper we examine how a science archive can deliver advanced visualization capabilities for the SKA science archive. In particular, we have conducted a thorough exploration of existing visualization software for astronomy and other fields to identify tools capable of addressing Big Data requirements. Using selected technologies, we have developed a prototype archive that provides access to interactive visualizations of 3D radio data through web-based interfaces, adhering to International Virtual Observatory Alliance (IVOA) recommendations to favour interoperability and Open Science practices. In addition, we discuss how current IVOA recommendations support these visualization capabilities and how they could be expanded. Our prototype archive includes a service to generate 3D models on the fly as a server operation, enabling remote visualizations in a flexible manner; for instance, a set of parameters can be used to customize the models and their visualization. We have used SKA precursor and pathfinder data to test its usability and scalability, concluding that remote visualization is a viable solution for handling high-volume data. However, our prototype is constrained by memory limitations, requiring techniques to reduce memory usage
- VS Code v1.99 Is All About Copilot Chat AI, Including Agent Mode (<https://visualstudiomagazine.com/Articles/2025/04/04/VS-Code-v1-99-Is-All-About-Copilot-Chat.aspx>)

- Compiled Listing of Astronomy Software (good sites to bookmark)
 - Astronomy Software (<http://www.midnightkite.com/index.aspx?URL=Software>)
 - NASA's High Energy Astrophysics Science Archive Research Center (HEASARC) Software Repository (<https://heasarc.gsfc.nasa.gov/docs/software.html>)
 - Sky and Telescope (<https://skyandtelescope.org/astronomy-resources/astronomy-software-public-domain-freeware-and-shareware/>)
 - Astronomy Online (<https://astronomyonline.org/AstronomySoftware.asp>)
 - Wikipedia list of software for astronomy research and education (https://en.wikipedia.org/wiki/List_of_software_for_astronomy_research_and_education)
- Remotely Operated Telescopes
 - Pictor Telescope (<https://pictortelescope.com/>)
 - Wikipedia list of radio telescopes (https://en.wikipedia.org/wiki/List_of_radio_telescopes)

Please let me know if you want any specific software topics covered. Some future projects that I have in mind are:

- Building a generic control system for use with Scope In A Box
- Building a database connecting and storing H1 observations by SARA members
- Building a remotely operated radio telescope (3 meters) for the local schools to (a) learn how to build and (2) use in their Computer Science, Physics and Earth and Space classes.
- Any other ideas for software projects, what software technology needs built for the amateur community?

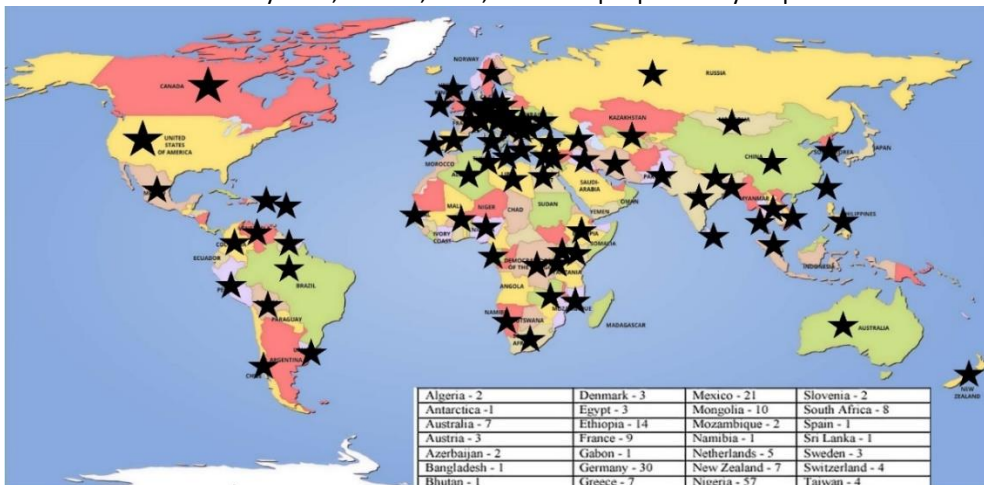
Marcus Fisher (Marcus.S.Fisher@gmail.com)



SuperSID
*Collaboration of Society
of Amateur Radio
Astronomers and
Stanford Solar Center*



- Stanford provides data hosting, database programming, and maintains the SuperSID website
- Society of Amateur Radio Astronomers (SARA) sells the SuperSID monitors for 48 USD to amateur radio astronomers and the funds are then used to support free distribution to students all over the world (image below as of Fall 2017)
- Jonathan Pettingale at SARA is responsible for building and shipping the SuperSID monitor kits: SuperSID@radio-astronomy.org
- SuperSID kits may be ordered through the SARA SuperSID webpage: <http://radio-astronomy.org/node/210>
- Questions about the SuperSID project may be directed to Steve Berl at Stanford: steveberl@gmail.com
- Jaap Akkerhuis at Stanford is responsible for the SuperSID software and SARA has provided financial support for his efforts
- SuperSID website hosted by Stanford: <http://solar-center.stanford.edu/SID/sidmonitor/>
- SuperSID database: <http://sid.stanford.edu/database-browser/>
- The data is searchable by time, station, date, and multiple plots may be placed on the same graph for comparison.



**SID Monitor
Distribution**
1078 instruments
82 countries
7 continents

Algeria - 2	Denmark - 3	Mexico - 21	Slovenia - 2
Antarctica - 1	Egypt - 3	Mongolia - 10	South Africa - 8
Australia - 7	Ethiopia - 14	Mozambique - 2	Spain - 1
Austria - 3	France - 9	Namibia - 1	Sri Lanka - 1
Azerbaijan - 2	Gabon - 1	Netherlands - 5	Sweden - 3
Bangladesh - 1	Germany - 30	New Zealand - 7	Switzerland - 4
Bhutan - 1	Greece - 7	Nigeria - 57	Taiwan - 4
Bolivia - 1	Guyana - 1	Pakistan - 4	Thailand - 5
Bosnia-Herzegovina - 2	Hungary - 1	Peru - 10	Tunisia - 9
Brazil - 11	India - 33	Philippines - 3	Turkey - 2
British Virgin Islands - 1	Indonesia - 2	Poland - 2	Uganda - 5
Bulgaria - 2	Iran - 4	Portugal - 3	UK - 32
Burkina Faso - 1	Iraq - 1	Rep of Congo - 3	Uruguay - 9
Canada - 33	Ireland - 9	Romania - 4	US Virgin Islands - 2
Chile - 1	Italy - 42	Russia - 3	USA - 491
China - 38	Kenya - 23	Rwanda - 1	Uzbekistan - 2
Columbia - 9	Korea (South) - 2	S Africa - 4	Venezuela - 2
Croatia - 7	Lebanon - 11	Senegal - 1	Vietnam - 1
Cyprus - 1	Libya - 1	Serbia - 1	Zambia - 2
Czech Republic - 1	Malaysia - 19	Singapore - 3	
D Rep of Congo - 4	Malta - 1	Slovak Repub - 2	

For official use only Monitor assigned: _____ Site name: _____ Country: _____
--

SuperSID Space Weather Monitor Request Form

<i>Your information here</i>	
Name of site/school (if an institution):	
Choose a site name: (3-6 characters) No Spaces	
Primary contact person:	
Email:	
Phone(s):	
Primary Address:	Name School or Business Street Street City Country
	State/Province Postal Code
Shipping address, if different:	Name School or Business Street Street City Country
	State/Province Postal Code
Shipping phone number:	
Latitude & longitude of site:	Latitude: _____ Longitude: _____

I understand that neither Stanford nor the Society of Amateur Radio Astronomers is responsible for accidents or injuries related to monitoring use. I will ensure that a surge protector and other lightning protection devices are installed if necessary.

Signature: _____ **Date:** _____

I will need:

<i>What</i>	<i>Cost</i>	<i>How many?</i>
SuperSID distribution USB Power	\$48 (assembled)	
USB Sound card 96 kHz sample rate (or provide this yourself)	\$40 (optional)	
Antenna wire (120 meters) (or you can provide this yourself)	\$23 (optional) with connectors attached and tested	
RG 58 Coax Cable (9 meters) (or provide this yourself)	\$14 (optional) with connectors attached and tested	
Shipping	US \$12 Canada & Mexico \$40 all other \$60	
	TOTAL	\$

_____ I have included a \$ _____ check (payable to SARA)

_____ I will make payment thru www.paypal.com to treas@radio-astronomy.org

or

_____ If you are a Minority-serving institution, in a Developing or economically deprived nation, and/or you are using the monitor with students for educational purposes, you may qualify for obtaining a monitor at reduced or no cost. Check here if you wish to apply for this designation. Then tell us how you want to use the SuperSID monitor. Include type of site, number of students involved, whether public or private school, grade levels, etc. and describe your program.

The goal of the SuperSID project is to provide as many students with systems as possible. If you are able to pay for a system, even if you qualify for a free one, please do so and help support our goal.

For more details on the Space Weather Monitor project, see: <http://sid.stanford.edu>

To set up a SuperSID monitor you will need:

¹ Access to power and an antenna location that is relatively free of electric interference (could be indoors or out)

² A **PC**** with the following minimal specifications:

a. A sound card that can record (sample) up to 96 kHz, or a USB port to connect such a sound card (for North and South America)

i. All other countries can use AC97 sound card with 48 kHz record (sample) rate.
Most computers made after 1997 will have AC97.

b. Windows 2000 or more recent operating system

c. 1 GHz Processor with 128 mb RAM

d. Ethernet connection & internet browser (desirable, but not required)

e. Standard keyboard, mouse, monitor, etc.

³ An inexpensive antenna that you build yourself. You'll need about 120 meters (400 feet) of **insulated** wire. Solid wire is easier to wind than stranded. Magnet wire will work but be more fragile. You can use anything from #18 to #26 size wire. The antenna frame can be made of wood, PVC pipe, or similar materials. We'll provide instructions. You can purchase the wire from us or obtain your own.

⁴ RG58 coax cable with a BNC connector at one end to run from the antenna to the SuperSID receiver. 9 meters is recommended, but the length will depend on where you place the antenna. You can purchase the coax from us or obtain your own.

⁵ Surge protector and other protection against a lightning strike

Return this form to: SuperSID@radio-astronomy.org

or mail to:

SARA Treasurer

c/o Thomas Jacobs

P. O. Box 4245

Wilmington, NC 28406.

Announcing Radio JOVE 2.0

The Radio JOVE Team



Radio JOVE students and amateur scientists from around the world observe and analyze natural radio emissions of Jupiter, the Sun, and our galaxy using their own easy to construct radio telescopes.

Our Project announces Radio JOVE 2.0, where participants assemble a 16-24 MHz radio spectrograph to observe solar, Jupiter, Galactic, and Earth-based natural radio emissions and share their observations with fellow participants.

In the Beginning

Radio JOVE started as a NASA sponsored educational outreach project in 1999. We developed a radio telescope kit suitable for receiving signals from Jupiter, the Sun, the Galaxy, and Earth-based radio emissions. The original kit comprised a radio receiver (RJ1.1) and a dual dipole antenna for 20.1 MHz. An important goal was to teach electronic principles including how to build, solder, and assemble the radio receiver and antenna.

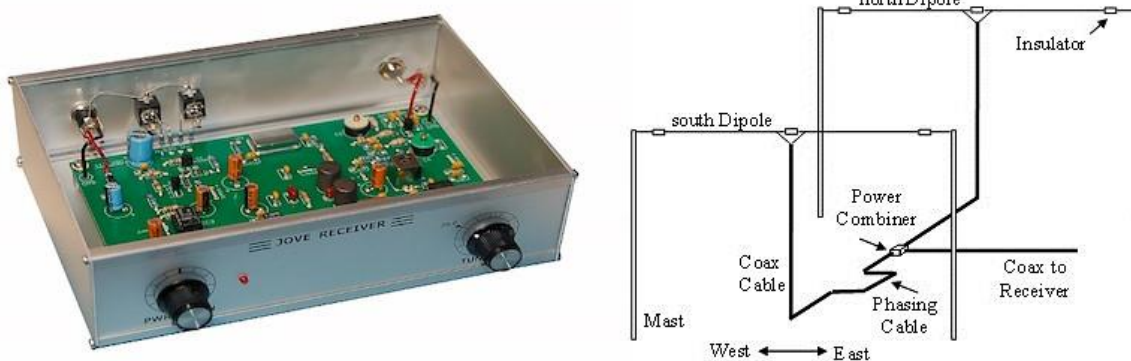


Figure 1. A Radio JOVE RJ1.1 receiver and a schematic of the dual-dipole antenna.

In addition to the hardware, three software packages were developed. These were Radio Jupiter Pro (Jupiter emission prediction program), Radio-SkyPipe (strip chart program) and Radio Sky Spectrograph (control and display of radio spectrograph data).

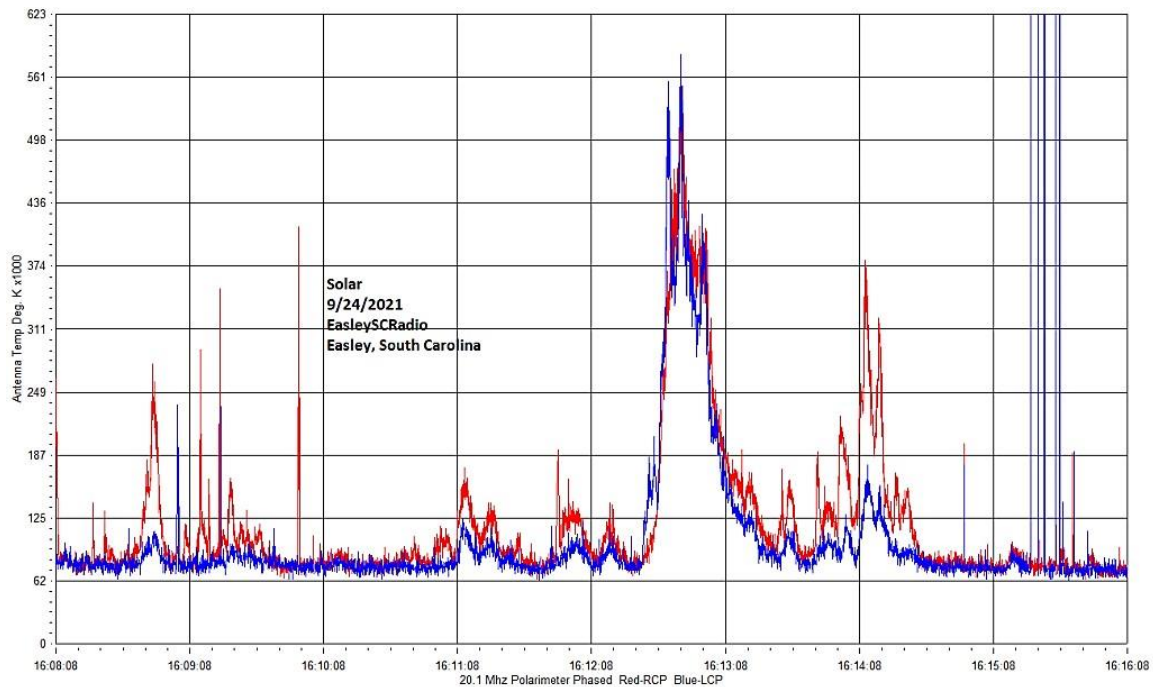


Figure 2. A SkyPipe strip chart showing multiple solar bursts using a JOVE receiver. John Cox, SC.

The Growth of Radio JOVE

As of Autumn 2021, over 2,500 kits have been sold at cost to schools and individuals around the world. Thousands of data submissions from observers have been made to the Radio JOVE data archive.

The Radio JOVE web site has always provided a wealth of information describing observation methods and various educational materials intended to teach radio astronomy techniques and scientific methods. Biannual newsletters are produced, and several telephone help sessions are held each year.

A sub-group of experienced observers known as the Spectrograph Users Group (SUG) evolved from the core JOVE group. These observers developed data collection and analysis techniques using more advanced equipment and techniques. SUG members have contributed to articles published in peer-reviewed scientific journals. This group remains active under the Radio JOVE listserv at <https://groups.io/g/radio-jove/>.

Moving Forward with New Technology

In the past, Radio JOVE provided the hands-on experience of building a radio kit. We have many RJ1.1 receivers in operation successfully contributing scientifically valuable data. It has, however, become increasingly difficult to obtain parts for the RJ1.1 receiver kits and we therefore decided to replace the RJ1.1 receiver with a new SDR-based design for the receiver portion of our radio telescope kits. While we continue to support the hardware and software for the original RJ1.1 receivers, the only kits now available for purchase from Radio JOVE contain this newly designed system.

In recent years, new technologies have made software defined radios (SDRs) ever more affordable. These radios can operate on a single frequency like the original JOVE receiver but can also generate spectrograms which depict radio activity as a function of both time and frequency. Such displays offer new insights into our studies of the Sun, Jupiter, the Galaxy, and both natural and artificial Earth-based radio emissions.

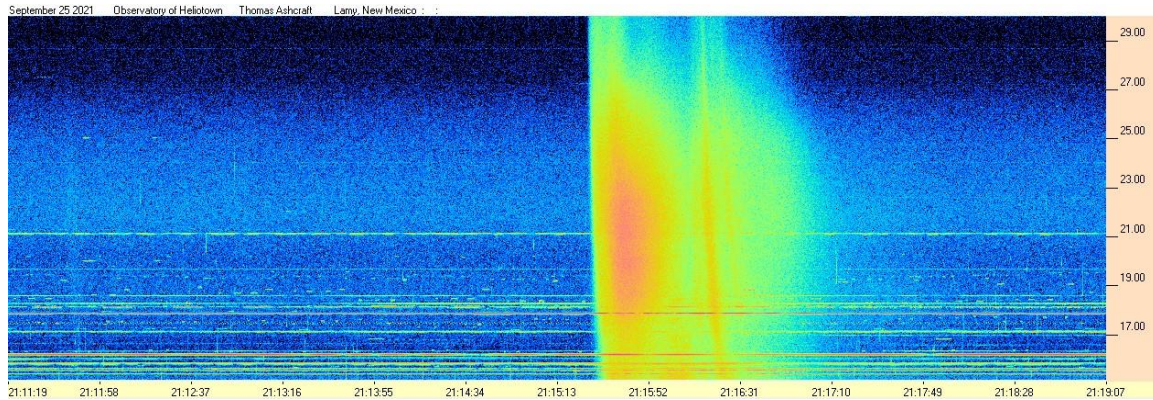


Figure 3. Radio spectrogram showing multiple solar bursts received by Tom Ashcraft in New Mexico. Horizontal scale is time, and the vertical scale is frequency. Amplitude is displayed using different colors corresponding to the strength of signals.

Radio JOVE continues to sell radio telescope packages including an antenna, receiver, and software; however, the receiver is now a commercially built SDR.



Figure 4. The JOVE team has had considerable success with the SDRPlay RSP1A unit and will provide support for using this instrument for our radio astronomy program. Not all SDR types can be supported, but it is our intent to provide support for some other SDRs as they become available during this period of rapid SDR development.

It continues to be our goal to introduce new observers to the scientific method and help them experience the thrill of receiving cosmic radio signals. Through a series of educational training modules and observing and analysis projects we aim to guide new observers to levels where they can contribute to Citizen Science projects.

We continue to support our large user base that uses JOVE RJ1.1 receivers – both in terms of technical support for the receivers but also with new and exciting observing projects for both RJ1.1 and SDR users.

We welcome both new and experienced observers to the JOVE 2.0 program as we share the excitement of receiving, studying, and understanding radio signals from our corner of the galaxy.

Please see the Radio JOVE web site at <https://radiojove.gsfc.nasa.gov> for more information.



RADIO JOVE 2.0 RADIO TELESCOPE KIT ORDER FORM

Order Online using PayPal™

* * * Please allow 2 to 3 weeks for delivery. * * *

IMPORTANT: Before you order the Jove receiver kit and/or the antenna kit, we suggest that you read the on-line manuals. You will need to provide additional materials and tools to complete the antenna. The cost of additional materials for the antenna support structure (masts, etc.) may be in the range of US\$75 to US\$100. Also note that the optimal antenna height can be up to 20ft, depending upon your latitude.

<p>Item # RJK2u – Complete 2.0 Kit: Receiver + Unbuilt Antenna Kit + Software</p> <p>This kit includes an SDRplay RSP1A, USB Cable, SMA/BNC cable, F-adapter, unbuilt Antenna Kit (RJA), printed assembly manuals, and Radio-Sky Spectrograph (RSS) software.</p> <p>Note: Kit does not include antenna support structure.</p> <p>Price: \$215 + Shipping (See reverse for shipping)</p>	<p>Item # RJK2p – Complete 2.0 Kit: Receiver + Professionally Built Antenna Kit + Software</p> <p>This kit includes an SDRplay RSP1A, USB Cable, SMA/BNC cable, F-adapter, Professionally Built Antenna Kit (RJA2), printed assembly manuals, and Radio-Sky Spectrograph (RSS) software.</p> <p>Note: Kit does not include antenna support structure.</p> <p>Price: \$384 + Shipping (See reverse for shipping)</p>
<p>Item # RJA – Unbuilt Antenna Kit</p> <p>The RJA Radio JOVE Antenna Kit includes a printed construction manual, stranded copper easy-to-solder antenna wire, ceramic insulators, RG-59 easy-to-solder coax cable, screw-on F connectors, and a power combiner.</p> <p>Note: Kit does not include antenna support structure. Assembly requires a soldering gun and other tools.</p> <p>Price: \$90 + Shipping (See reverse for shipping)</p>	<p>Item # RJA2 – Professionally Built Antenna Kit</p> <p>The RJA2 Radio JOVE Antenna Kit includes a printed installation manual, two professionally assembled dipole antennas constructed of #14 Copperweld wire with Budwig center insulators and center support rope attachment points, high quality RG-6 coax with pre-installed commercial grade connectors, and a power combiner.</p> <p>Note: Kit does not include antenna support structure.</p> <p>Price: \$249 + Shipping (See reverse for shipping)</p>
<p>Item # LTJ2 – Listening to Jupiter, 2nd Ed. by R. S. Flagg</p> <p>PDF download of Richard Flagg's book "Listening to Jupiter, 2nd Ed., 2005". The file is downloaded from a secure website.</p> <p>Price: \$10 + \$0 shipping (PDF file download)</p>	<p>Item # RJR2 – Radio JOVE 2.0 Receiver-Only Kit</p> <p>This kit includes one SDRplay RSP1A SDR receiver, USB Cable, SMA/BNC cable, and F-adapter, printed assembly manuals, and Radio-Sky Spectrograph (RSS) software.</p> <p>Price: \$135 + Shipping (See reverse for shipping)</p>

RADIO JOVE 2.0 RADIO TELESCOPE KIT ORDER FORM (continued)

Order Online at https://radiojove.net/kit/order_form.html

OR

Complete this form and mail with payment

Payment may be made by Credit Card via PayPal™, U.S. Check, U.S. Money Order, International Money Order in U.S. funds drawn on a U.S. bank, or Western Union Money Transfer made payable to **The Radio JOVE Project**. No bank-to-bank wire transfers are accepted. Purchase Orders are accepted from U.S. Institutions.

Send to: The Radio JOVE Project
 1301 East Main St
 MTSU Box 412
 Murfreesboro, TN 37132, USA
 email: chiggins@mtsu.edu
 FEIN: 20-5239863

Item	Description	Quantity	Item Price	Shipping (see below)	Subtotal
RJK2u	Complete Radio JOVE 2.0 Kit Receiver + unbuilt Antenna		\$215		
RJK2p	Complete Radio JOVE 2.0 Kit Receiver + Professionally Built Antenna		\$384		
RJA2	Professionally Built Antenna-Only Kit		\$249		
RJA	Unbuilt Antenna-Only Kit		\$90		
RJR2	Receiver-Only Kit		\$135		
LTJ2	Listening to Jupiter, 2 nd Ed., by R.S. Flagg (PDF download)		\$10	\$0	
Total:					

Shipping Fees for Radio JOVE: We ship all packages using USPS Priority Mail flat rate boxes.
 U.S.A.: \$17.00
 Canada: \$57.00
 All Other International Shipping: \$85.00

Ship to: (Please print clearly)

Name: _____
 Address: _____
 City, State, Postal Code: _____
 Province, Country: _____
 Email: _____

Visit the Radio JOVE web site and fill out the team application form at https://radiojove.net/sign_up_form.php even if you are just an interested individual so that you can receive important information about kit updates, online services, and activities within the project as they occur!



The British Astronomical Association
A company limited by guarantee
Registered Charity No. 210769

PO Box 702, Tonbridge, TN9-9TX 020-7734 4145
www.britastro.org



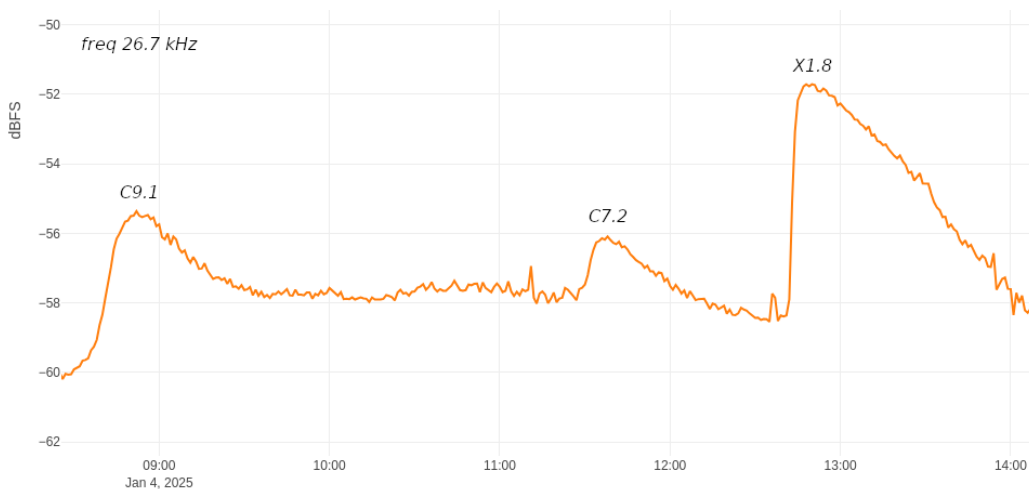
Please send questions, reports, and observations to John Cook: jacook@jacook.plus.com
BAA Radio Astronomy Section, Director: Paul Hearn

RADIO SKY NEWS

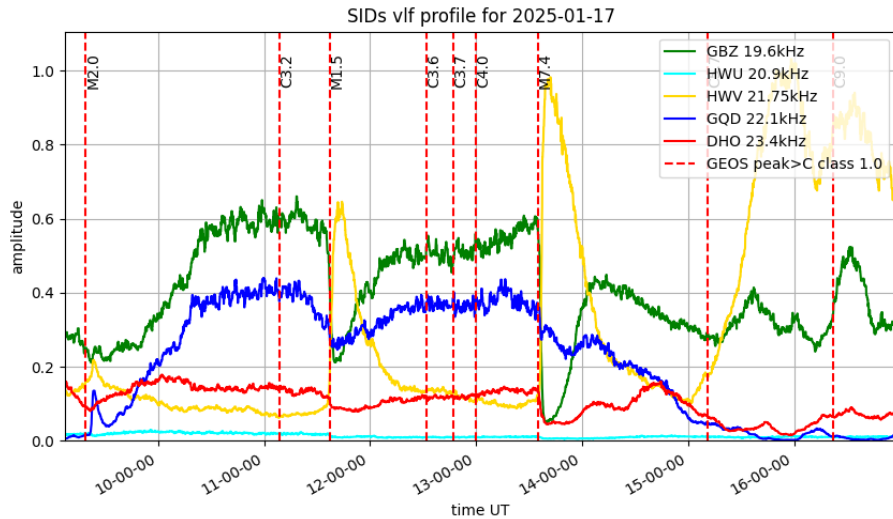
2025 JANUARY

VLF SID OBSERVATIONS

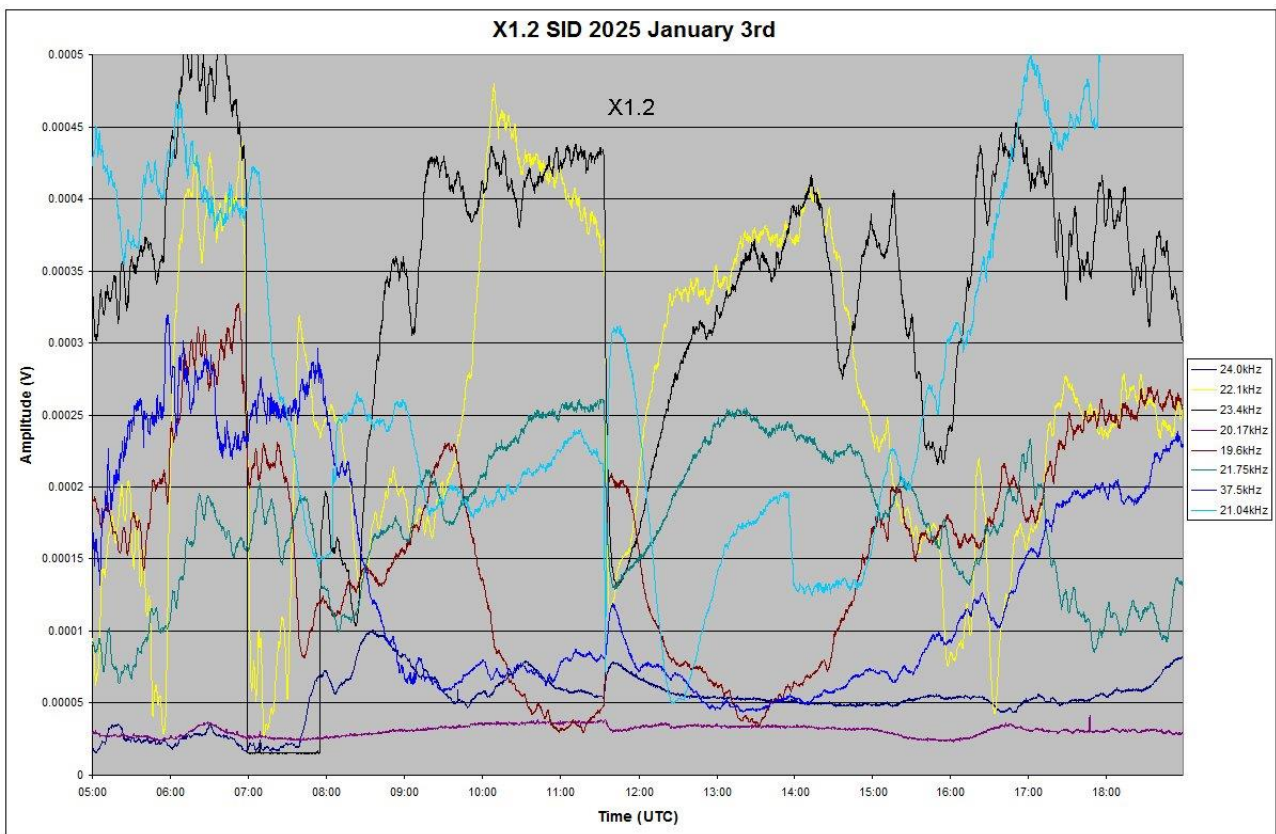
Solar activity in January was very low in comparison with previous months, just forty-five classified flares being recorded. There were two X-class flares early in the month, but they were followed by a week in which we did not record any SIDs. The satellite data shows some weaker flares during the gap from the 6th to 13th, along with a couple of M-flares that we have missed. The ionosphere was very unstable during this period, hiding any genuine events.



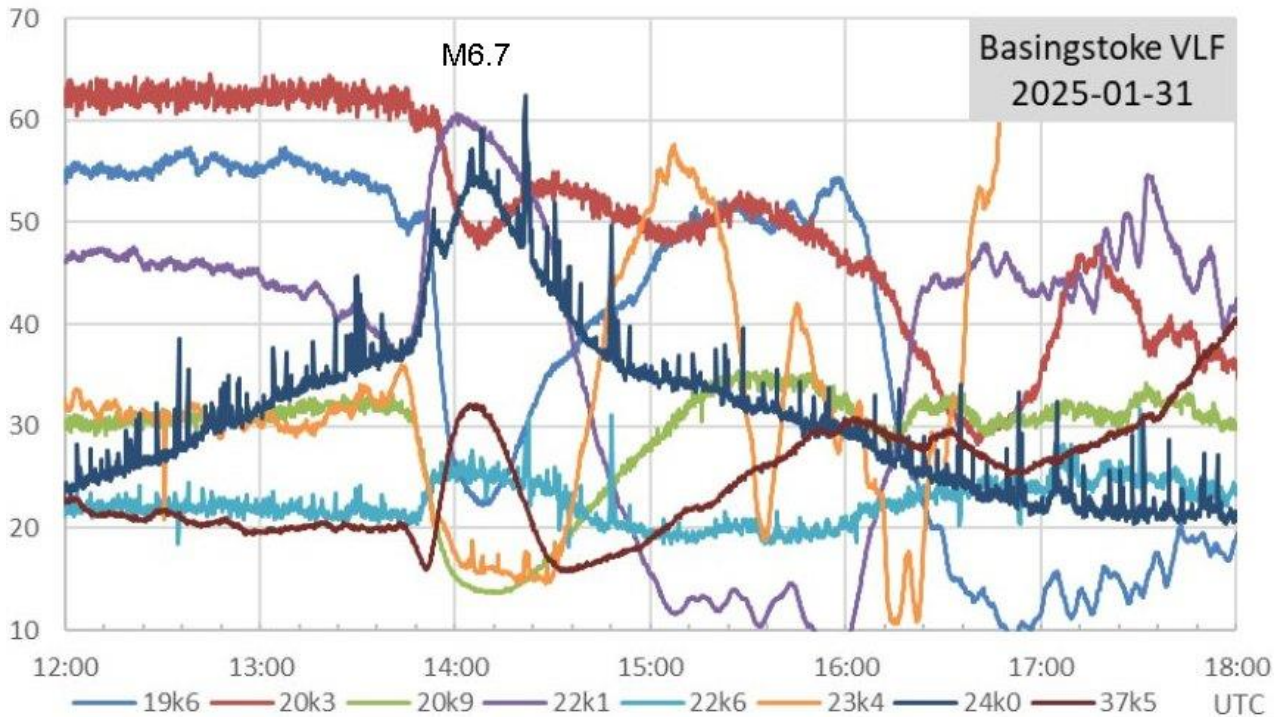
The X1.8 flare on the 4th was widely recorded, well timed at 12:50UT. The recording by Thomas Mazzi in Italy was made at 26.7kHz, a Turkish signal. The C9.1 and C7.2 flares have also produced good SIDs.



Mark Prescott's recording from the 17th shows a more active day, with two strong M-flares. 23.4kHz has not responded as well as the other signals to either of the M-flares. None of the signals show any trace of the weaker C-flares. The M2.0 flare at 09:20UT has produced a fairly weak SID at 22.1kHz and 21.75kHz.



The X1.2 flare on the 3rd was again well timed at 11:40UT, shown in Mark Edwards' recording. All of the signals show general instability. 21.04kHz shows a very strong 'spike and wave' SID, while the other signals show an ordinary 'shark fin'.

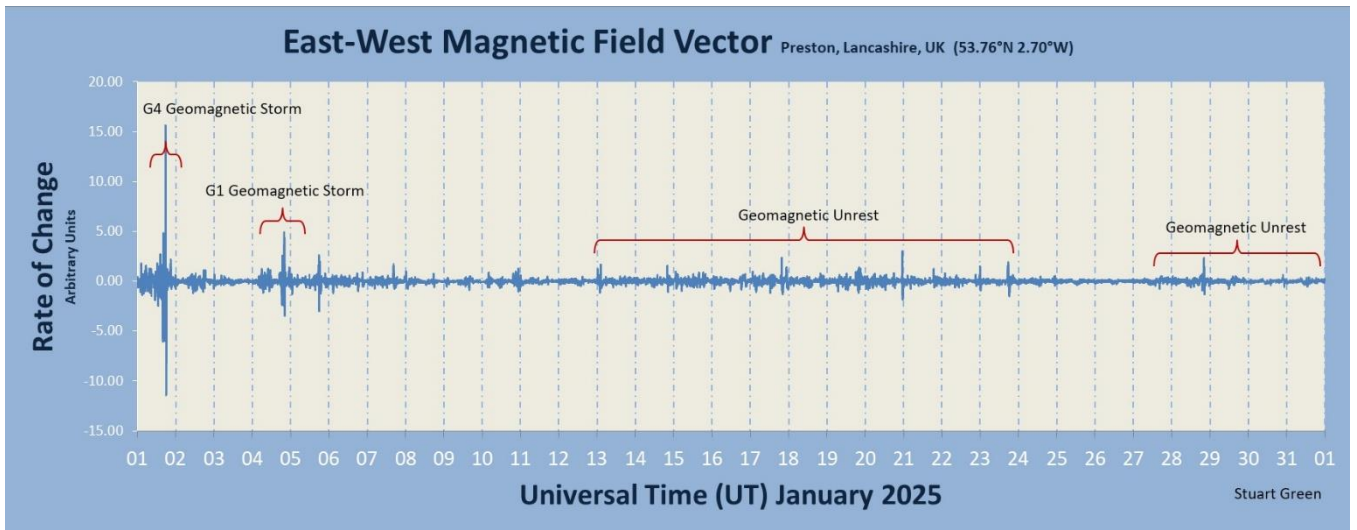


Activity increased again with a strong M6.7 flare on the 31st, shown in the recording by Paul Hyde. Most of the signals show a clear SID, but the background noise is also very strong. The series of smaller flares after 15:00UT are not easy to identify.

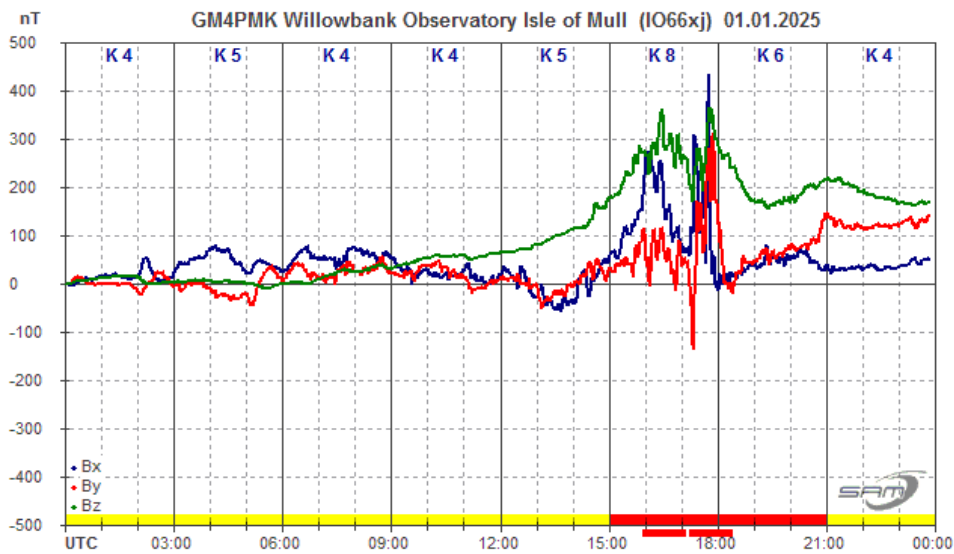
Unfortunately, I made an error in the December report. In Paul's chart from December 8th. I said that 37.5kHz had shown the strongest SID, where I should have said 22.1kHz. It can be tricky to correctly identify the colours used when there are lots of signals present.

We have a small partial eclipse to look forward to on March 29th. The greatest eclipse will be seen from northeastern Canada, but the path then crosses the Atlantic to reach the UK, ending in Italy. The maximum eclipse here in the UK is about 45 to 50%, just after 11UT, depending on location. There are charts and timings in the February Journal. We should see some effects on many of our signals, so worth checking. I also hope for some clear weather for a visual observation.

MAGNETIC OBSERVATIONS

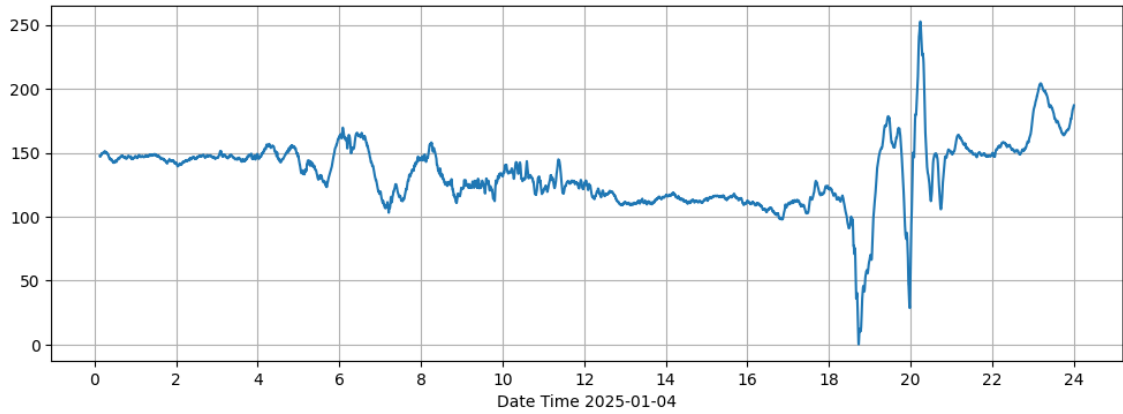


Stuart Green has re-scaled his chart of the month's magnetic activity to show the strong G4 storm on January 1st. The rest of the month looks very quiet, but the Bartels chart does show gentle disturbance through most of the month. Roger Blackwell has also re-scaled his chart from the 1st:

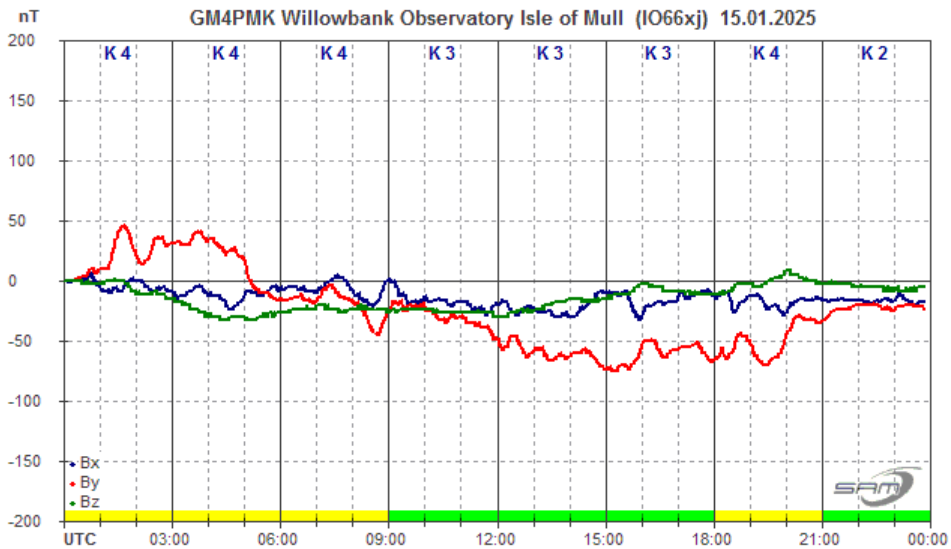
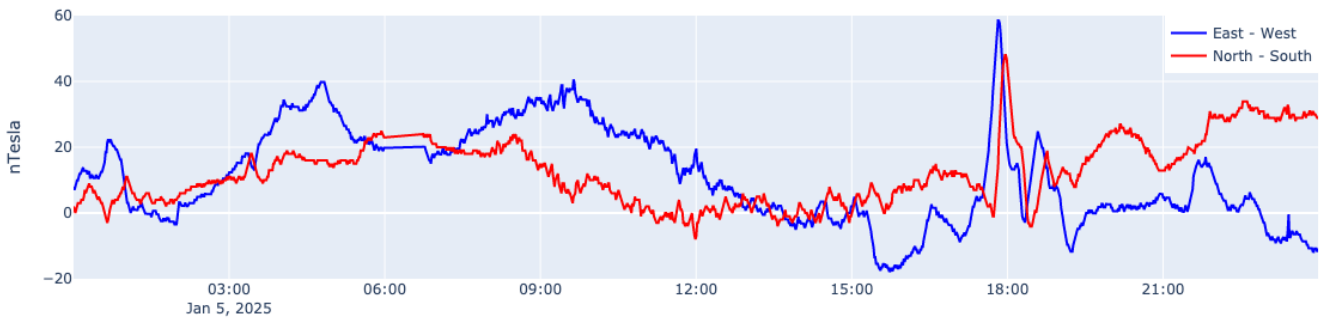


This disturbance appears to be from a number of CMEs from the flaring at the end of December. It continued into the 2nd, although much weaker, followed on the 4th with the addition of a stronger solar wind. Callum Potter's chart shows stronger disturbance in the evening of the 4th, Nick Quinn's chart showing more activity in the evening of the 5th.

Wasbister Magnetometer (59.17N,3.06W)



Steyning Magnetometer (50.8 North, 0.3 West)

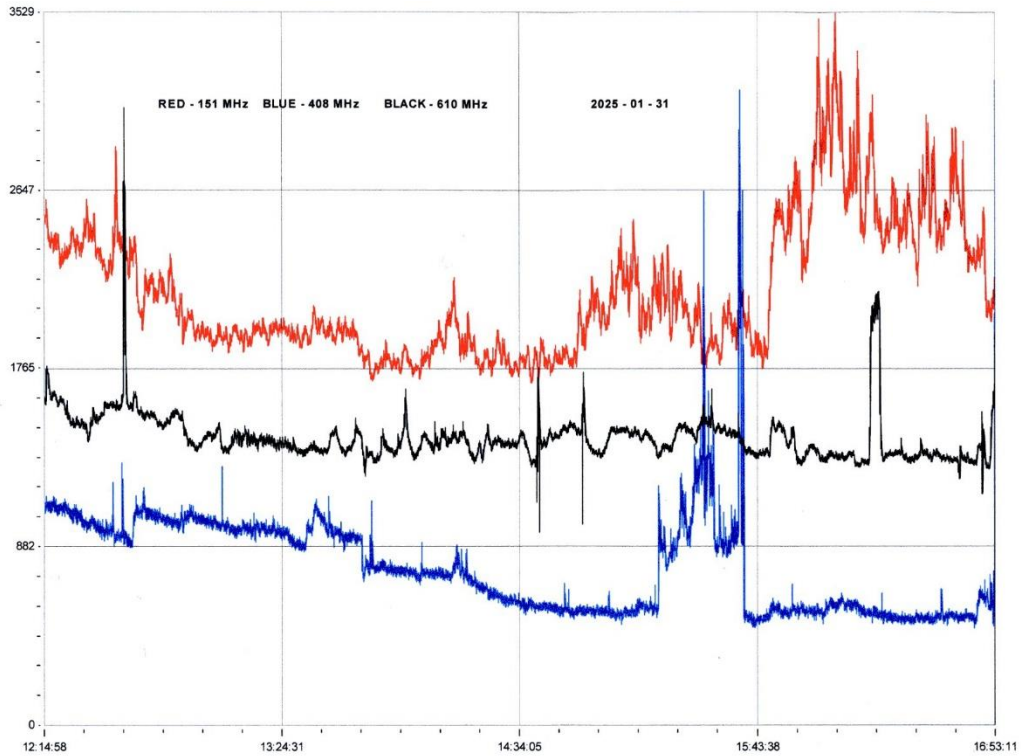


The remainder of the month's activity was much weaker, Roger Blackwell's recording from the 15th being typical. This appears to be mostly from some mild solar wind.

Magnetic observations received from Roger Blackwell, Stuart Green, Callum Potter, Nick Quinn, and John Cook.

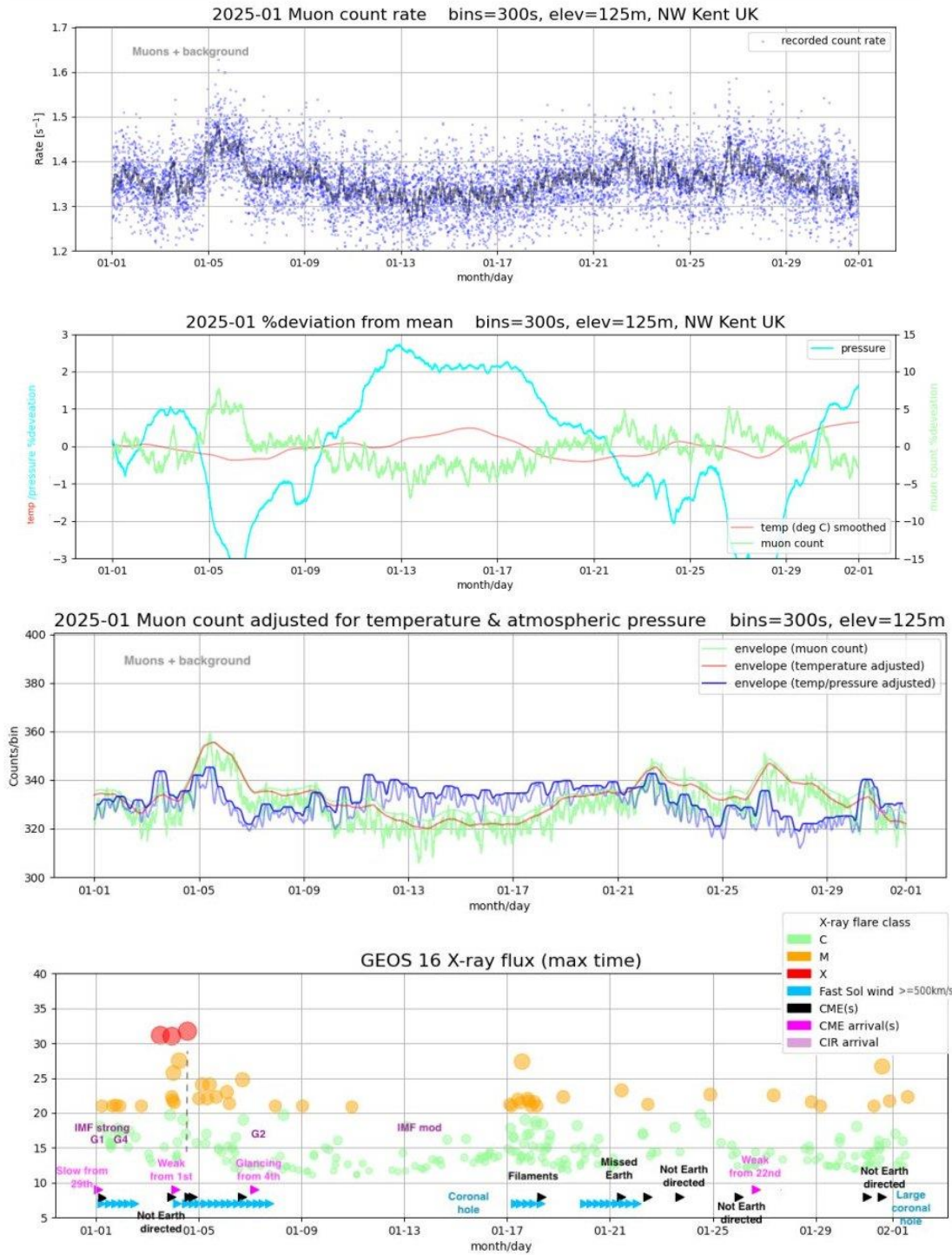
SOLAR EMISSIONS

Colin Clements reports a very quiet month for radio emissions, nothing being recorded from either of the early X-flares. He did record some activity on the 31st, with what appears to be a delayed noise burst from the M6.7 flare.



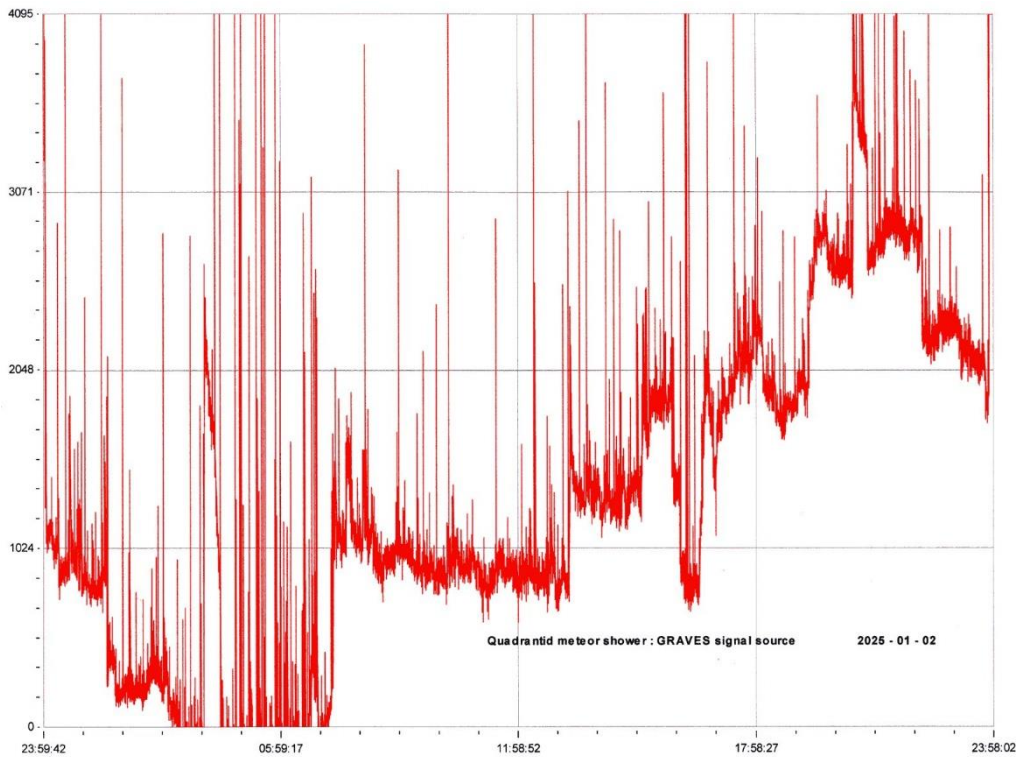
408MHz (blue) starts at about 15:14, continuing for about 30 minutes. 151MHz (red) emissions start shortly afterwards, continuing to the end of the recording.

MUONS



Mark Prescott's muon recordings show some strong variation through January. The chart on the previous page also shows that we had some very strong atmospheric pressure changes. The temperature / pressure corrected chart above still shows a muon increase following the strong flares early in the month. Through the middle of the month, it is rather more stable, but does show a large drop after the 23rd, with another peak right at the end of the month.

QUADRANTIDS



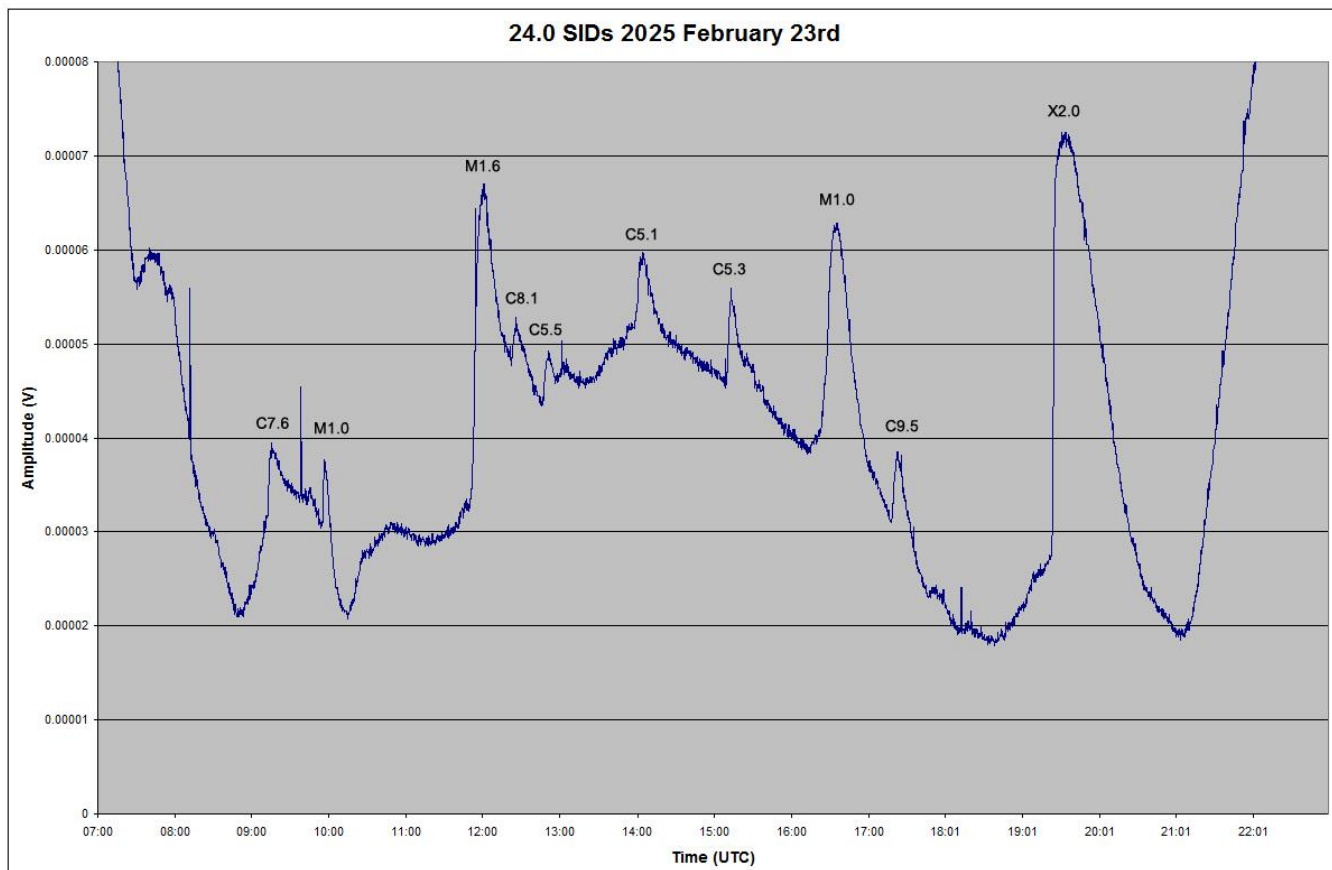
Colin Clements recorded the Quadrantid meteor shower using the GRAVES signal. His chart covers the full 24 hours on 2nd January and shows rising activity through the day. The most active period is in the evening, fading a little in the last hour.

I have already mentioned the partial solar eclipse on March 29th. It will be interesting to compare recordings from different parts of the country as we have done for previous eclipses.

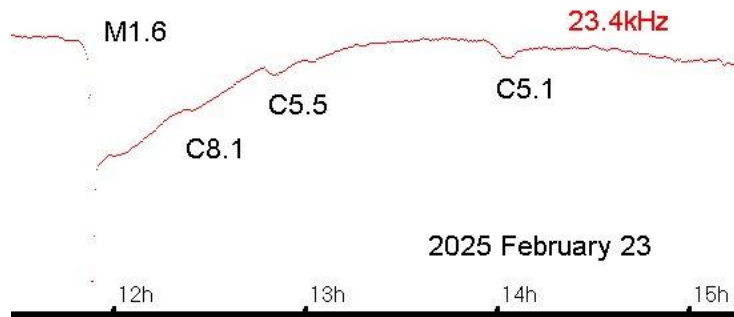
The Historical section newsletter was published earlier this week and includes a very interesting article by Wayne Orchiston about Dr Elizabeth Alexander and her part in the development of Radio Astronomy after World War II. We all know of the work done by Sir Bernard Lovell, but much more was being done at the time and has since been overlooked. Well worth looking for Historical Section Newsletter 31 on the website.

VLF SID OBSERVATIONS

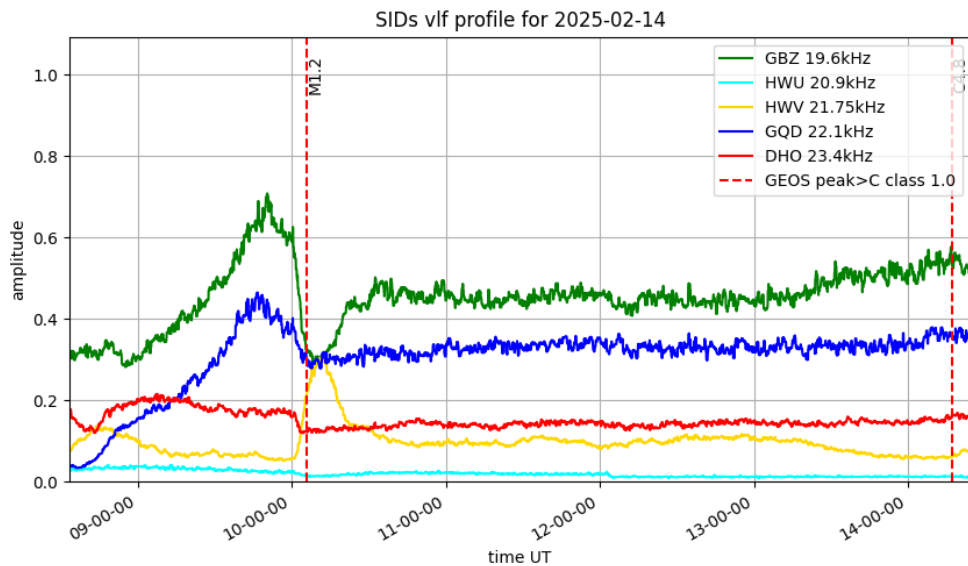
Solar flare activity increased in February, back up to the level last seen in 2024 November. We recorded SIDs from eighty classified flares, including a single X-flare. This was the only one shown in the satellite data, and we were lucky to record it on the 24kHz signal peaking at 19:32UT on the 23rd. This was also the busiest day of the month, shown in Mark Edwards’ 24kHz recording:

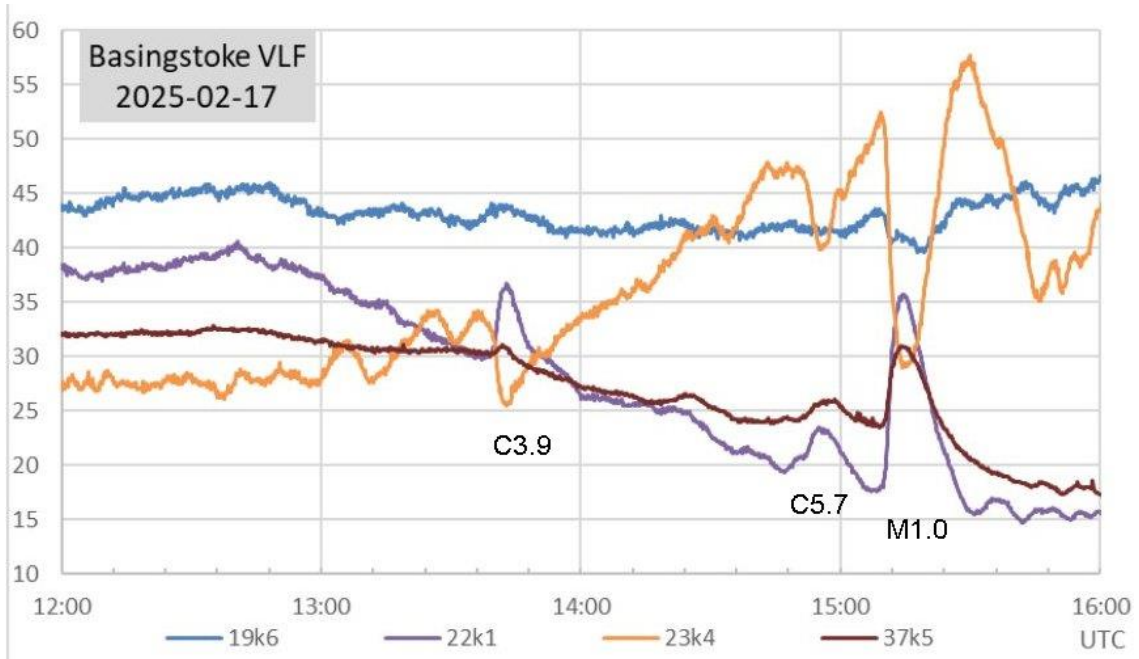


The Satellite flare list in the SWPC weekly report does not include the four peaks shown in Mark’s chart between 12:20UT and 16UT. They have been classified here by reference to the daily X-ray chart on the SWPC web site. I indicate these in the timing tables with ‘?’, as the X-ray chart covers a maximum of seven days, well past by the time that I am analysing our reports. They are however often significant flares, the C5.1 at 14:05 producing SIDs for eight of our nine observers.

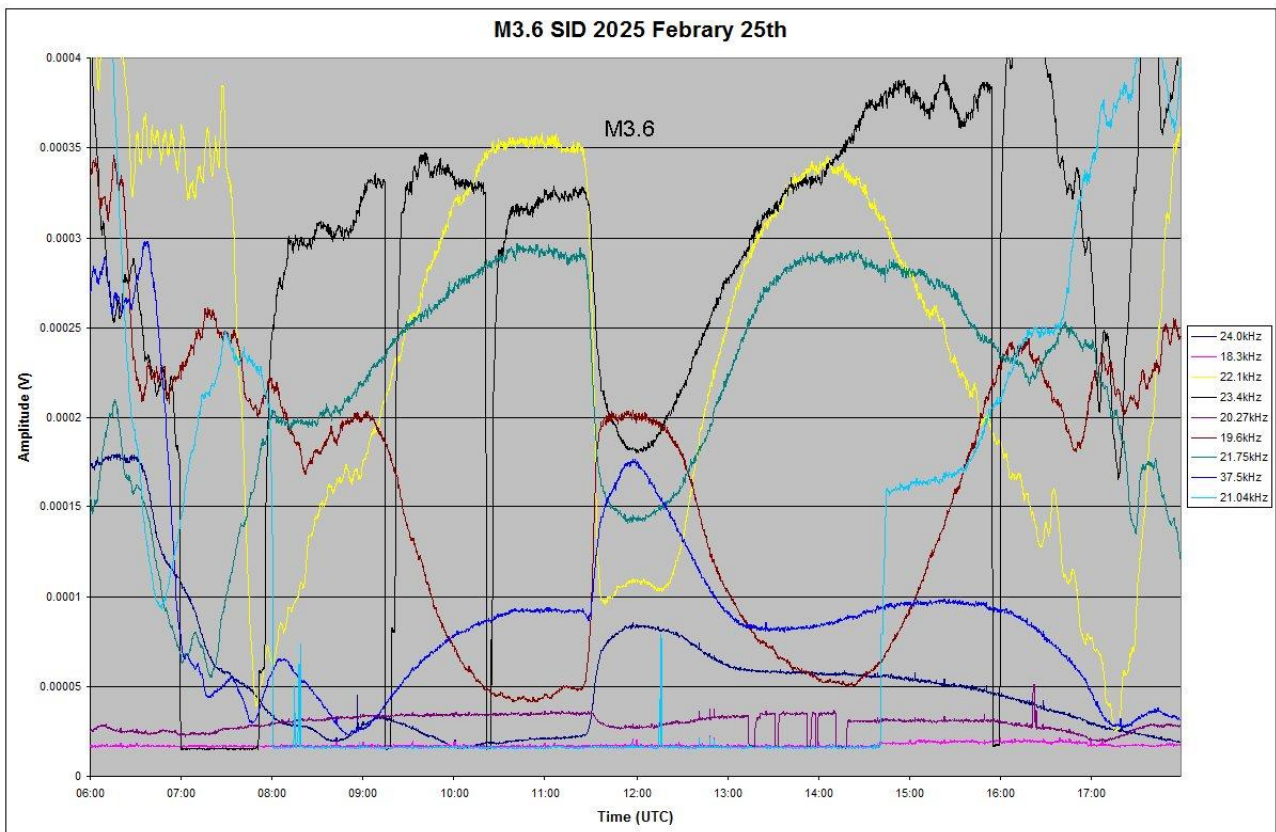


My own 23.4kHz recording also shows these events following the strong M1.6 flare. The M1.6 SID is slightly distorted by a transmitter glitch just as it starts. Flaring activity faded from the 9th for several days, increasing again after the 13th. Mark Prescott's recording shows a single SID from the M1.2 flare just after 10UT on the 14th. The rest of the day is very flat, with minimal effects from the C4.8 flare at the end of the chart.



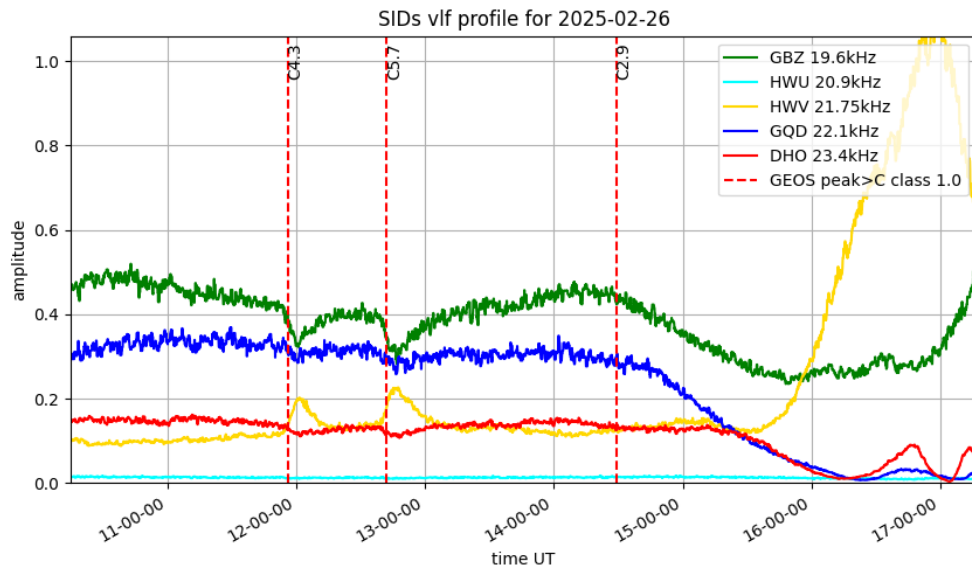


Paul Hyde’s recording from the 17th shows a very disturbed 23.4kHz signal. 22.1kHz and 37.5kHz are much clearer and show the three flares. The C4.4 flare just before 16UT does not show, the rise at 23.4kHz being most likely the start of sunset.



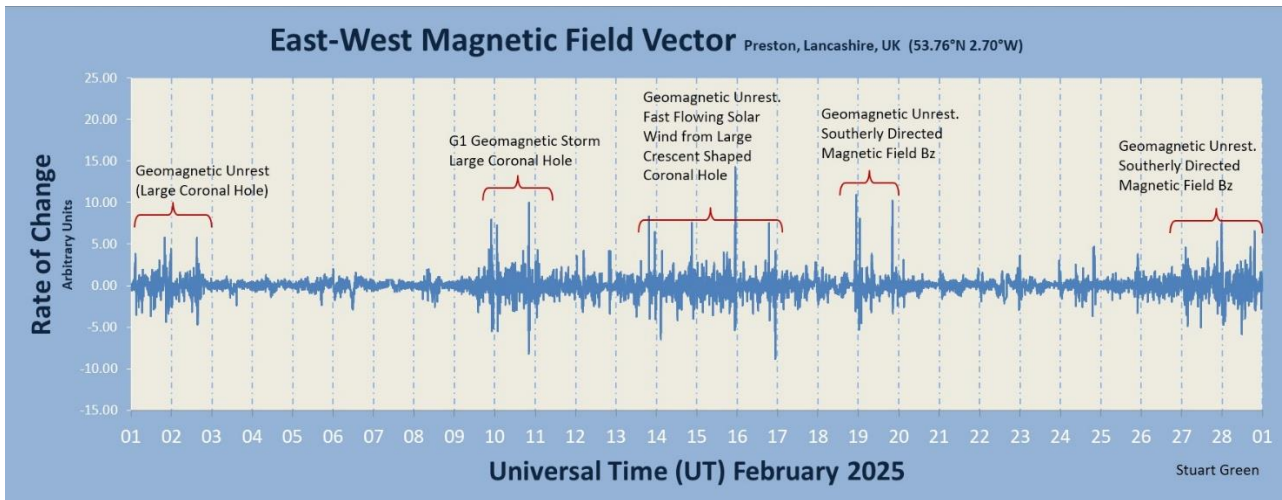
Mark Edwards’ recording from the 25th shows the M3.6 flare, well timed at midday. It also shows more problems with 23.4kHz, with a series of dropouts following the usual 7-8 break. 22.1kHz shows a small ‘spike-and-wave’ SID, while the other signals have the normal ‘shark’s fin’ SID.

There was a series of smaller flares on the 26th, shown in the recording by Mark Prescott:



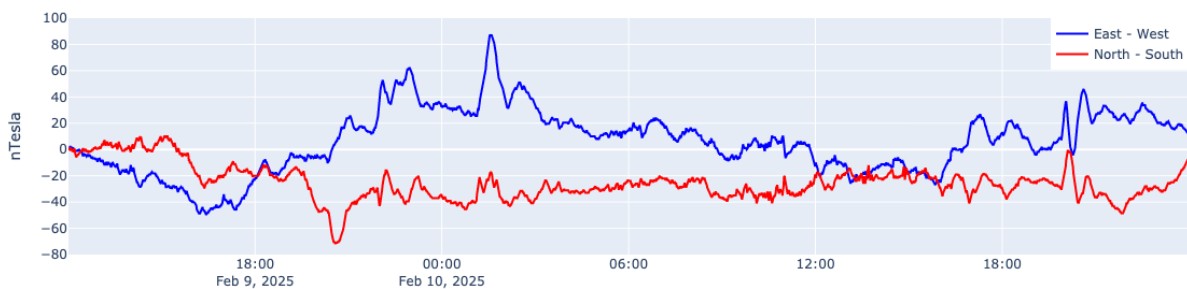
Both the C4.3 and C5.7 show well, and there is perhaps a small hint of a SID at 13:30 for the unclassified flare on the 19.6kHz signal.

MAGNETIC OBSERVATIONS

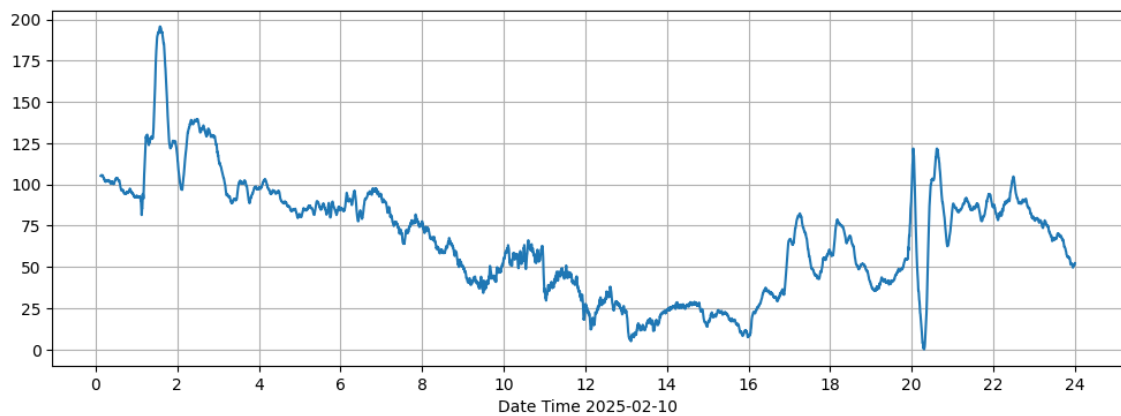


Stuart Green's summary of magnetic activity in February shows some disturbance on most days. Our SID statistics include plenty of M-class flares, but CMEs seem to have been very mild and mixed in with strong solar winds from coronal holes. The satellite images seem to show that most CMEs were directed well away from the Earth. None of our recordings show any sign of a distinct CME arrival. Some the strongest disturbance was over the 9th to 11th, the recording by Nick Quinn showing its start:

Steyning Magnetometer (50.8 North, 0.3 West)

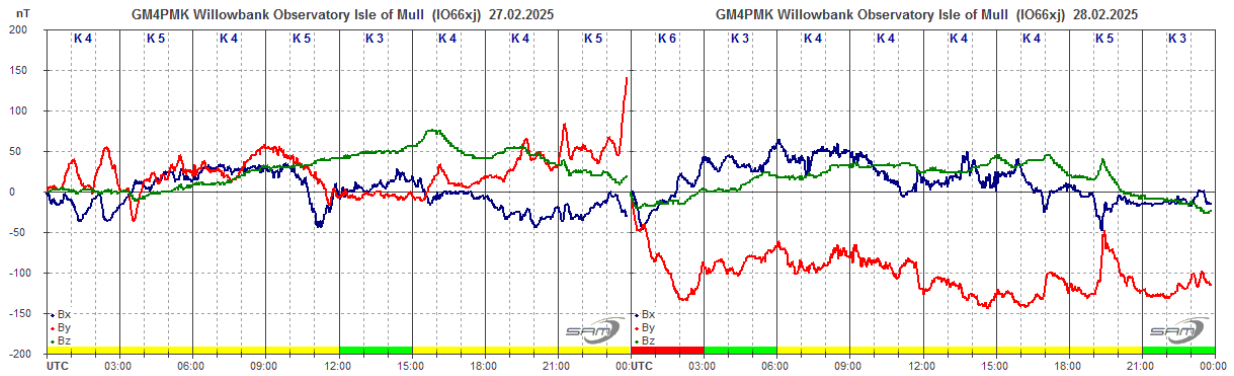


Wasbister Magnetometer (59.17N,3.06W)



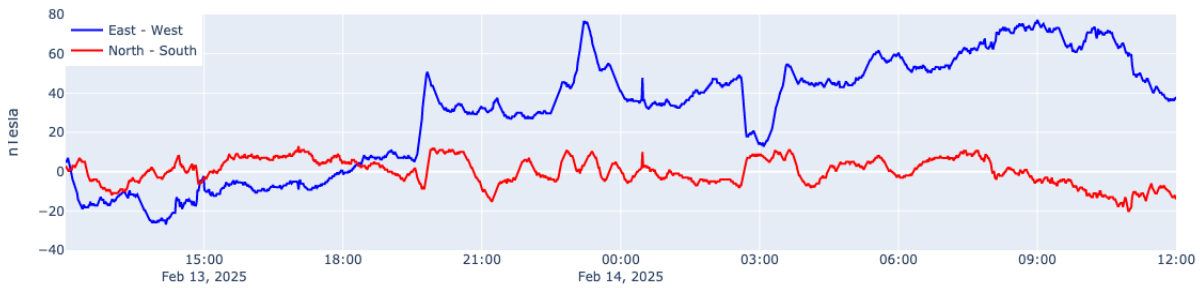
Callum Potter's recording on the 10th is similar, but with greater amplitude.

The most active period was at the end of the month, shown here by Roger Blackwell:



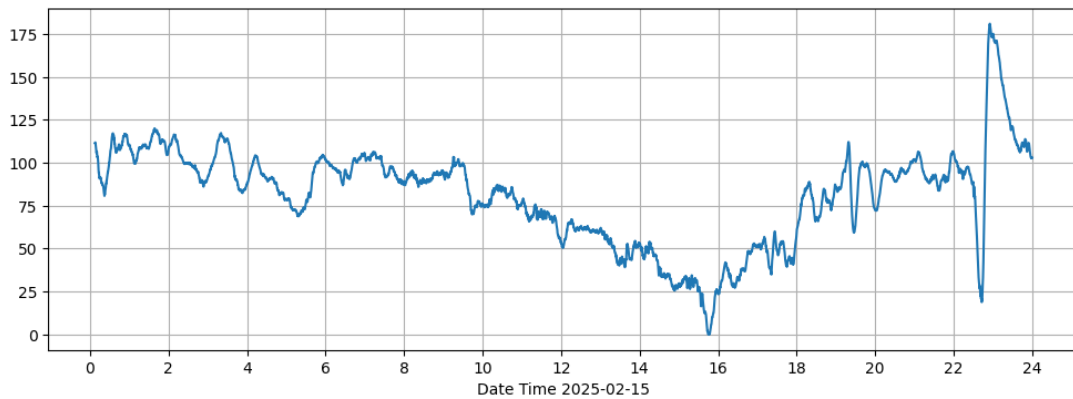
This shows the 27th and 28th, the large disruption in the **By** (red) trace being due to a sensor reset at midnight. The Earth – Solar magnetic field alignment at this time of year allows the best interaction (an ideal time for aurora watching) and so maximises the effect that the solar wind has.

Steyning Magnetometer (50.8 North, 0.3 West)



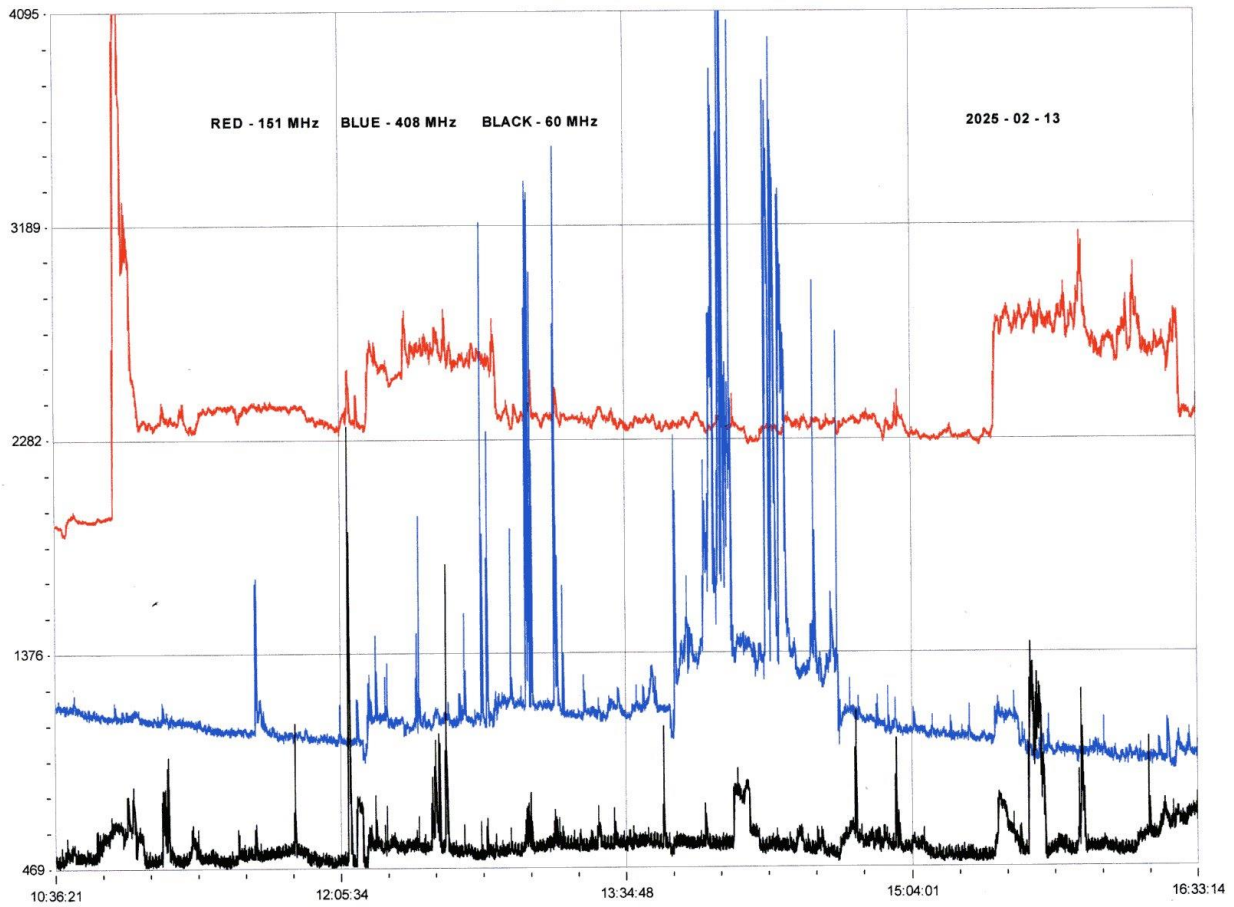
Solar wind from a large coronal hole produced another period of disturbance mid-month, Nick Quinn's recording showing the 13th and 14th. There is a sharp field change around 19:30 on the 13th, although I have not found any reference to a CME impact at this time. A similar effect is seen in charts from other observers. The disturbance continued for several days, Callum Potter's recording showing more activity on the 15th.

Wasbister Magnetometer (59.17N,3.06W)

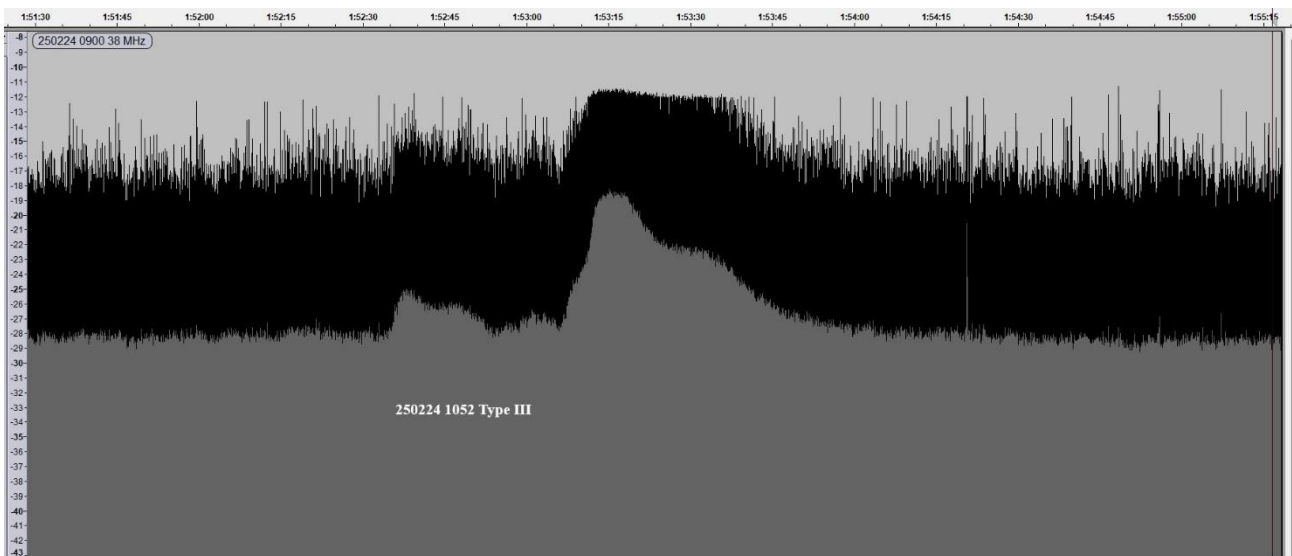


Magnetic observations received from Roger Blackwell, Stuart Green, Callum Potter, Nick Quinn, and John Cook.

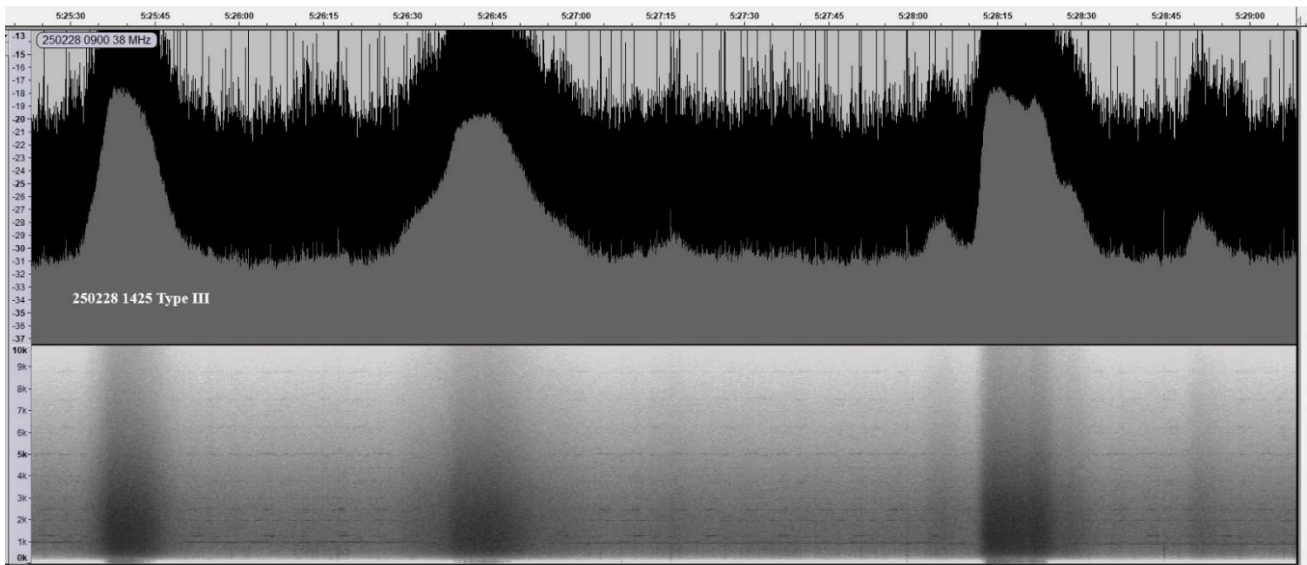
SOLAR EMISSIONS



Colin Clements' HF/VHF recording from the 13th shows some strong activity, particularly at 408MHz (blue). The strong spike at 151MHz (red) may be related to the M1.0 flare peaking at 11:10. There is also a small response at 60MHz (black). The 408MHz signal starting just after 12UT matches the C3.3 and C3.2 flares that we recorded, while the source of the stronger burst after 14:00 is unknown.

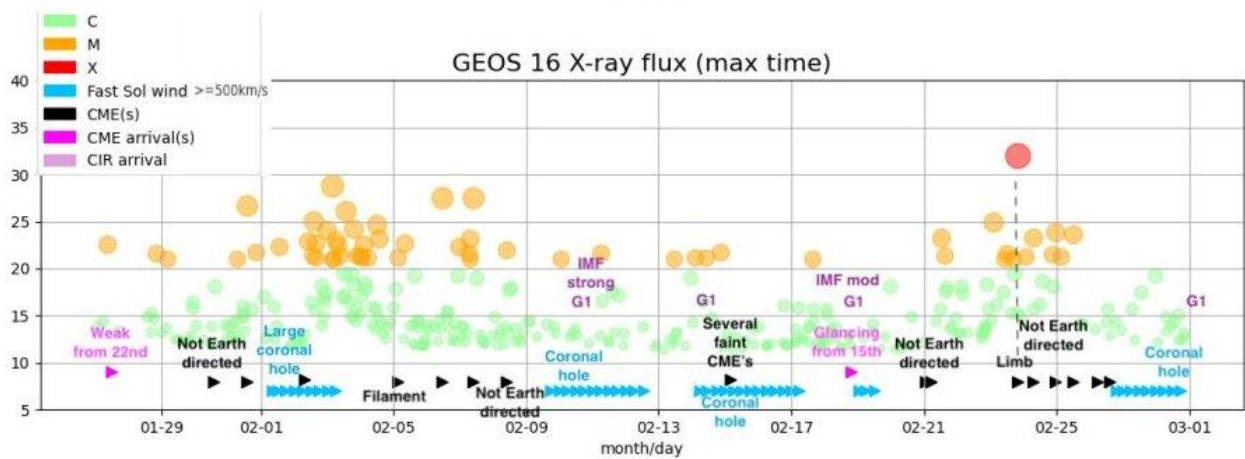
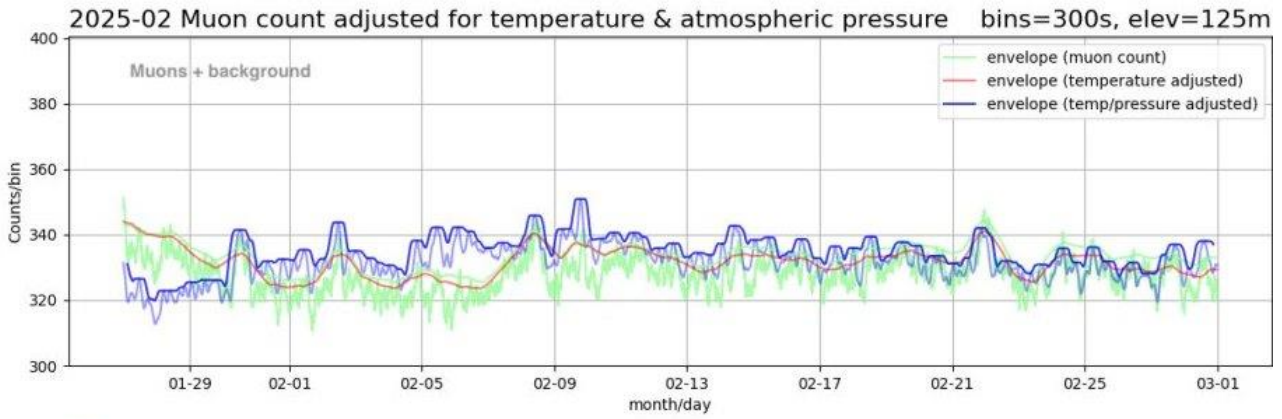
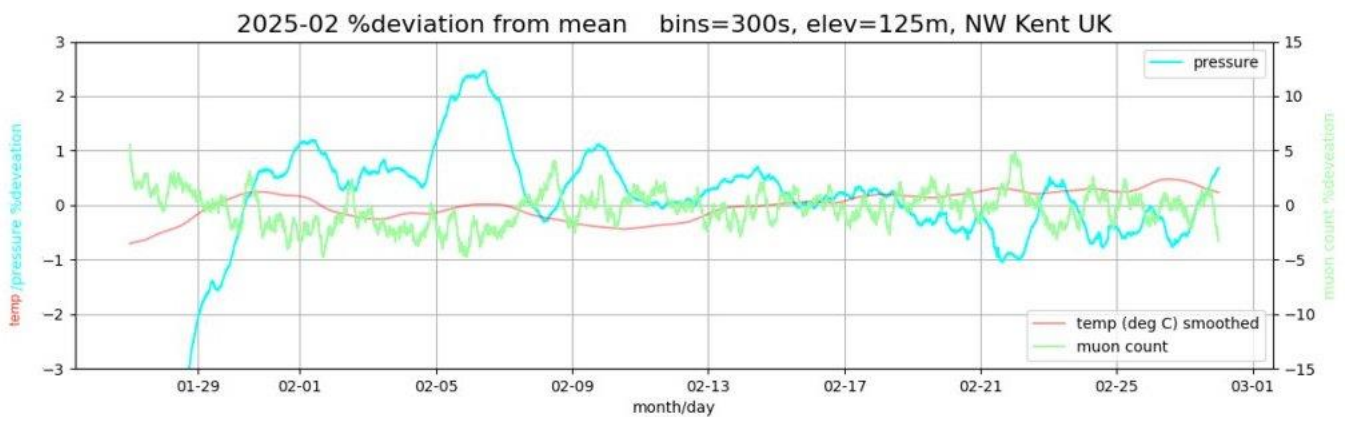
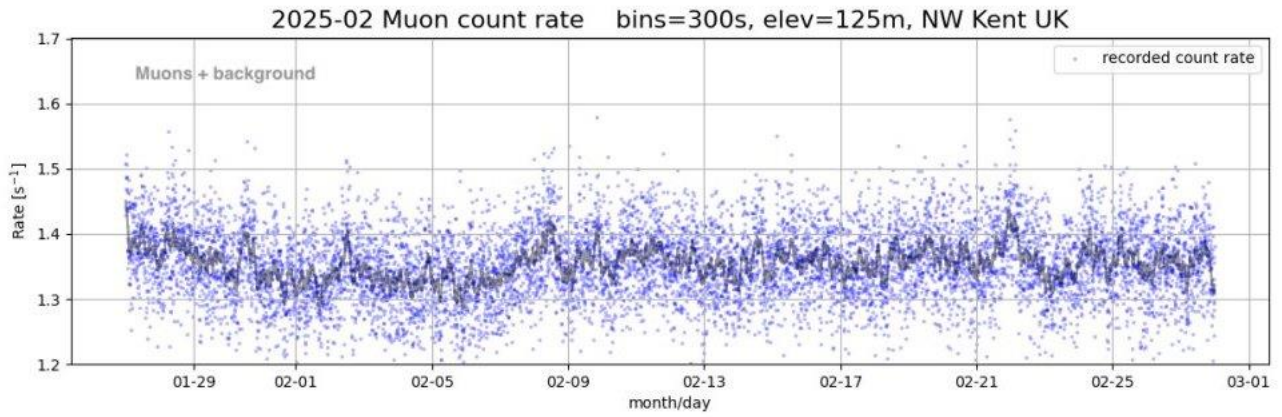


Colin Briden's 38MHz recording from the 24th shows a type III emission starting at 10:52UT and lasting about 90 seconds with an amplitude of 10dB.



His recording from the 28th starts at 14:25, with a series of peaks over a period of 3 minutes with an amplitude of 12dB. This type III emission is the start of a run of thirteen similar peaks that make a type VI emission. The lower part of the chart shows the noise over a 10kHz bandwidth.

MUONS



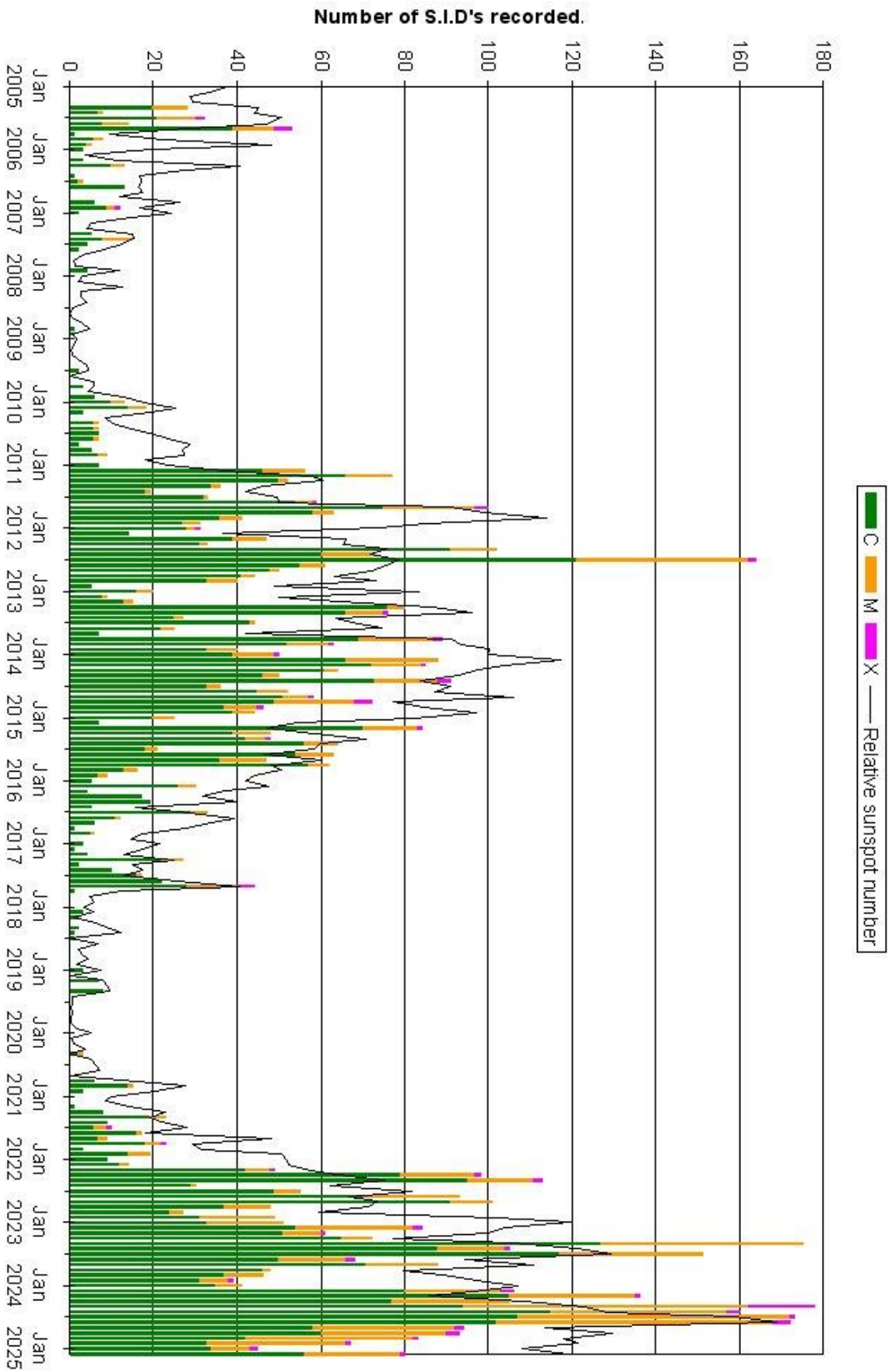
Mark Prescott's muon charts show a gentle rise at the start of February, following the drop at the end of January. Atmospheric pressure also increased on the 1st, then remaining rather unstable through the rest of the month. The muon counts generally reflect this behaviour. They also seem to drop during the period of strong flaring over the 2nd to 5th. The coronal hole solar wind was also more active after the 10th, with a gentle drop in the muon flux recorded up to the end of the month.

The partial solar eclipse on March 29th offers about 40% cover over the UK, the maximum being around 11UT depending on location. I very much hope that the clouds behave and stay out of the way. Our VLF and HF/VHF observations should not be affected either way, but it will be good to watch how the environment responds to the changing light.

BARTELS CHART

ROTATION	KEY:	DISTURBED.	ACTIVE	SFE	B, C, M, X = FLARE MAGNITUDE.	Synodic rotation start (carington's)
2575	F	21 22 23 24 25 26 27 28 29 30 31	2258	2022 June	1 2 3 4 5 6 7 8 9 10 11 12 13 14 15 16	
2576	F	17 18 19 20 21 22 23 24 25 26 27 28 29 30	2259	2022 July	1 2 3 4 5 6 7 8 9 10 11 12 13	
2577	F	14 15 16 17 18 19 20 21 22 23 24 25 26 27 28 29 30 31	2260	2022 August	1 2 3 4 5 6 7 8 9 10 11 12 13 14 15 16	
2578	F	10 11 12 13 14 15 16 17 18 19 20 21 22 23 24 25 26 27 28 29 30 31	2261	2022 September	1 2 3 4 5 6 7 8 9 10 11 12 13 14 15 16	
2579	F	6 7 8 9 10 11 12 13 14 15 16 17 18 19 20 21 22 23 24 25 26 27 28 29 30 31	2262	2022 October	1 2 3 4 5 6 7 8 9 10 11 12 13 14 15 16	
2580	F	3 4 5 6 7 8 9 10 11 12 13 14 15 16 17 18 19 20 21 22 23 24 25 26 27 28 29 30	2263	2022 October	1 2 3 4 5 6 7 8 9 10 11 12 13 14 15 16	
2581	F	30 31 1 2 3 4 5 6 7 8 9 10 11 12 13 14 15 16 17 18 19 20 21 22 23 24 25	2264	2022 November	1 2 3 4 5 6 7 8 9 10 11 12 13 14 15 16	
2582	F	26 27 28 29 30 1 2 3 4 5 6 7 8 9 10 11 12 13 14 15 16 17 18 19 20 21 22	2265	2022 December	1 2 3 4 5 6 7 8 9 10 11 12 13 14 15 16 17 18 19 20 21 22	
2583	F	23 24 25 26 27 28 29 30 31 1 2 3 4 5 6 7 8 9 10 11 12 13 14 15 16 17 18	2266	2023 January	1 2 3 4 5 6 7 8 9 10 11 12 13 14 15 16 17 18	
2584	F	19 20 21 22 23 24 25 26 27 28 29 30 31 1 2 3 4 5 6 7 8 9 10 11 12 13 14	2267	2023 February	1 2 3 4 5 6 7 8 9 10 11 12 13 14 15 16	
2585	F	15 16 17 18 19 20 21 22 23 24 25 26 27 28 29 30 31 1 2 3 4 5 6 7 8 9 10 11 12 13	2268	2023 March	1 2 3 4 5 6 7 8 9 10 11 12 13 14 15 16	
2586	F	14 15 16 17 18 19 20 21 22 23 24 25 26 27 28 29 30 31 1 2 3 4 5 6 7 8 9	2269	2023 April	1 2 3 4 5 6 7 8 9 10 11 12 13 14 15 16	
2587	F	10 11 12 13 14 15 16 17 18 19 20 21 22 23 24 25 26 27 28 29 30 1 2 3 4 5 6	2270	2023 May	1 2 3 4 5 6 7 8 9 10 11 12 13 14 15 16	
2588	F	7 8 9 10 11 12 13 14 15 16 17 18 19 20 21 22 23 24 25 26 27 28 29 30 31 1 2	2271	2023 June	1 2 3 4 5 6 7 8 9 10 11 12 13 14 15 16	
2589	F	3 4 5 6 7 8 9 10 11 12 13 14 15 16 17 18 19 20 21 22 23 24 25 26 27 28 29	2272	2023 July	1 2 3 4 5 6 7 8 9 10 11 12 13 14 15 16	
2590	F	30 1 2 3 4 5 6 7 8 9 10 11 12 13 14 15 16 17 18 19 20 21 22 23 24 25 26	2273	2023 August	1 2 3 4 5 6 7 8 9 10 11 12 13 14 15 16	
2591	F	27 28 29 30 31 1 2 3 4 5 6 7 8 9 10 11 12 13 14 15 16 17 18 19 20 21 22	2274	2023 September	1 2 3 4 5 6 7 8 9 10 11 12 13 14 15 16	
2592	F	23 24 25 26 27 28 29 30 31 1 2 3 4 5 6 7 8 9 10 11 12 13 14 15 16 17 18	2275	2023 September	1 2 3 4 5 6 7 8 9 10 11 12 13 14 15 16	
2593	F	19 20 21 22 23 24 25 26 27 28 29 30 31 1 2 3 4 5 6 7 8 9 10 11 12 13 14 15	2276	2023 October	1 2 3 4 5 6 7 8 9 10 11 12 13 14 15 16	
2594	F	16 17 18 19 20 21 22 23 24 25 26 27 28 29 30 31 1 2 3 4 5 6 7 8 9 10 11 12	2277	2023 November	1 2 3 4 5 6 7 8 9 10 11 12 13 14 15 16	
2595	F	13 14 15 16 17 18 19 20 21 22 23 24 25 26 27 28 29 30 31 1 2 3 4 5 6 7 8 9	2278	2023 December	1 2 3 4 5 6 7 8 9 10 11 12 13 14 15 16	
2596	F	10 11 12 13 14 15 16 17 18 19 20 21 22 23 24 25 26 27 28 29 30 31 1 2 3 4 5	2279	2024 January	1 2 3 4 5 6 7 8 9 10 11 12 13 14 15 16	
2597	F	6 7 8 9 10 11 12 13 14 15 16 17 18 19 20 21 22 23 24 25 26 27 28 29 30 31 1	2280	2024 February	1 2 3 4 5 6 7 8 9 10 11 12 13 14 15 16	
2598	F	2 3 4 5 6 7 8 9 10 11 12 13 14 15 16 17 18 19 20 21 22 23 24 25 26 27 28	2281	2024 February	1 2 3 4 5 6 7 8 9 10 11 12 13 14 15 16	
2599	F	29 1 2 3 4 5 6 7 8 9 10 11 12 13 14 15 16 17 18 19 20 21 22 23 24 25 26	2282	2024 March	1 2 3 4 5 6 7 8 9 10 11 12 13 14 15 16	
2600	F	27 28 29 30 31 1 2 3 4 5 6 7 8 9 10 11 12 13 14 15 16 17 18 19 20 21 22	2283	2024 April	1 2 3 4 5 6 7 8 9 10 11 12 13 14 15 16	
2601	F	23 24 25 26 27 28 29 30 31 1 2 3 4 5 6 7 8 9 10 11 12 13 14 15 16 17 18 19	2284	2024 May	1 2 3 4 5 6 7 8 9 10 11 12 13 14 15 16	
2602	F	20 21 22 23 24 25 26 27 28 29 30 31 1 2 3 4 5 6 7 8 9 10 11 12 13 14 15	2285	2024 June	1 2 3 4 5 6 7 8 9 10 11 12 13 14 15 16	
2603	F	16 17 18 19 20 21 22 23 24 25 26 27 28 29 30 31 1 2 3 4 5 6 7 8 9 10 11 12	2286	2024 July	1 2 3 4 5 6 7 8 9 10 11 12 13 14 15 16	
2604	F	13 14 15 16 17 18 19 20 21 22 23 24 25 26 27 28 29 30 31 1 2 3 4 5 6 7 8	2287	2024 August	1 2 3 4 5 6 7 8 9 10 11 12 13 14 15 16	
2605	F	9 10 11 12 13 14 15 16 17 18 19 20 21 22 23 24 25 26 27 28 29 30 31 1 2 3 4	2288	2024 September	1 2 3 4 5 6 7 8 9 10 11 12 13 14 15 16	
2606	F	5 6 7 8 9 10 11 12 13 14 15 16 17 18 19 20 21 22 23 24 25 26 27 28 29 30 31	2289	2024 September	1 2 3 4 5 6 7 8 9 10 11 12 13 14 15 16	
2607	F	2 3 4 5 6 7 8 9 10 11 12 13 14 15 16 17 18 19 20 21 22 23 24 25 26 27 28	2290	2024 October	1 2 3 4 5 6 7 8 9 10 11 12 13 14 15 16	
2608	F	29 30 31 1 2 3 4 5 6 7 8 9 10 11 12 13 14 15 16 17 18 19 20 21 22 23 24	2291	2024 November	1 2 3 4 5 6 7 8 9 10 11 12 13 14 15 16	
2609	F	25 26 27 28 29 30 31 1 2 3 4 5 6 7 8 9 10 11 12 13 14 15 16 17 18 19 20 21	2292	2024 December	1 2 3 4 5 6 7 8 9 10 11 12 13 14 15 16	
2610	F	22 23 24 25 26 27 28 29 30 31 1 2 3 4 5 6 7 8 9 10 11 12 13 14 15 16 17	2293	2025 January	1 2 3 4 5 6 7 8 9 10 11 12 13 14 15 16	
2611	F	18 19 20 21 22 23 24 25 26 27 28 29 30 31 1 2 3 4 5 6 7 8 9 10 11 12 13	2294	2025 February	1 2 3 4 5 6 7 8 9 10 11 12 13 14 15 16	
2612	F	14 15 16 17 18 19 20 21 22 23 24 25 26 27 28 29 30 31 1 2 3 4 5 6 7 8 9 10 11 12	2295	2025 March	1 2 3 4 5 6 7 8 9 10 11 12 13 14 15 16	

VLF flare activity 2005/25



Operation and Comparison of Total Power, Dicke and Correlation Radiometers

Peter W East

Abstract

Radiometer receivers used for amateur radio astronomy require high RF gains preceding modern software defined radios (SDR). However, most active subsystems suffer from temperature induced gain drift and also, their electronic devices often add low frequency flicker or $1/f$ noise. This article compares the basic total power receiver stability performance with the Dicke switch and pseudo-correlation receiver types designed to overcome these instabilities to flatten data baselines and improve recognition of weak radio sources.

Introduction

The operation, sensitivity and data extraction processes of the total power, Dicke switch and pseudo-correlation receivers employing SDRs is compared and examined using hydrogen-line data collected by an experimental pseudo-correlation receiver [1]. A pseudo-correlation receiver is a variant of the correlation receiver comprising twin phase tracking, band-limited channels feeding a multiplier [2]. The pseudo-correlation receiver discussed in this paper is based upon those used in the WMAP and PLANCK space observatories launched to measure the cosmic microwave background [3,4].

The paper is divided into five parts, the first summarizing the target background and power levels received. Part 2 describes the structure, theory of operation, detection and processing requirements of the three receiver types. Part 3 introduces a pseudo-correlation hardware test bed, using a pair of RTL2832U SDRs for the 1420 MHz hydrogen-line band. This is used to collect some test data that is analyzed to demonstrate and compare the performance of the three receiver types in Part 4. Finally, Part 5 suggests future improvements.

Part 1. Background

Janskys and Receiver Power

The strength of radio astronomy sources is expressed in Janskys (J); the source flux corresponding to 1 Jansky is, $1J = 10^{-26}$ Watts/m²/Hz.

The equivalent resistor thermal noise input power in terms of Boltzmann's constant, k , RF bandwidth and effective temperature is, $kT_J B_r$ Watts, where $k = 1.38 \cdot 10^{-23}$ Watts/K/Hz; T_J is device temperature measured in °K and B_r is the measurement RF bandwidth in Hz.

For an antenna effective capture area of A m², intercepting a radio target flux of 1 Jansky, the received antenna terminal power is, JAB_r . Equating the powers in these expressions,

$$J A B_r \cdot 10^{-26} = k T_J B_r = 1.38 \cdot 10^{-23} T_J B_r \text{ Watts,}$$

$$\text{or, } J A = 1380 T_J$$

Rearranging the equality, the equivalent source temperature, T_J supplied by an antenna, effective area A m² is given by,

$$T_J = J A / 1380 \text{ K (1)}$$

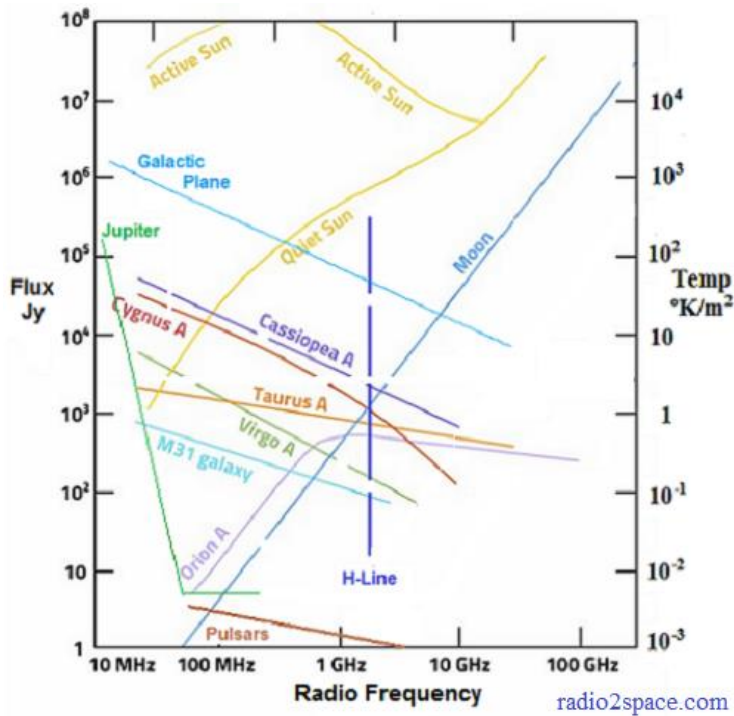


Figure 1. Chart of Typical Radio Telescope Sources of Interest to Amateurs

Figure 1 plots some common radio source flux ranges with flux (indicated at left-hand ordinate) and equivalent source temperature as collected by a 1 m² aperture radio telescope antenna and calculated from Equation 1 (indicated at the right-hand ordinate).

The chart shows that most galactic sources of amateur interest, using a typical 1 m² antenna system produce modest temperatures in the region of 0.1 to 10 K.

Hydrogen line clouds are much more accommodating and are the preferred targets for some amateurs.

Part 2. Theory

Radio Telescope Receivers

Figure 2 illustrates a generic power-measuring receiver, comprising an antenna, low noise RF amplifier, driving a software defined radio (SDR) producing digital data for processing to extract the target data.

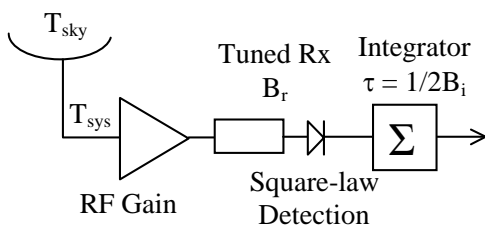


Figure 2. Total Power Radiometer (Square-law Detector)

With an SDR implementation, digital in-phase and quadrature (I/Q) outputs are squared and added in the data processing to simulate square-law detection. The integrator in this case is in the form of a data averaging, simulating a low-pass data filter over the observation window. With most SDRs, data processing is mostly carried out off-line although GNU Radio seems to be the preferred software for SDR data collection and any data pre-processing required.

For target source plus sky background noise temperature of $T_{sky} = T_{source} + T_{skyback}$ and system temperature T_{sys} (made up of feeder loss, mismatch loss and input LNA noise), the output signal voltage V from a square-law detector followed by an integrator contains both AC, (V_{AC}) and DC, (V_{DC}) components, given by (see Appendix 1 for the squaring analysis),

$$\begin{aligned} V &= V_{AC} + V_{DC} \\ &= kG(T_{sky} + T_{sys})\sqrt{2B_r B_i}|_{AC} + kGB_r(T_{sky} + T_{sys})|_{DC} \end{aligned} \quad (2)$$

where, k is Boltzmann's constant.

G is the total receiver power gain.

B_r is the detector input RF bandwidth and B_i the post-detector integrator equivalent bandwidth.

(τ , the total integration time in seconds is equal to $1/2B_i$).

The DC output usually includes the wanted target response (T_{source}) but it also includes a measure of the sky background + system noise temperature, whilst the AC component adds uncertainty to the result. Estimation of the system temperature from component parameters allows computation of the wanted noise source.

This is a simplification, as the temperature received by the antenna may, in addition to the wanted source, comprise background components and ground noise entering via antenna side and back lobes.

The target source signal-to-noise ratio (SNR) is, from Equation 2,

$$\begin{aligned} SNR &= \frac{kGB_r T_{source}}{kG(T_{sky} + T_{sys})\sqrt{2B_r B_i}} \\ &= \frac{B_r T_{source}}{(T_{sky} + T_{sys})\sqrt{2B_i B_r}} \quad (3) \\ &= \frac{T_{source}\sqrt{B_r \tau}}{T_{sky} + T_{sys}} \end{aligned}$$

Indicating an independence of RF gain fluctuations. However, as Equation 2 shows, the wanted source measure sits on a DC baseline that is RF gain dependent and whilst T_{sys} may dominate T_{sky} , it may be susceptible to antenna pointing changes and/or vary across wide RF bands.

The DC baseline level is RF gain (G) dependent, and is proportional to $kGB_r(T_{skyback} + T_{sys})$

This equation shows that the output indicated baseline temperature is dominated by the integrated system noise temperature and amplitude varied by ambient temperature gain changes. Also, the AC noise variation is reduced by the square root integration term in Equation 3.

Modern SDRs draw more component heating power when recording data and it is not unusual for gain drift significantly during recordings. It may be useful in some instances to stabilize the RF chain gain in some way; by means of a temperature-controlled oven, for example.

For wideband spectrum monitoring, with total power receivers, the data baseline follows the receiver gain/frequency response shape which may also obscure the wanted source component.

With post-recording digital processing, it may be possible to track and correct for both gain drift and frequency band shapes. This is often the simplest option for amateurs.

The radiometer temperature sensitivity over the observation time τ , is usually defined by inverting the final equality (SNR=1) in Equation 3 giving,

$$\Delta T = \frac{T_{sky} + T_{sys}}{\sqrt{B_r \tau}} = \frac{T_{sys}}{\sqrt{B_r \tau}} \quad (4)$$

As is usual, in the second equality of Equation 4, T_{sys} includes T_{sky} .

Dicke Radiometer

The Dicke switch receiver was invented to electronically correct for gain drift and variations during a recording but at the expense of at least, a 3dB reduction in sensitivity.

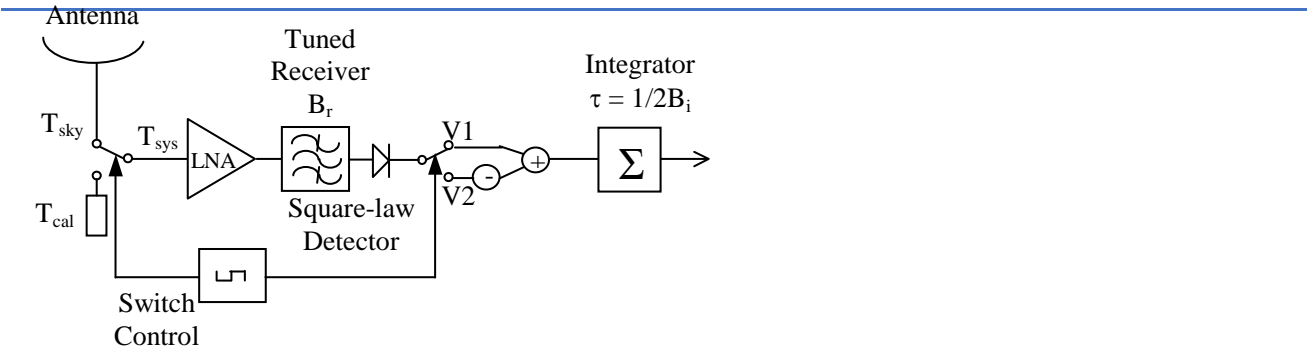


Figure 3. Dicke Switch Radiometer

In the conventional Dicke switched receiver, the two switches in Figure 3 are switched synchronously with a 50:50 duty cycle, so that the difference between the antenna path signal and a calibration reference path signal is integrated after square-law detection.

The aim of this architecture is to minimize the effect of RF gain variations on the detected total power DC baseline output, by switching sufficiently fast so that both channels see the same instantaneous gain. The two channel's data are subtracted before integration. The switching rate is usually chosen in the kiloHerz region to track the highest expected rate of amplifier gain variations and/or to minimize the inverse frequency ($1/f$) noise generated in most semiconductor devices.

The analysis approach is similar to that above. For the two integrated 50:50 switched paths $V1$ and $V2$, and system gain G ,

$$\begin{aligned} V &= V_{AC} + V_{DC} \\ V1 &= kG(T_{sky} + T_{sys})\sqrt{2B_r B_i} \Big|_{AC} + kGB_r(T_{sky} + T_{sys}) \Big|_{DC} \\ V2 &= kG(T_{cal} + T_{sys})\sqrt{2B_r B_i} \Big|_{AC} + kGB_r(T_{cal} + T_{sys}) \Big|_{DC} \end{aligned} \quad (5)$$

	Switch section 1 average, $\Sigma V1$	Switch section 2 average, $\Sigma V2$
DC	$kG[T_{sky} + T_{sys}] B_r/2$	$kG[T_{cal} + T_{sys}] B_r/2$
AC	$kG[T_{sky} + T_{sys}] \sqrt{2B_r B_i} / \sqrt{2}$	$kG[T_{cal} + T_{sys}] \sqrt{2B_r B_i} / \sqrt{2}$

Table 1. Switch state detector noise voltages integrated over a full switch cycle

When averaging over a full switch cycle, half-cycle DC components in Table 1 are reduced by a factor of 2 and half-cycle AC noise components' amplitudes are reduced by a factor of $\sqrt{2}$; finally resulting in the entries listed in Table 2.

Uncorrelated AC noise voltage terms in the switch half-cycles on addition, combine as the square root of the sum of their squares to produce the result in Table 2.

DC	$kG[T_{sky} - T_{cal}] B_r/2$
AC	$kG \left[\sqrt{(T_{sky} + T_{sys})^2 + (T_{cal} + T_{sys})^2} / \sqrt{2} \right] \sqrt{2B_r B_i}$

Table 2. Final DC and AC Components Difference ($\Sigma V1 - \Sigma V2$).

The integrated wanted source DC power within T_{sky} , T_{source} leads to its SNR,

$$\begin{aligned}
 SNR &= \frac{kGB_r T_{source}}{kG\sqrt{2} \left[\sqrt{(T_{sky} + T_{sys})^2 + (T_{cal} + T_{sys})^2} \sqrt{2B_r B_i} \right]} \\
 &= \frac{T_{source} \sqrt{B_r \tau}}{\sqrt{2} \left[\sqrt{(T_{sky} + T_{sys})^2 + (T_{cal} + T_{sys})^2} \right]} \quad (6) \\
 &\approx \frac{T_{source} \sqrt{B_r \tau}}{2(T_{sky} + T_{sys})} \Big|_{T_{cal}=T_{sky}}
 \end{aligned}$$

The DC baseline level variation is much reduced now proportional to, $kGB_r(T_{sky} - T_{cal})$, since in the final subtraction, the system temperature T_{sys} has been cancelled out, any data baseline level variation is theoretically nulled when the calibration temperature is set equal the current sky background temperature.

The Dicke receiver improvement, as expected, is at the expense of halving the achievable source signal-to-noise ratio compared to the total power receiver.

The system temperature sensitivity is now given by,

$$\Delta T = \frac{\sqrt{2} \sqrt{(T_{sky} + T_{sys})^2 + (T_{cal} + T_{sys})^2}}{\sqrt{B_r \tau}} \rightarrow \frac{2(T_{sky} + T_{sys})}{\sqrt{B_r \tau}} \Big|_{T_{cal} \approx T_{sky}} \quad (7)$$

For this Dicke switch implementation, T_{sky} is separated from T_{sys} to show that not only is the sensitivity reduced by a factor of 2 over the total power case but to minimize baseline drift, the calibration noise level should be chosen to be equal to the sky background noise and if not, this also can further degrade the eventual system sensitivity.

Calibration Reference Adjustment - the Gain Modulation Factor

In cases where the calibration reference noise level does not equal the sky background level, it is possible to compensate for this in post-processing by introducing the gain modulation factor, R ; this is the ratio of the integrated average of the DC terms in the sky and calibration switch half-cycles.

$$R = \frac{\sum_{\tau} (V1)}{\sum_{\tau} (V2)} = \frac{T_{sky} + T_{sys}}{T_{cal} + T_{sys}} \Big|_{DC} \pm \sqrt{\frac{2}{B_r \tau} \left((T_{sky} + T_{sys})^2 + (T_{cal} + T_{sys})^2 \right)} \Big|_{AC} \quad (8)$$

The AC term represents the rms error in estimating the mean value of R .

Multiplying $V2$ half-cycles by R before Table 2 subtraction and integration over time τ , attempts to make $(T_{cal} + T_{sys}) = (T_{sky} + T_{sys})$ on average, to zero the DC baseline aiming at the optimum sensitivity result of Equation 7 when $T_{cal} = T_{sky}$. Without this procedure, it is seen from Equations 6 and 7 that if the calibration reference level is much greater than the background sky level, then the Dicke receiver sensitivity is further degraded. To minimize the effect of the AC noise component, derivation of the value of R normally requires averaging the whole data set first, probably off-line before final target estimation and display. From Equation 8, if the calibration noise level is too excessive, there may still be some uncertainty remaining in the value of R , also if the target source level is significant, this can add to any baseline offset. The main object however is still to limit the effects of gain variations.

The Pseudo-Correlation Receiver

The pseudo-correlation receiver design suppresses $1/f$ noise, any baseline variation due to receiver gain changes and also improves sensitivity over the Dicke switch system. A pseudo-correlation receiver design was used in both the WMAP and PLANCK space observatories launched to measure the cosmic microwave background and achieved considerable temperature measurement accuracy.

Figure 3 shows an example implementation. It requires two identical receiver chains with matched LNA gains and close phase tracking in the first section (up to the indicated stage 4 marker).

The first two low noise RF amplifiers (LNA) lie between a pair of 180° 3 dB couplers (see Appendix 2 for 90° coupler analysis). In this instance, the couplers ensure the antenna and calibration signals enjoy the same RF gain passing through both LNAs so that any RF gain variations with time, track in both channels.

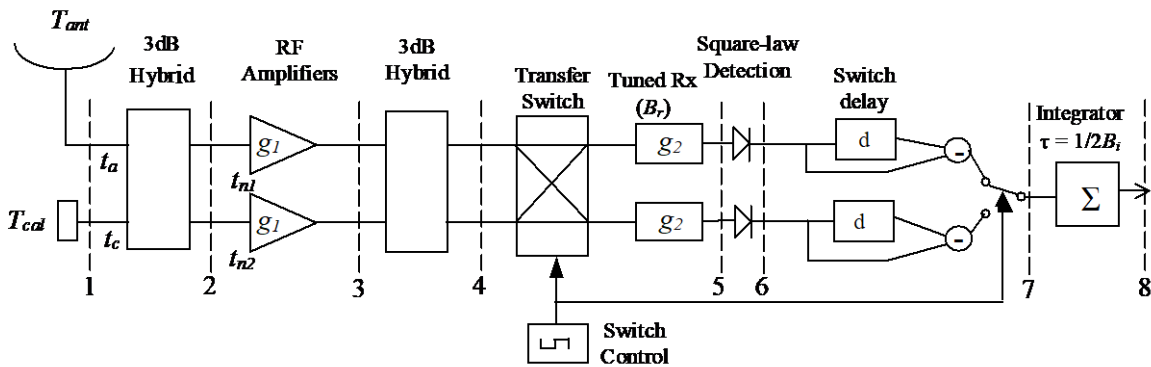


Figure 3 Ideal Pseudo Correlation Receiver

In the output section (markers 4 to 8), which also aims to minimize back-end red noise and balance the path gains, a transfer switch swaps the two signals to a pair of amplified tuned receivers. Once again the switch waveform is 50:50 duty cycle and the receiver cycles differenced. A detailed description follows.

The first section comprises a pair of 3dB hybrid couplers, coupled by a pair of matched low noise RF amplifiers to a second recombining coupler as shown in Figure 3. The two hybrids are identical. For this analysis, 180° couplers are assumed. The first hybrid inputs are fed from the antenna and a fixed calibration source with equivalent source temperature voltages t_a and t_c . The 180° hybrid output voltages, as shown in Table 1 are the sum and difference of the input signal and calibration voltages reduced by a factor $\sqrt{2}$ (halves the input power sharing to the output ports). In this way both input signals are amplified by both LNAs. The second hybrid coupler recombines the LNA outputs and separates the equally amplified input signals.

This technique ensures that any LNA gain changes affect both signal and calibration signals equally so that when eventually compared, any differences are nulled. This section has the property that the signals input to the first coupler pass through both LNAs equally and exit separately at the outputs of the second coupler with the gain and noise figure equivalent to that of a single amplifier. For information, this arrangement doubles the potential power output.

The back-end receiver section comprises a transfer switch and a pair of amplified RF band-restricted SDR receivers followed by square-law detection and data processing. The transfer switch is driven by a 50/50 pulsed drive followed by signal synchronous processing and integration. The switching operation passes the two comparison signals through both SDR receivers to now enable suppression of back-end gain variations. In this example the transfer switch function replaces a similar function used in the PLANCK receiver, which actually uses 180° phase shifters in the feeds to the second hybrid coupler to accomplish data switching. For amateur use, the transfer switch option eases a difficult requirement to find/develop an accurate fast-switching 180° RF phase shifter.

The post-detector processing is sometimes better done off-line. To best utilize the data for maximum sensitivity, it is necessary to re-arrange data between switch half-cycles, requiring a half-cycle delay as indicated in the back end of Figure 3.

The circuit analysis follows, indicating the signal processing progression stages. For simplicity, in this ideal case, the parallel receiver parameters are assumed identical and the hybrid-LNA-hybrid section, phase tracks perfectly.

Stage	1	2	3	4	5-switch 1	5-switch 2
Upper	t_a	$\frac{t_a}{\sqrt{2}} + \frac{t_c}{\sqrt{2}}$	$\left(\frac{t_a + t_c}{\sqrt{2}}\right)g^{1+t_{n1} \cdot g^1}$	$t_a g^1 + \frac{t_{n1} \cdot g^1 + t_{n2} \cdot g^1}{\sqrt{2}}$	$g^1 g^2 \left(t_a + \frac{t_{n1} + t_{n2}}{\sqrt{2}}\right)$	$g^1 g^2 \left(t_c + \frac{t_{n1} - t_{n2}}{\sqrt{2}}\right)$
Lower	t_c	$\frac{t_a}{\sqrt{2}} - \frac{t_c}{\sqrt{2}}$	$\left(\frac{t_a - t_c}{\sqrt{2}}\right)g^{1+t_{n2} \cdot g^1}$	$t_c g^1 + \frac{t_{n1} \cdot g^1 - t_{n2} \cdot g^1}{\sqrt{2}}$	$g^1 g^2 \left(t_c + \frac{t_{n1} - t_{n2}}{\sqrt{2}}\right)$	$g^1 g^2 \left(t_a + \frac{t_{n1} + t_{n2}}{\sqrt{2}}\right)$

Table 3. Circuit Upper and Lower channel equivalent voltages at numbered stages along the Figure 3 diagram.

t_{n1} and t_{n2} represent the LNA noise temperatures and g_1 and g_2 the LNA and SDR section voltage gains.

Stage 6	Detector Output Voltage, Switch position 1 (s1)	Detector Output Voltage, Switch position 2 (s2)
Upper (u)	s1u $kG_1G_2 \left(T_a + \frac{T_{n1} + T_{n2}}{2}\right) \sqrt{2B_r B_i} + kG_1G_2 \left(T_a + \frac{T_{n1} + T_{n2}}{2}\right) B_r$	s2u $kG_1G_2 \left(T_c + \frac{T_{n1} + T_{n2}}{2}\right) \sqrt{2B_r B_i} + kG_1G_2 \left(T_c + \frac{T_{n1} + T_{n2}}{2}\right) B_r$
Lower (l)	s1l $kG_1G_2 \left(T_c + \frac{T_{n1} + T_{n2}}{2}\right) \sqrt{2B_r B_i} + kG_1G_2 \left(T_c + \frac{T_{n1} + T_{n2}}{2}\right) B_r$	s2l $kG_1G_2 \left(T_a + \frac{T_{n1} + T_{n2}}{2}\right) \sqrt{2B_r B_i} + kG_1G_2 \left(T_a + \frac{T_{n1} + T_{n2}}{2}\right) B_r$

Table 4. Square-law Detector Voltages (AC + DC) Terms

Note: G_1G_2 now refer to component power gains and equivalent temperatures T_a T_c replace T_{ant} and T_{cal} .

Also, 's1' and 's2' refer to the switch position first and second half cycles, 'u' and 'l' refer to the upper and lower receiver channels respectively.

Stage 7	Detector Voltage, Switch1 - delayed upper	Detector Voltage, Switch2 - delayed lower
Upper	s1u $kG_1G_2 (T_a + T_n) \sqrt{2B_r B_i} + kG_1G_2 (T_a + T_n) B_r$	-s1l $-kG_1G_2 (T_c + T_n) \sqrt{2B_r B_i} - kG_1G_2 (T_c + T_n) B_r$
Lower	-s2u $-kG_1G_2 (T_c + T_n) \sqrt{2B_r B_i} - kG_1G_2 (T_c + T_n) B_r$	s2l $kG_1G_2 (T_a + T_n) \sqrt{2B_r B_i} + kG_1G_2 (T_a + T_n) B_r$

Table 5. Swap and Negate Calibration terms - to simplify, noise terms T_{n1} and T_{n2} are assumed equal at T_n

Table 5 swapping and negating these apparently identical half switch cycle detector voltage terms in blue type at Stage 7, ensures that on combining the upper and lower channels, the AC noise terms are de-correlated in time to ensure maximum sensitivity as indicated in Table 6, below.

Stage 8	Output Voltage, Switch 1 output	Output Voltage, Switch 2 output
DC	s1u - s2u = $kG_1G_2 (T_a - T_c) B_r$	s2l - s1l = $kG_1G_2 (T_a - T_c) B_r$
AC	$kG_1G_2 \sqrt{\left(T_a + \frac{T_{n1} + T_{n2}}{2}\right)^2 + \left(T_c + \frac{T_{n1} + T_{n2}}{2}\right)^2} \sqrt{2B_r B_i}$	$kG_1G_2 \sqrt{\left(T_a + \frac{T_{n1} + T_{n2}}{2}\right)^2 + \left(T_c + \frac{T_{n1} + T_{n2}}{2}\right)^2} \sqrt{2B_r B_i}$

Table 6. Final path sum

From Stage 8, Table 6, the integrated source SNR is,

$$\begin{aligned}
 SNR &= \frac{kG_1G_2B_rT_{source}}{kG_1G_2\left[\sqrt{(T_a + T_{sys})^2 + (T_c + T_{sys})^2}\right]\sqrt{2B_rB_i}} \\
 &= \frac{T_{source}\sqrt{B_r/2B_i}}{\sqrt{(T_a + T_{sys})^2 + (T_c + T_{sys})^2}} \quad (9) \\
 &\approx \frac{T_{source}\sqrt{B_r\tau}}{\sqrt{2}(T_a + T_{sys})} \Big|_{T_c=T_a} \\
 \text{where, } T_{sys} &= \frac{T_{n1} + T_{n2}}{2}
 \end{aligned}$$

And the temperature sensitivity is,

$$\Delta T = \frac{\sqrt{(T_a + T_{sys})^2 + (T_c + T_{sys})^2}}{\sqrt{B_r\tau}} \rightarrow \frac{\sqrt{2}(T_a + T_{sys})}{\sqrt{B_r\tau}} \Big|_{T_c \approx T_a} \quad (10)$$

Showing that the optimum sensitivity lies between that of the total power and Dicke receiver types.

Applying the Gain Modulation Factor

A cooled calibrated noise source equal to the antenna temperature is needed to feed the switch port to balance the DC baseline. With typical background temperatures of 10 to 15 K, this may be difficult for amateurs to achieve. An alternative is to employ a second antenna pointing at a quiet area of the sky.

The other option where sensitivity is not an issue, as described for the Dicke radiometer, is to use a standard matched load at ambient or a more convenient cooled temperature and after estimating or measuring the antenna temperature, to derive and weight the calibration measure by the gain modulation factor or R in Stage 8 processing, (as for example, $s1u - R.s2u$ and $s2l - R.s1l$) where,

$$R = \frac{1}{\tau} \sum_{\tau} \frac{s1u + s2l}{s1l + s2u} = \frac{1}{\tau} \sum_{\tau} \frac{T_a + \frac{T_{n1} + T_{n2}}{2}}{T_c + \frac{T_{n1} + T_{n2}}{2}} = \frac{1}{\tau} \sum_{\tau} \frac{T_a + T_{sys}}{T_c + T_{sys}} \Big|_{T_{n1}=T_{n2}=T_{sys}} \quad (11)$$

The function, $\frac{1}{\tau} \sum_{\tau}$ implies the summation or average value over the observation time τ .

As before, with applying the gain modulation factor R , within limits, approaching the optimum sensitivity of Equation 10 is possible.

To illustrate the gain compensation property of the correlation receiver, the DC component of square-law detector outputs (Table 4 above), are now listed assuming unmatched LNA and SDR gains G and G' and the resulting path and switch state responses are presented in Table 7. The four channel/switch components are renamed $s1u$, $s2u$, $s1l$, $s2l$, to indicate switch positions 1 and 2 for the upper and lower receiver channels as referenced to Figure 3.

Stage 6	Detector Voltage, Switch 1	Detector Voltage, Switch 2
Upper	$s1u$ $kG_2 \left(\begin{array}{l} \frac{T_a}{4} (G_1 + G_1' + 2\sqrt{G_1 G_1'}) \\ + \frac{T_c}{4} (G_1 + G_1' - 2\sqrt{G_1 G_1'}) \\ + \frac{G_1 T_{n1} + G_1' T_{n2}}{2} \end{array} \right) B_r$	$s2u$ $kG_2 \left(\begin{array}{l} \frac{T_c}{4} (G_1 + G_1' + 2\sqrt{G_1 G_1'}) \\ + \frac{T_a}{4} (G_1 + G_1' - 2\sqrt{G_1 G_1'}) \\ + \frac{G_1 T_{n1} + G_1' T_{n2}}{2} \end{array} \right) B_r$
Lower	$s1l$ $kG_2' \left(\begin{array}{l} \frac{T_c}{4} (G_1 + G_1' + 2\sqrt{G_1 G_1'}) \\ + \frac{T_a}{4} (G_1 + G_1' - 2\sqrt{G_1 G_1'}) \\ + \frac{G_1 T_{n1} + G_1' T_{n2}}{2} \end{array} \right) B_r$	$s2l$ $kG_2' \left(\begin{array}{l} \frac{T_a}{4} (G_1 + G_1' + 2\sqrt{G_1 G_1'}) \\ + \frac{T_c}{4} (G_1 + G_1' - 2\sqrt{G_1 G_1'}) \\ + \frac{G_1 T_{n1} + G_1' T_{n2}}{2} \end{array} \right) B_r$
Stage 8 Difference	$s1u - s2u$ $kG_2 (T_a - T_c) \sqrt{G_1 G_1'} B_r$	$s2l - s1l$ $kG_2' (T_a - T_c) \sqrt{G_1 G_1'} B_r$

Table 7 Stage 6 Detector Voltages with non-equal path gains (DC terms only)

Using the results of Table 7, the integrated Stage 8 DC output is,

$$k \left(\frac{G_2 + G_2'}{2} \right) (T_a - T_c) \sqrt{G_1 G_1'} B_r \quad (12)$$

showing that both signal and calibration inputs T_a and T_c are equally amplified by both channel gains but there is still some baseline dependence on gain fluctuations if the sky and calibration levels differ.

Applying the gain modulation factor R in post processing (at Stage 8, Tables 6 and 7) is therefore, a necessary process; that is, $(s1u - s2u) \rightarrow (s1u - R.s2u)$ and $(s2l - s1l) \rightarrow (s2l - R.s1l)$.

Part 3. Experimental System

Hydrogen Line Correlation Receiver Breadboard

The receiver test system comprises a quad 22-element Yagi tuned to 1420MHz with a gain of about 23 dB and 13° beamwidth feeding a correlation receiver assembly providing data suitable for investigating all three receiver types described.



Figure 4. Hydrogen Line 22-element Quad Yagi Antenna

The preamplifier/correlation receiver (Figure 5) uses two 90° 3dB couplers from Anaren (1-2GHz type: 10015-3) and two low noise amplifiers (Mini-circuits ZX60-P162LN+) with a transfer switch (Sivers type PM7553) at the output. The couplers may be 90° or 180° types (see Appendix 2 for 90° coupler analysis).



Figure 5. Hybrid LNA Correlation Receiver Section

The first coupler (the blue component to the left of Figure 5) splits the input signals equally between the two similar amplifier channels (Figure 6), whilst the output coupler recombines the amplified signals and splits them to the output ports such that the amplified input signals are isolated and exit different ports. A 50 Ω matched load, represents the ambient level calibration source, feeds one coupler input and the second open input shown is connected to the antenna. Effectively, both calibration and antenna input signals pass through both amplifiers and so are equally affected by any amplifier gain changes so that any subsequent comparison preserves that of the two inputs. Here, the output coupler ports feed a wide-band, electrically operated, mechanical transfer switch.

This first hardware section ideally requires phase tracking low noise amplifiers with equal gain responses. In this case the two Mini-circuits amplifiers were purchased from the same batch and together with equal standard connectors between the couplers, no phase adjustment appeared necessary.

The transfer switch outputs are amplified and interdigital band-filtered in secondary twin channel units (one) shown in Figure 6 that feed a corresponding pair of RTL2832U SDR dongles.

Operation of the transfer switch re-directs the preamplifier output signals to the opposite amplifier chain and SDR dongle. This enables compensation of the two channel amplifier/detection gain differences.

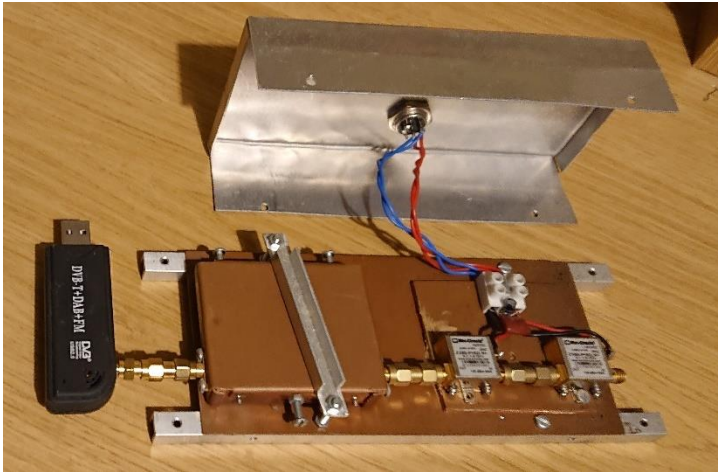


Figure 6. Single Channel of the post Transfer Switch SDR Detection Section

Both SDRs are initiated at nominally the same time to record digitized data for about 50 seconds. With the transfer switch in the crossover position immediately after for a further 50 seconds, the SDRs are again initiated for the same duration to generate a second pair of data files.

To achieve near simultaneous recording, two PC terminal windows, one for each SDR, run a copy of the control software that is set with the desired recording parameters.

Typical control software commands to run two SDRs (-d 0 and -d 1) on a single computer for MS WINDOWS with an RF bandwidth of 2.048 MHz are [5],

```
>RN_RTLAT.exe "./rtl_sdr.exe dat1.bin -f 1420e6 -d 0 -g 49 -n 100e6" 256 14 24 00
>RN_RTLAT.exe "./rtl_sdr.exe dat2.bin -f 1420e6 -d 1 -g 49 -n 100e6" 256 14 24 00
```

These programs are run in the working directory, which must also contain the Osmocom *rtl_sdr* tools.

The RN_RTLAT command programs trigger the start for recording data from both SDRs at 14hr 24m 0s in this example, using the Osmocom *rtl_sdr.exe* program. On collection of 100 million samples at a 2.048 MHz rate in the dat.bin files, the data is then analyzed in 256 point blocks using an FFT algorithm and outputs averaged spectrum text files dat1.txt and dat2.txt.

Operating the transfer switch and resetting the software commands as required, a second set of files dat3.txt and dat4.txt are generated. This is repeated, effectively completing two switch cycles.

Inputting these data text files into Excel or Mathcad software, the data collected is analyzed in Part 4. below.

Experiment Limitations

SDR Synchronizing

Whilst the intention is to trigger the SDRs to start simultaneously with the software described, the PC and RTL recording software do not appear to allow this and delays of 10 to 20 ms are usually observed. However, transfer switching the output data in real time, operating a fast transfer switch normally should ensure data processing synchronism after SDR initiation.

Slow Switch Frequency

In practical systems, the switch cycle frequency would be in the kiloHerz range to ensure tracking of fast $1/f$ and slow gain temperature changes. Although these should be suppressed considerably if the reference calibration noise equals the antenna sky background and pre-first coupler losses/match were compensated. With only two switch cycles of 100 seconds period for the reported data some short term variations could be expected.

Part 4. Evaluation of Receivers

Test Measurements

Two sets of measurements were made at Galactic Latitude 0° , around Galactic Longitude 100° and the spectral responses shown for two transfer switch positions in Figure 7. In this test, the switch was operated for two cycles, each cycle of 100 seconds period and 50% duty cycle. The data spectrum is analyzed over the SDR bandwidth, 2.048 MHz centered on 1420 MHz and presented here in 256 FFT frequency bins.

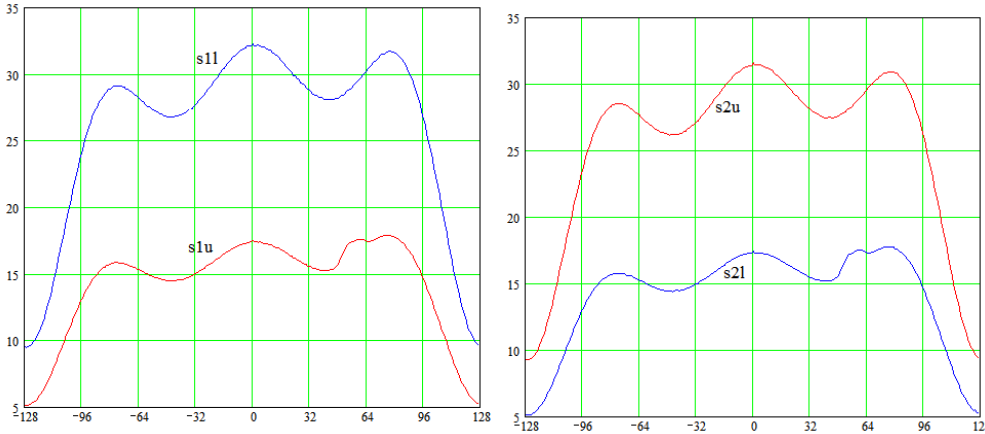


Figure 7 Switch Position 1 (s1) and 2 (s2), Upper (u-red)/Lower (l-blue) Channel Spectra

The plots in Figure 7 exhibit the typical RTL2832U SDR band response shape. As in the schematic in Figure 3, the upper channel is fed from the antenna, and the lower channel records the calibration reference; in this case an RF $50\ \Omega$ matched load at ambient temperature.

The amplitude ratios of these plots can be used to provide a rough calibration of the system as detailed below.

Temperature Calibration

Trx the receiver/LNA noise temperature (0.6 dB NF = 43°K)

$Tcal$ the calibration reference load temperature - 290°K

Tu the unwanted noise components (ambient ground temperature entering the antenna sidelobes)

$Tcon$ the noise loss in the antenna connecting cable (0.1 dB) and antenna mismatch loss (0.5dB) and connector loss, 0.2 dB (0.8 dB $\sim 59^\circ\text{K}$)

Th the hybrid coupler loss (0.25 dB $\sim 17^\circ\text{K}$)

Sky background is assumed equal to 15°K

When switched to the calibration reference input load, the receiver input noise power is proportional to,
 $Tc = Tcal + Th + Trx = 290 + 17 + 43 = 350^\circ\text{K}$

When switched to the antenna, the receiver input noise power is proportional to,
 $Ta = Tsky + Tu + Tcon + Th + Trx = 15 + Tu + 58 + 17 + 43 = 134 + Tu$

From the plots in Figure 7, the base-noise DC ratios $\frac{s2l}{s1l}$ & $\frac{s1u}{s2u} \approx 0.55$, plotted in Figure 8. The baseline differences are indicative of the channel gain drift over the long measurement duration.

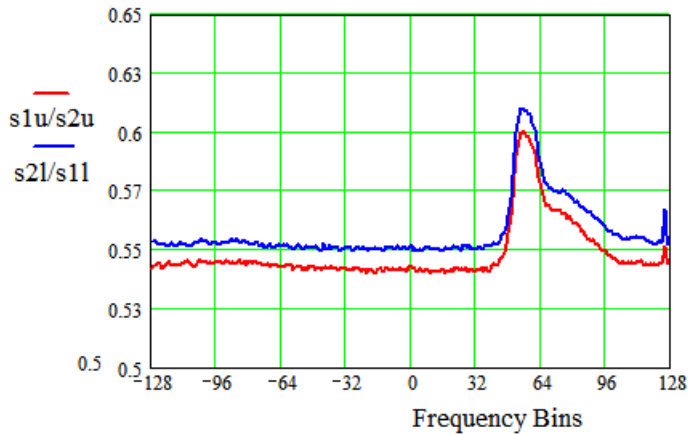


Figure 8. Channel Ratios

Therefore, $Ta = Tc \times 0.55 = 350 \times 0.55 = 193$, so $Tu = 193 - 134 = 59 \text{ }^\circ \text{K}$

This estimate of background noise entering the sidelobes of the Yagi array is not unreasonable, as for the measurements reported, this quad Yagi antenna was sited close to some brick buildings [6].

Total Power Receiver Simulation

The red partial $s1u$ plot in Figure 9 is the result expected for a simple total power spectrum receiver. To recover the hydrogen line response, either the basic SDR response is estimated and subtracted or curve-matching software used to accomplish the same result.

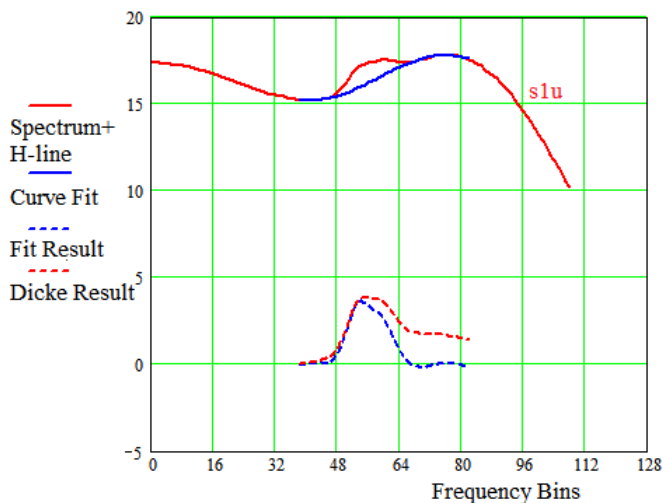


Figure 9 Total Power Spectrum - Data recovered with Simple Sin wave Curve Fit

For example, the blue solid plot in Figure 9 is a simple sine wave, part-band curve-fitting approximation, adjusted by eye to predict the SDR band response. The resulting blue dashed estimate, by subtraction of the H-line response is plotted below. The red dashed plot is the H-line estimate derived from the Dicke receiver simulation. It appears that the weaker frequency hydrogen response is washed out, indicating a potential weakness of this method even though the peak SNR is quite large.

An alternative is to repeat the measurement with the antenna replaced by a matched load to recover the band shape more accurately and either subtract the amplitude weighted plot from the H-line measurement or divide the two data files to produce a ratio plot.

Dicke Switch Simulation

The single channel plots $s1u$ and $s2u$ can be used to demonstrate the operation of the Dicke receiver albeit by accepting a very low switch integration rate. Also, as it is not usually possible for amateurs to use a calibration source as low as the antenna temperature, it is usual to attenuate the load switch-cycle response by means of the gain modulation factor R , to closely match the antenna background level before comparison.

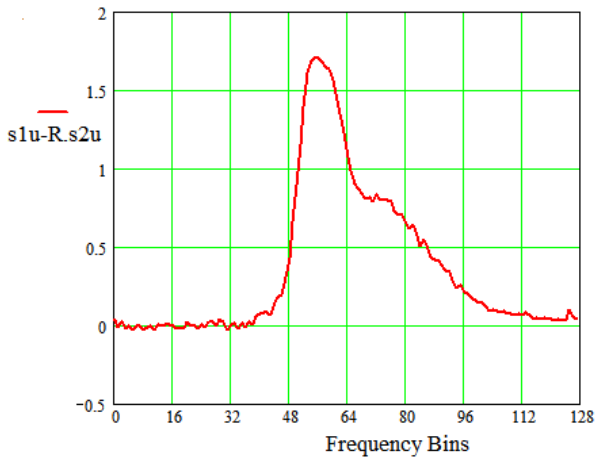


Figure 10. Dicke Switch Receiver Simulation with Gain Modulation Factor Adjustment

The result using a single channel of the pseudo-correlation receiver data is plotted in Figure 10.

The value of $R = 0.546$, calculated from Equation 8, effectively zeroing the plot baseline. This confirms the expected baseline nulling capability of the well-proven Dicke switch radiometer.

Pseudo-Correlation Receiver Result

Figure 11 represents the correlation receiver operation for comparison with the Dicke receiver result of Figure 10. The H-line structure is similar, and a lower level of baseline noise may be recognized. The plot now illustrates the full receiver bandwidth, and it is noticed that the baseline is largely zeroed but there is a slight deviation around bin -85, possibly some low level RFI, as it appeared in both recording cycles.

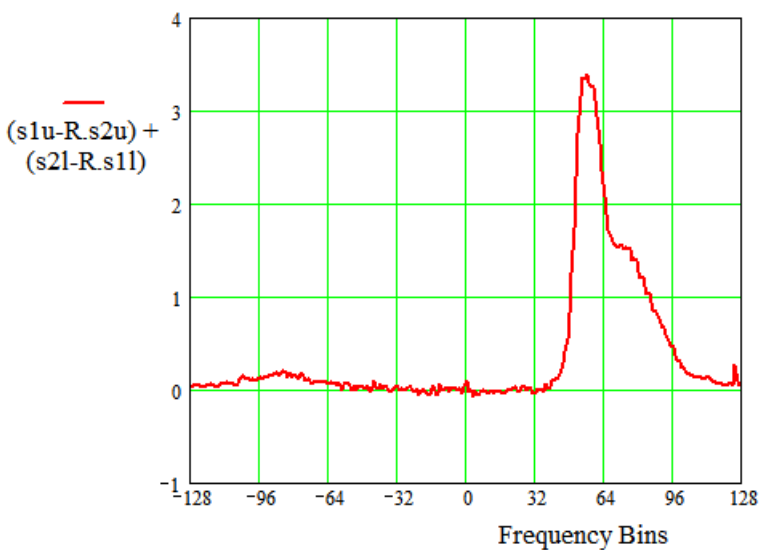


Figure 11. Correlation Receiver Hydrogen Line Spectrum

The small spike at bin zero was a known RTL/FFT artifact and the spike at bin 125, possibly RFI. Both the Dicke and pseudo-correlation receiver operations clearly work well, even with such a simplification using 2 switch cycles with the large 100 second period.

Part 5. Receiver Improvements and Conclusions

Improvements

The main limitation of the experimental pseudo-correlation receiver is the speed of the transfer switch. This mechanical transfer switch is limited in its minimum switching time of 15 ms, whilst the WMAP and PLANCK receivers operate at around 4 kHz and use electronic control to switch the phase shifter, the latter probably requiring operation in tens of nanoseconds.

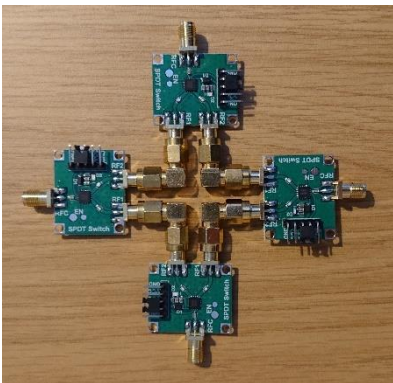


Figure 12. Fast, Wide-band Transfer Switch Option

Here, the mechanical transfer switch can be replaced by four suitable electrically operated single pole double throw (SPDT) switches, such as the Analog Devices HMC849, shown in Figure 12, which operates in RF bands up to 6 GHz with switching times of 150 nanoseconds.

Signals in the East-West ports are directed North-South or the South-North ports in Figure 12 electronically as required. With only 1 dB loss below 2 GHz, these switch devices would also be suitable for Dicke radiometers in H-line studies.

Whilst the use of the RTL2832U SDR is convenient and cheap, there are a number of modern SDRs with flatter band pass characteristics, wider bandwidth, flatter response and better stability and possibly dual phase tracking channels which may be more suitable as the basis of practical radio astronomy receivers.

Conclusions

The pseudo-correlation receiver design and operation has been described and compared to the basic Total Power and Dicke switch radiometers. The Total power receiver is the easiest and most sensitive to implement, but suffers from time/temperature gain variations, $1/f$ noise and difficulty in tracking the baseline variations. The Dicke switch receiver is a little more complicated to implement and drops 3 dB or more in sensitivity because of the 50:50 signal/reference switching and possibly further losses due to the input switch loss. It really requires a calibrated noise reference source to balance the data baseline, but this can be corrected for any reference setting by off-line measurement and applying the gain modulation factor. The pseudo-correlation receiver is further complicated by extra hardware and processing but recovers 1.5 dB of the Dicke sensitivity loss, removes the need for an input RF switch but suffers possibly an extra 0.5 dB loss of the input coupler. This is the preferred receiver concept by professionals requiring very accurately calibrated measurements. The application of the gain modulation factor to zero the DC baseline and 'optimize' the sensitivity equations may have some consequences if the calibrated noise level significantly exceeds the sky background; it also adds a data post-processing requirement. For this comparison exercise, a simpler design variation has been used to collect hydrogen-

line data [7]. If very high sensitivity, data integrity and/or $1/f$ noise is not so important, the switching rates can be reduced to very low levels; as shown with the test measurements used for this paper. Switching periods of a few seconds may be sufficient to cope with turn-on device warm-up, for example. Gain measurements on the experimental receiver show that in the correlation receiver section, the amplifiers in both channels appear to match well in both gain and phase. Isolation in the coupler-coupler section was better than 20dB.

For amateur use, the simplicity and sensitivity offered by the total power receiver type is generally preferred. In this case, the database line can be coarsely adjusted to zero, gain variations controlled by maintaining a constant temperature environment and spectrum frequency response by careful calibration or accurate curve matching. Care needs to be taken with the latter route as some baseline approximations may obscure the weaker target features.

For more serious investigations, Dicke or pseudo-correlation receivers have definite benefits, but for specific targets, some specialized post-processing algorithms may be required to recover source detail and fidelity.

References

1. Dicke, RH., "The Measurement of Thermal Radiation at Microwave Frequencies", Rev. Sci. Instr., Vol 17, 1946, pp268-279.
 2. Harris et al, "Design Considerations for Correlation Radiometers", http://www.astro.umd.edu/~harris/kaband/gbt_memo254.pdf
 3. Mennella et al, "Advanced pseudo-correlation radiometers for the Planck-LFI instrument", <http://www.deepspace.ucsb.edu/wp-content/uploads/2013/02/Advanced-Pseudo-Correlation-Radiometers-for-the-Planck-LFI-Instrument-Proceedings-20031.pdf>
 4. Seiffert M. et al, $1/f$ Noise and other Systematic Effects in the Planck-LFI Radiometers. <https://arxiv.org/abs/astro-ph/0206093>
 5. RTL Data Processing Software. <http://www.y1pwe.co.uk/RAProgs/NewSW.zip>
-
6. East, PW. "Taking the Guesswork out of Antenna Ground and Spillover Noise", SARA Journal Sept/Oct 2024.
 7. East PW. "Low Cost Hydrogen Line Radio Telescope using the RTL SDR - Phase 3", <http://www.y1pwe.co.uk/RAProgs/pdf/HLRrtI3.pdf>
-

Appendix 1. Noise in the Square-law Detector

Band-limited Gaussian noise can be represented by a large set of sinusoidal RF components with random amplitudes and phases of the form,

$$n(t) = \sum_p a_p \cos(2\pi f_p t + \phi_p)$$

where f is within the band B_1 to B_2 , and $B_2 - B_1 = B_r$, and the power is given by,

$$\overline{n^2(t)} = \frac{1}{2} \sum_p a_p^2 = PB_r$$

where, P is the input noise power density (per Hz) in the band B_r and $P = kT$

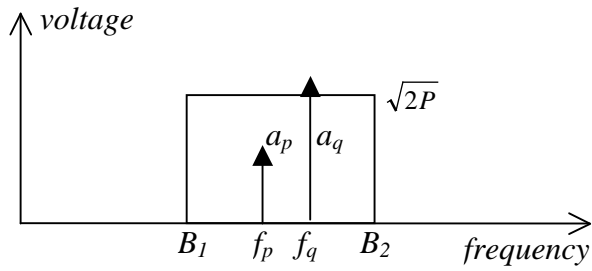


Figure A1.1 Input Noise Representation

The detector squaring output voltage, assuming two random input frequency components labeled p and q , produces both sum and difference frequencies,

$$n^2(t) = \sum_{p=q} a_p^2 \cos^2(2\pi f_p t + \phi_p) + \sum_{p \neq q} \sum_{q \neq p} a_p a_q \cos(2\pi f_p t + \phi_p) \cos(2\pi f_q t + \phi_q)$$

The multiplication function produces low frequency difference terms and sum frequency terms centered on double the band center frequency (see Figure A1.2). In detection analysis, the low frequency terms are of interest and the low frequency detector output is,

$$n^2(t) = \sum_p \frac{a_p^2}{2} + \sum_{p \neq q} \sum_{q \neq p} \frac{a_p a_q}{2} \cos(2\pi (f_p - f_q)t + \phi_p - \phi_q) + \sum_{p \neq q} \sum_{q \neq p} \frac{a_p a_q}{2} \cos(2\pi (f_q - f_p)t + \phi_q - \phi_p)$$

The DC component is the sum of B_r frequencies with total output power $P_{dc} = P^2 B_r^2$.

The low frequency AC terms show that there are two possible components at the same difference frequency, one above f_p and one below f_p . (or at positive and negative frequencies).

For any difference frequency $f_p - f_q = f$, there are $B - f$ instances, so the output power spectrum exhibits a triangular shape as shown in Figure A1.2.

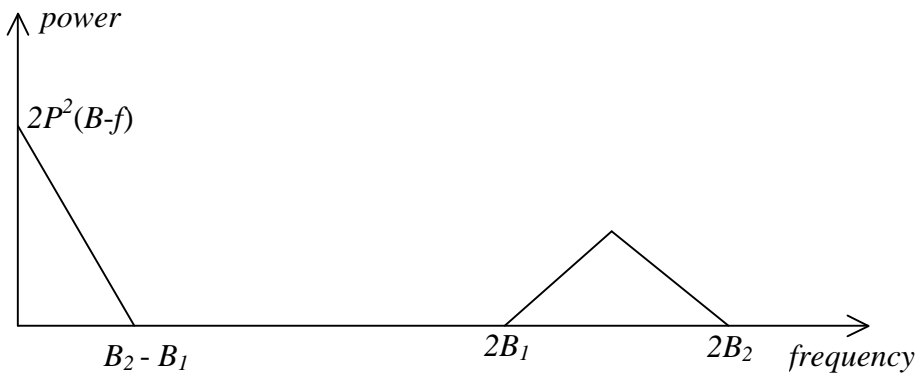


Figure A1.2 Low Frequency Output Noise Spectrum

Following the detector with a low-pass video filter, B_i the video AC power from integrating under the curve is,

$$P_{ac} = 2P^2(B_r B_i - B_i^2 / 2) \rightarrow P_{ac} = 2P^2(B_r B_i) \text{ if } B_i \ll B_r$$

If B_i is much smaller than B_r i.e. long video integration time, τ , the square-law detector AC noise output voltage approximates to, $P\sqrt{2B_r B_i}$. The DC signal-to-noise ratio is,

$$SNR = \frac{PB_r}{P\sqrt{2B_r B_i}} = \sqrt{\frac{B_r}{2B_i}} = \sqrt{B_r \tau}$$

This result agrees with the alternative less descriptive analysis approach of first, deriving the detector noise power output correlation function, applying the Wiener-Kinchine transform to determine the power spectrum and finally, integrating the result over the video bandwidth.

Appendix 2. Correlation Receiver RF Analysis 90° 3dB Couplers

Figure A2.1 shows the correlation receiver with 90° 3dB couplers and the corresponding stage signal voltages. The complex mathematics symbol, j represents 90° phase shift and j^2 , 180° phase shift or signal negation (since, $j^2 = -1$).

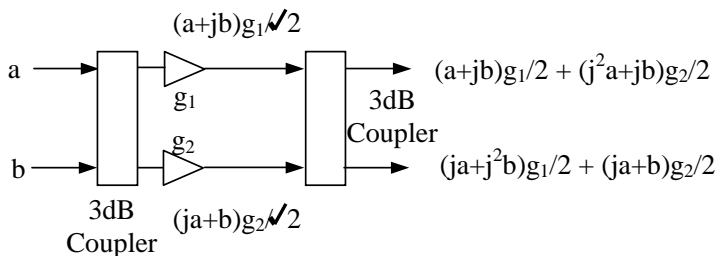


Figure A2.1 Correlation Receiver using 90° 3 dB Couplers

The output signal components simplify to, $a(g_1-g_2)/2 + jb(g_1+g_2)/2$, and $ja(g_1+g_2)/2 + b(g_2-g_1)/2$.

This shows that the signal a appears at the lower output port amplified by the sum of the two amplifier voltage gains, g_1 and g_2 with a 90° phase shift and the b signal exits the upper output port similarly phase shifted. Suppression of the opposing input depends on both the phase and gain match of the amplifiers.

As for the 180° coupler version analyzed in the main body, there are similar error components should the amplifier gains be unequal.

PW East March 2025



Peter East, pe@y1pwe.co.uk is retired from a Defense Electronics career in radar and electronic warfare system design. He has authored a book on Microwave System Design Tools, is a member of the British Astronomical Association since the mid '70s and joined SARA in 2013. He has had a lifelong interest in radio astronomy; presently active in amateur detection of pulsars using SDRs and researching low SNR pulsar recognition and analysis. He has recently written another book, 'Galactic Hydrogen and Pulsars - an Amateurs Radio Astronomy' describing his work in Radio Astronomy.

He maintains an active RA website at <http://www.y1pwe.co.uk>

HAARP Riometer Observations ~ 17 March 2025

Whitham D. Reeve



Introduction: The *Relative Ionospheric Opacity Meter*, or Riometer, is a very stable receiver and antenna system used to measure radio wave absorption in the D-region of the terrestrial ionosphere. The signal source for the Riometer is the Galactic synchrotron radiation that pervades the Milky Way Galaxy (figure 1). The Riometer frequency is set far above the ionosphere's E- and F-region critical frequencies so that any decrease in the received Galactic background radiation is attributed to D-region absorption. The measured absorption at the Riometer frequency may then be translated to other frequencies of interest using empirically derived formulas.

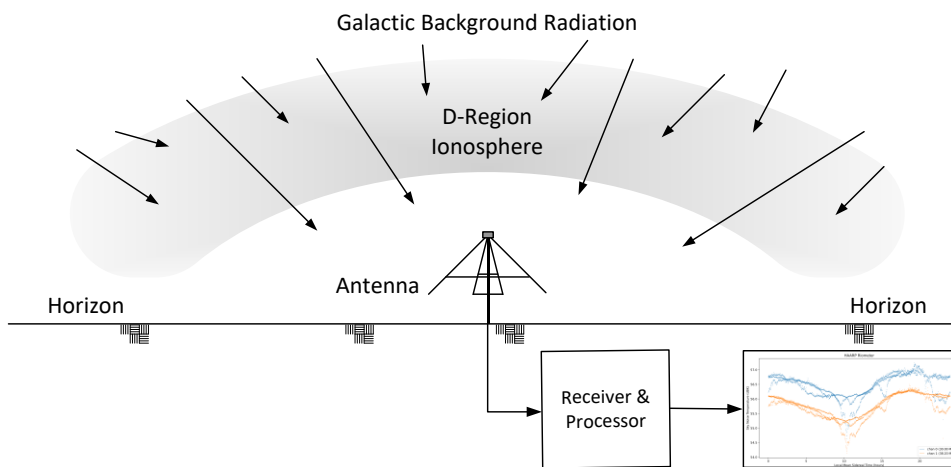


Figure 1 ~ The ever-present Galactic background radiation received on the ground follows a consistent pattern throughout each day when the ionosphere is quiet. When the ionosphere is disturbed, the absorption increases in the D-region and is seen as a reduction in the received power compared to a quiet day.

A new Riometer was commissioned at the HAARP facility in Alaska in January of 2025 and its data is the basis for this article. The new Riometer is one of several diagnostic instruments located near the *Ionospheric Research Instrument* (IRI) at the HAARP facility. It complements the existing ionosonde, which is a diagnostic instrument used to determine the critical frequencies for heating experiments in the ionosphere's E- and F-regions. However, D-region absorption often prevents the ionosonde from determining the upper region critical frequencies, so the Riometer is used to determine when those conditions occur and what changes to an experiment are necessary.

Absorption: D-region absorption has three primary causes, which depend somewhat on the latitude. At lower latitudes ($< 60^\circ$ magnetic) solar flare radiation can deeply penetrate Earth's atmosphere and reach the ionosphere's D-region, causing a sudden increase in electron density and the possibility of electron collisions with neutral atmospheric particles. The higher collision rate leads directly to a significant and rapid increase in the amount of absorption. Absorption from solar flares is a daytime phenomenon.

Absorption caused by solar flares at higher latitudes ($\geq 60^\circ$ magnetic) does occur but is less frequent than at lower latitudes because the flare radiation penetrates the atmosphere obliquely, losing its energy as it travels farther to the D-region. HAARP's magnetic latitude is 63° north and, depending on magnetic conditions, it sits near the southern edge or directly below the *Auroral Oval*. The Auroral Oval is the donut shaped region at high latitudes that marks the footprints of magnetic field lines where aurora and other electromagnetic phenomena are produced.

Absorption at higher latitudes is more commonly from two sources of *particle precipitation*. In general, precipitation patterns are controlled by Earth's magnetic field and the sources of the particles (figure 2). These phenomena can produce absorption during the day or night:

- ⚙ **Solar Energetic Particles (SEP).** SEPs, mostly protons, are associated with particularly strong solar flares. The highly energetic protons, travelling at fractions of light speed, are able to enter the magnetosphere where they become trapped by Earth's densely packed magnetic field lines whose footprints map to Earth's polar cap. As the protons spiral down the magnetic field lines (precipitate), they collide with atmospheric molecules and atoms in the D-region, which increases the ionization. The electrons are excited by radio waves, in this case the sky noise, and have a higher probability of collisions and, thus, absorption. This phenomenon ordinarily occurs within roughly 20° latitude of the magnetic poles and so is called *Polar Cap Absorption (PCA)*. However, during magnetically disturbed periods, the protons may precipitate into the Auroral Oval. PCA events are indicated on the D-Region Absorption Prediction (D-RAP) plots posted by NOAA at: <https://www.swpc.noaa.gov/products/d-region-absorption-predictions-d-rap> ;
- ⚙ **Magnetic disturbance.** If the Interplanetary Magnetic Field (IMF), which is blown by the solar wind, has a southward component, it is able to merge with Earth's magnetic field and cause a magnetic disturbance. Energetic electrons in the solar wind, enhanced by a coronal hole high-speed stream (CHSS) or coronal mass ejection (CME), are able to enter the magnetosphere where they are trapped by the terrestrial magnetic field lines marked by the Auroral Oval. A related source of energetic electrons is the magnetotail. The electrons are temporarily stored there, and the process of reconnection in the magnetotail, related to a previous merging event on the Sunward side, convects them toward Earth where they precipitate along the magnetic field lines marked by the Auroral Oval. The precipitating electrons collide with neutral atmospheric particles, increasing the ionization and the likelihood of further collisions and absorption. This cause of absorption is far more common at higher latitudes than any other.

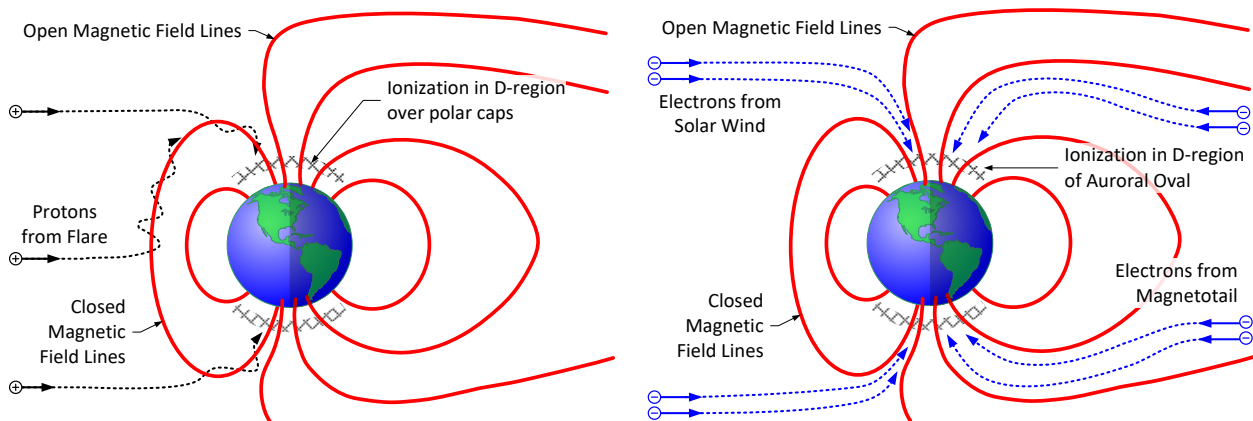


Figure 2 ~ Energetic particle precipitation. Left: Protons accelerated by a strong solar flare reach Earth in minutes to hours where they are trapped by closed magnetic field lines; Right: Energetic electrons from coronal hole high-speed streams or coronal mass ejections reach Earth days after leaving the Sun. They enter the magnetosphere along open magnetic field lines during a magnetic disturbance or are convected along field lines during reconnection in the magnetotail.

Events of 17 March: Even though there is a lower likelihood of solar flare effects on absorption at higher latitudes, two solar x-ray flares (table 1) occurred during the local morning and afternoon on 17 March, both of which led to absorption events in the D-region above the HAARP facility. Coincidentally, these events occurred only three days before the Spring (Vernal) Equinox when the Sun is directly above the equator.

Table 1 ~ Flares relevant to absorption events on 17 March. Times are UTC.

Type	Begin	Max	End	Magnitude	Data source: Space Weather Prediction Center Events Report: ftp://ftp.swpc.noaa.gov/pub/indices/events/
X-Ray	1545	1604	1614	C6.6	
X-Ray	1925	1933	1940	M1.0	

Particle precipitation related to a magnetic disturbance, specifically a magnetic bay (decrease in the local magnetic field flux density), caused absorption that preceded the solar flares. The absorption of Galactic background radiation caused by particle precipitation reached a maximum at about 1430 while the bay reached a minimum field intensity at about 1500.

The first flare peaked at 1604. The associated absorption was signified by a relatively sharp decrease similar to the preceding precipitation event. The second flare peaked at 1933 and caused a somewhat broad double-dip decrease in the received Galactic background radiation. Figure 3 shows the Riometer data from 17 March overlaid with the x-ray flux measured by the GOES spacecraft (<https://www.swpc.noaa.gov/products/goes-x-ray-flux>) and the local magnetic flux density measured by the HAARP SAM-III magnetometer (https://reeve.com/SAM/SAM-HAARP/SAM-HAARP_simple.html).

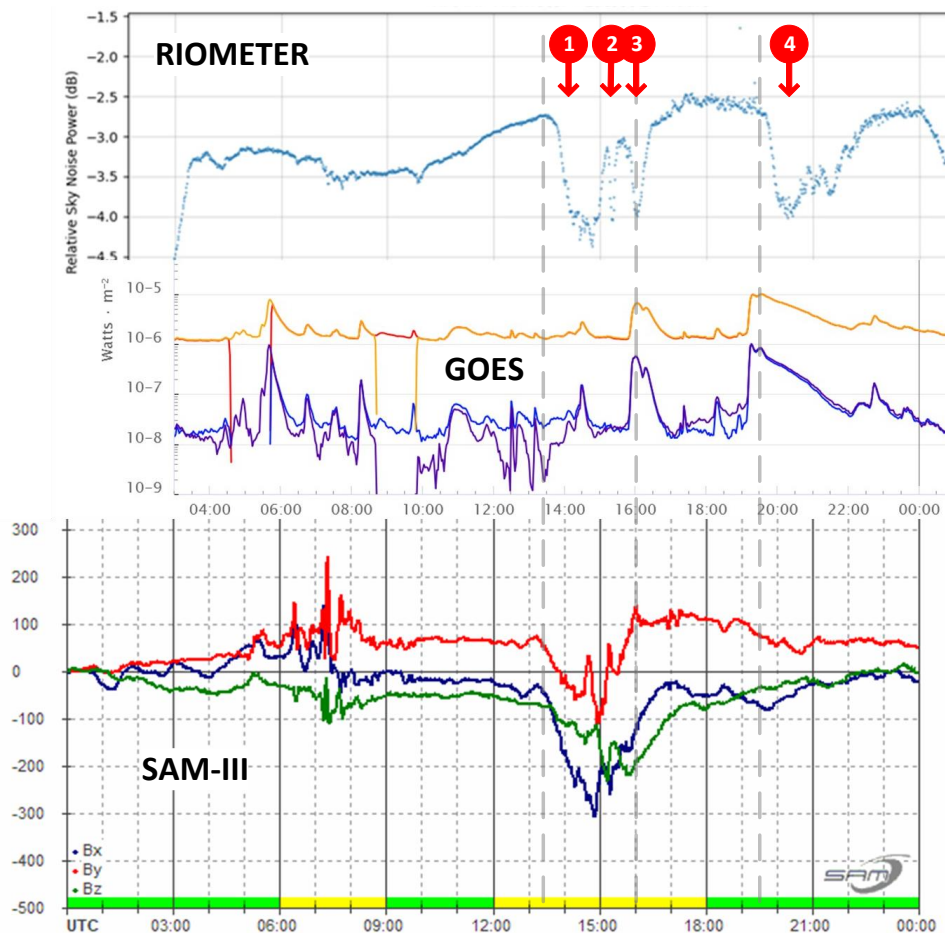


Figure 3 ~ Overlaid plots from 17 March with the same time scale. See text for explanations of each trace and time lines.

The upper (light-blue) trace is the HAARP Riometer 30.3 MHz receiver channel. The plot does not include a quiet day curve, which normally would be used to establish relative received power levels when no absorption is present. The trace shows the ratio of received sky noise to the Riometer’s internal reference noise source in dB.

Directly below the Riometer trace are the x-ray flux plots from the two GOES spacecraft. Shown are the GOES short wavelength channel (0.5 to 4 Å, blue traces) and long wavelength channel (1 to 8 Å, orange traces). Below the GOES plots is the magnetogram from the local SAM-III magnetometer located about 2.3 km southeast of the Riometer. The three magnetic field components are: Bx (north-south, red trace); By (east-west, blue trace); Bz (vertical, green trace).

The gray vertical dashed lines mark the following UTC epochs:

- ⚙ 1320: Beginning of magnetic bay that reached approximately -300 nT at 1500. The first significant absorption event ❶, dipping about 1.25 dB at 30.3 MHz and lasting 1.5 hours, started only a few minutes into the bay. It was followed at 1500 by a second absorption event ❷, a sharp 0.9 dB decrease lasting about 15 minutes. The second event appears to be related to magnetic fluctuations within the bay;
- ⚙ 1604: Peak of C6.6 x-ray flare. The third absorption event ❸, about 1 dB at 1600, correlates well with this flare. Note that the flare flux required about 1 hour to decay to the background level while the received sky noise recovered much faster.
- ⚙ 1933: Peak of M1.0 x-ray flare. The fourth absorption event ❹, almost 1.5 dB, correlates well with this flare and is much broader than the previous event. Also, unlike the previous event, the absorption recovered at about the same rate as the flare flux.

Instrumentation:

- ⚙ Riometer with LWA Antenna, 2-channel, 30.3 MHz & 38.2 MHz, Keo Scientific, Calgary, Alberta, Canada
- ⚙ SAM-III Magnetometer, 3-axis, Reeve Engineers, Anchorage, Alaska USA
- ⚙ GOES (Geostationary Operational Environmental Satellite), NOAA, <https://www.goes-r.gov/>

Does adding WTMicrowave Chinese Hydrogen Cavity Filter improve hydrogen signal detection over Nooelec SAWBird H1 Low Noise Amplifier Alone?

Dr Andrew Thornett, M6THO, Lichfield Radio Observatory, Lichfield, UK www.astronomy.me.uk

The need for effective filtering of the hydrogen signal for Milky Way galactic mapping.

The availability of cheap and effective off the shelf antennae from companies such as Nooelec and software defined radios (SDRs) and instructions in the SARA “Scope in the Box” project have led to a need for effective filtering of received radio signals to isolate the hydrogen band, and a small range around it to incorporate Doppler shifted signal, for processing using software such as Easy Radio Astronomy Suite (ezRA).

The Milky Way is composed mostly of hydrogen and, therefore, mapping of galactic arms and Doppler shift calculations are best done using the frequency for hydrogen (1420.405MHz). Unfortunately, this area of the electromagnetic spectrum is subject to quite a lot of radio interference in many of the areas in which we live, a situation made worse as more houses are built and increased use of electronic devices in the modern home.

Nooelec SAWBird H1 LNA

Many amateur radio astronomers use the Nooelec SAWBird H1 low noise amplifier (LNA) to achieve this filtering (<https://www.nooelec.com/store/sdr/sdr-addons/sawbird.html>), available for \$44.95 at the time of writing of this article on amazon.com (<https://www.amazon.com/Nooelec-SAWbird-H1-Applications-Frequency/dp/B07XPV9RX2>). The SAW filter in this device provides significant attenuation at +/- 30 MHz either side of 1420 MHz and also provides a dual cascaded low noise amplifier within a small compact unit.

Cavity Filters

Some observers recommend the addition of a cavity filter before the SAWBird to improve attenuation of out of band signals. However, a cavity filter also introduces some additional attenuation within band. This current paper explores the effect of adding in a cavity filter to a radio telescope already containing a Nooelec SAWBird H1 low noise amplifier on signal detection, in order to determine whether such an addition is beneficial.

Cavity Filters are a type of radio frequency (RF) filter used in communication systems to filter out noise and select signals at specific frequencies. They are typically composed of one or more hollow metal cavities containing conductor structures (www.temwell.com/en/pages/what-is-cavity-filter).

Cavity Filters operate using resonance. They contain a resonator with a tuning screw (to fine-tune the frequency) inside a conducting box. An RF or microwave resonator is a closed metallic structure (i.e., waveguides with both ends terminated in a short circuit). The resonator oscillates with higher amplitude at a specific set of frequencies, called resonant frequencies. When an RF signal passes through the cavity filter, a resonator acts as a band-pass filter and passes RF signals at specific resonant frequencies while blocking other nearby non-resonant frequencies. The resonant frequency of the cavity resonator depends on its dimension (length, width, height), mode number, dielectric constant (ϵ_r), and magnetic permeability (μ_r) of the material of construction. In a cavity filter, the resonator is fitted with a screw to tune the frequency range which allows to modify the physical length (inner space length) of the resonator as well as its capacitance to the ground, hence tuning the resonant frequency. Cavity filters are used in the MHz/GHz frequency range. They provide high Q-factor (i.e., high-selectivity/sharply attenuates the unwanted signals), low insertion loss, and robust

temperature stability when compared to other forms of filters commonly used in amateur radio astronomy. These advantages make cavity filters ideal for use in microwave and millimetre-wave systems, particularly in professional systems, which need filters with high-Q factor, lower insertion loss, and temperature stability. Advantages of cavity filters: (1) High Q-factor (up to the order of 10⁶), low insertion loss, and robust temperature stability. (2) Superior selectivity and good frequency stability. (3) Reduces the transmitter sideband noise and protects receivers against desensitization. (4) Better performance in microwave range (including 1420MHz that we use for hydrogen detection) when compared to other common forms of filter (<https://www.everythingrf.com/community/what-are-cavity-filters>).

Traditionally, amateur radio astronomers have had to make their own cavity filters if they wished to use one, a labour-intensive exercise requiring some skill and a lot of fiddling and ideally additional expensive equipment to tune the filter accurately. Commercial versions have been very expensive, limiting their use to professional observatories. However, like most areas of technology, new ranges of these devices have become available from China at much more competitive prices, which remain very low even with the new tariffs currently being introduced in the USA for imports from China. These new models provide an opportunity to consider these filters for amateur applications, in a way that was not possible previously.

In the current study, I used a cavity filters covering the hydrogen band, made by WTMicrowave (www.wtmicrowave.com), based in China. The company is also prepared to produce custom-designed filters, should amateurs have a need for them. Prices for the filter discussed in this article are around \$150 each plus carriage. The filter used is the WT-A9940-Q08 cavity filter. which is designed to cover 1400-1427 MHz and gives up to 69 dB attenuation either side of this. This gives a range of -20 MHz to +7 MHz from 1420 MHz, an improvement over the +/-30 MHz of the Nooelec SAWBird H1 LNA.

WTMicrowave WT-A9940-Q08 cavity filter 1400-1427 MHz (below):

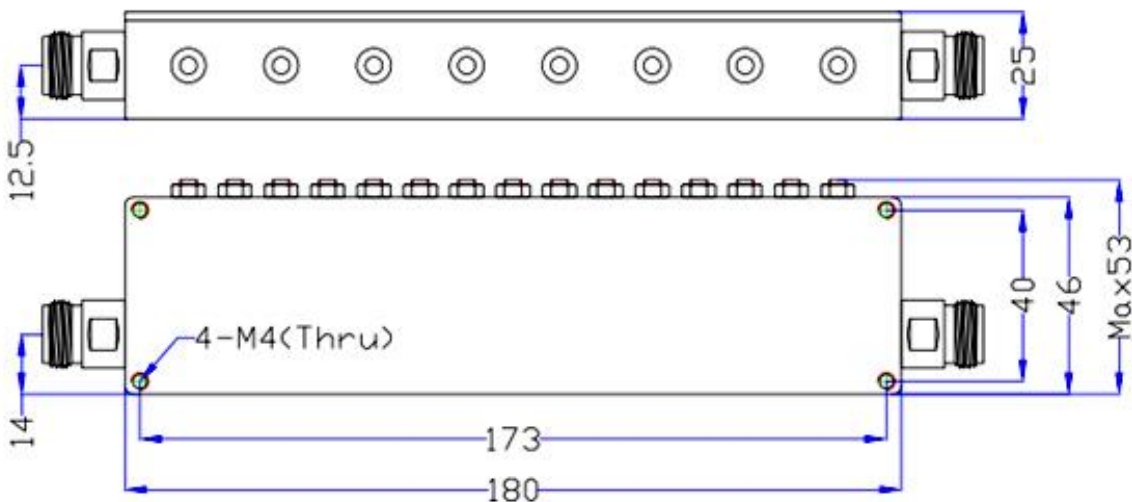


This cavity filter has N-type connectors at either end, so adapters are required to use with cables terminated with SMA connectors commonly used in amateur radio astronomy stations where software-defined radios are usually used, or the connector needs to be changed on the cable. Those users who control their systems with an amateur radio transceiver should be able to directly connect to the filter.

Specifications of the WT-A9940-Q08 cavity filter (below):

S/N	Item	Parameters
1	Center Frequency(F0)	1413.5MHz
2	Pass Band Frequency	1400 ~ 1427MHz **
3	Pass Band Insertion Loss	≤1.5dB
4	Pass Band Ripple	≤0.6dB
5	Pass Band Return Loss	≥23dB
6	Stop Band Rejection	≥50dB @ DC ~ 1375MHz ≥50dB @ 1452 ~ 3500MHz
7	Impedance	50 Ohms
8	Power Handling	200W Max.
9	Connectors	N-Female
10	Surface Finish	Painted Black
11	Temperature Range	-30°C ~ +70°C
12	Material	Housing: 6061 Aluminum alloy Resonant column: H59 Copper alloy Cover: LY12 Aluminum alloy Connectors: H59 Copper, Plated ternary alloy Tuning screw: H62 Copper alloy Other screw: Stainless Steel
13	Dimensions	180*46*25mm
14	Net weight	0.374 KG

Outline Drawing of the WT-A9940-Q08 Cavity Filter (below, dimensions units: mm, dimension tolerance +/- 0.5mm):

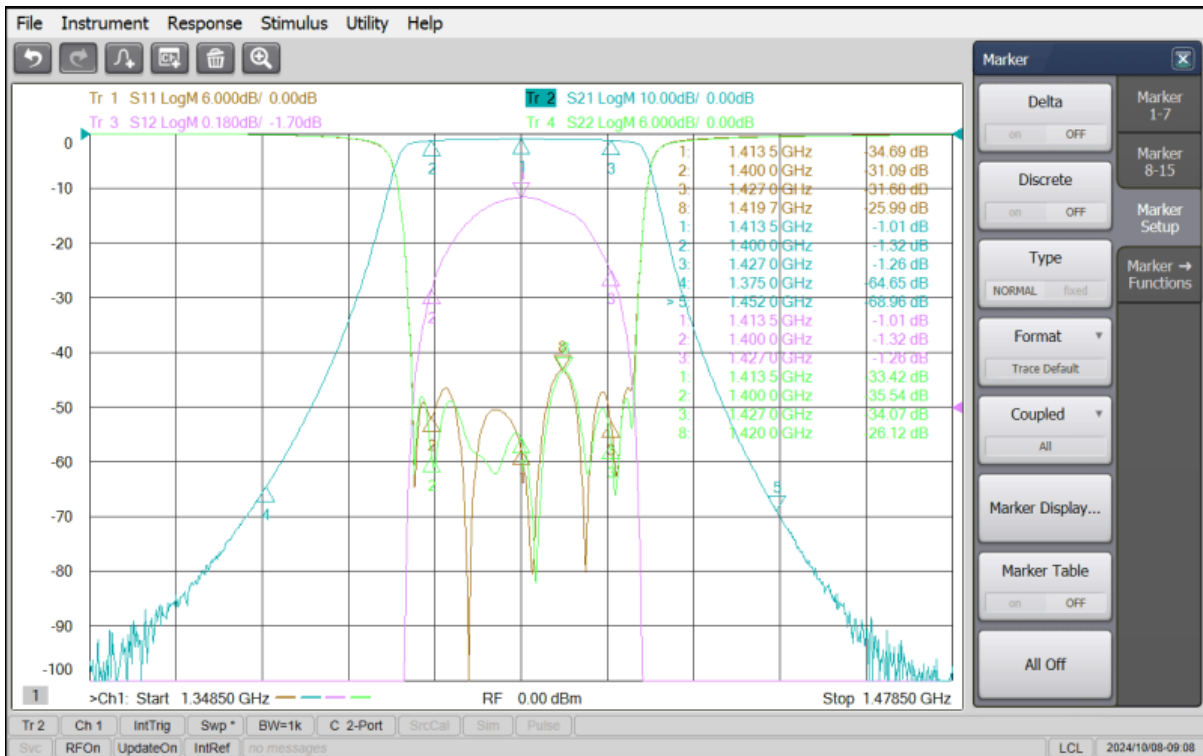


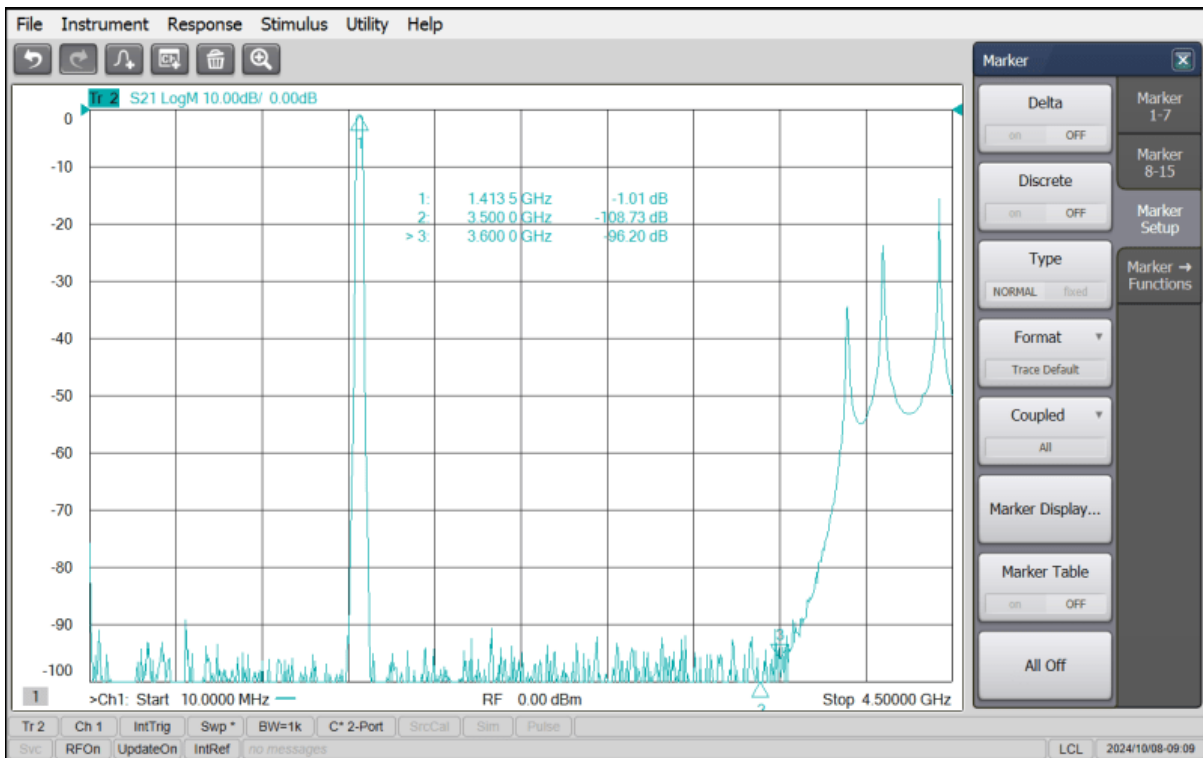
** The actual design bandwidth will be greater than the Pass Band Frequency, and there is no bandwidth limit.

The plots below show test report and curves for an example of these filters that I have been sent by the company (below).

Product Inspection Records

Model	WT-A9940-Q08	Item	Cavity Band Pass Filter	Quantity	3pcs		
Test Data							
Appearance	Major Parameter				Other Parameter		
	Pass Band 1400 ~ 1427MHz F0=1413.5MHz			Stop Band		Connectors	Surface Finish
Reference value	Insertion Loss	Ripple	Return Loss	DC ~ 1375MHz	1452 ~ 3500MHz	N-Female	Painted Black
S/N	<1.5dB	<0.6dB	≥23dB	≥50dB	≥50dB		
1	1.32	0.31	25.9	64	69	N-Female	Painted Black
2	1.29	0.27	27.2	63	69		
3	1.33	0.31	27.1	66	71		
Verdict:		Inspection way: Full inspection			Data recording mode: Full record		
Test Equipment: N5227B		Date: 2024-10-08		Tester: Liqiong Yong		Check: Xiaotao Yang	

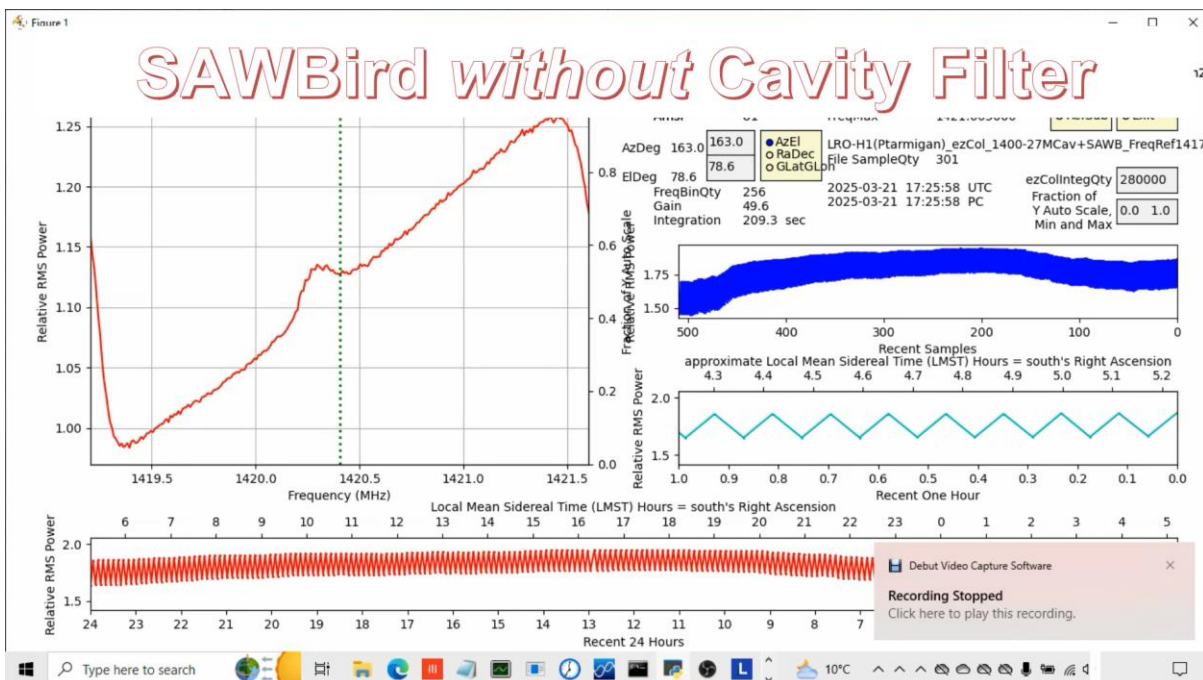




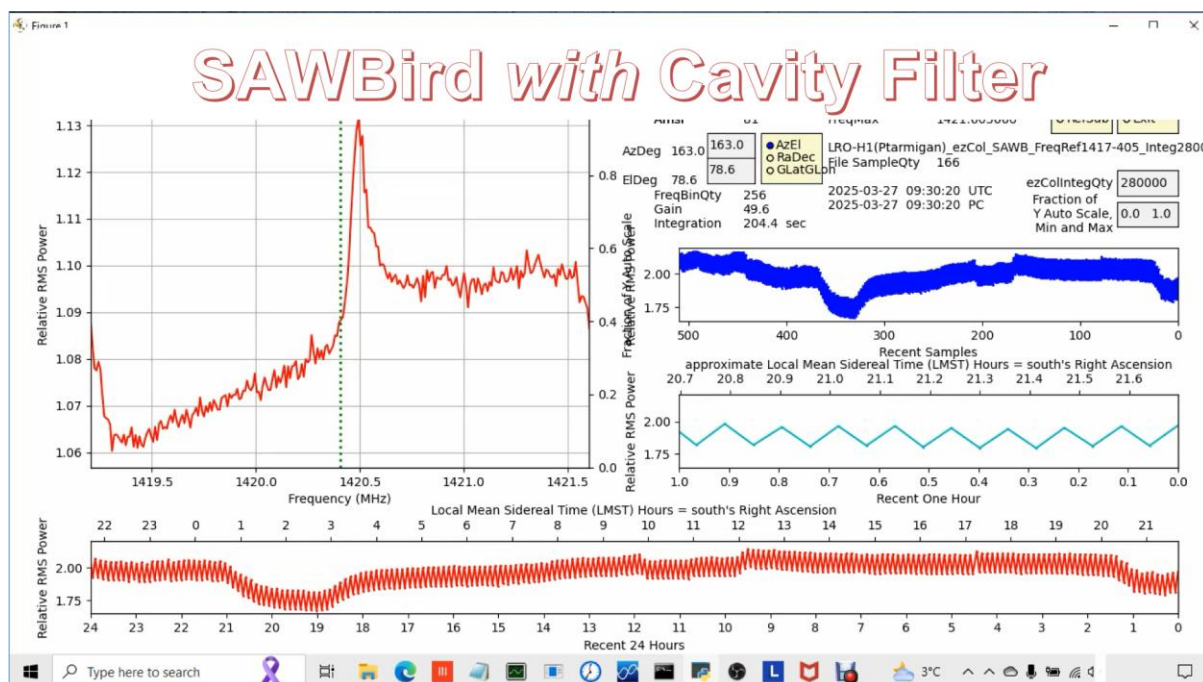
Comparison of results from processing LRO-H1(Ptarmigan Array Data) collected by ezCol.py (ezRA software suite) with three filter arrangements 1st to 12th January 2025.

I have installed the cavity filter in line before the SAWBird H1 on the Lichfield Radio Observatory LRO-H1 radio telescope (based on an ex-military Ptarmigan dipole array), located in Lichfield, UK (www.astronomy.me.uk), just north of Birmingham in the centre of England.

Maximum signal detection with cavity filter and SAWBird H1 LNA (ezCol.py from Easy Radio Astronomy (ezRA) <https://github.com/tedblue/ezRA>)



Maximum signal detection with SAWBird H1 LNA alone (ezCol.py from Easy Radio Astronomy (ezRA))
<https://github.com/tedcline/ezRA>:



Conclusion:

Adding the cavity filter dramatically reduces the level signal level, and reduces signal to noise ratio, suggesting that Nooelec SAWBird H1 LNA alone is more effective as method of collecting hydrogen line data for mapping Milky Way than SAWBird plus cavity filter.

Further information.

Further information about this project is available on the www.astronomy.me.uk website or by contacting me using the "contact us" page on that website.

Plotting of interpolated velocity against galactic longitude in 3D for large data set at Lichfield Radio Astronomy (LRO-H1 Data from Second Lichfield Radio Astronomy Milky way Map) using new functionality in Easy Radio Astronomy Software Suite (ezRA).

Andrew Thornett, M6THO, Lichfield Radio Observatory, Lichfield, UK www.astronomy.me.uk

The Lichfield LRO H1 Radio Telescope.

Lichfield Radio Observatory (LRO) is located at latitude 52.6815 north, longitude -1.8255 (1.8255 west) in Staffordshire, central England, UK, roughly 16 mi (26 km) north of Birmingham. The LRO H1 Radio Telescope is composed of a Ptarmigan Triffid ex-military 4x4 dipole array, measuring 86cm x 86cm in size. Filtering is two-stage using a 1400-1427MHz cavity filter, followed by a Nooelec SAWBird H1 LNA/filter. The system uses an RTL-SDR Blog V3 Software Defined Radio and data for this paper was recorded using Easy Radio Astronomy Software Suite (ezRA; Ted Cline; <https://github.com/tedcline/ezRA>).

The telescope is mounted on a simple wooden mount that allows variation in elevation. It points at the same azimuth constantly – data is collected using 24-hour drift scans which allow individual azimuth points to be calculated by the software during the sidereal day.

The Second Lichfield Radio Astronomy Milky Way Map.

The plots below are based on a substantial data set collected using the LRO-H1 Ptarmigan 86cm x 86cm 4 x 4 Dipole Array between 6 January 2024 and 1 November 2024, which constitutes the Second Lichfield Radio Astronomy Map of the Milky Way Radial Arms.

The data is comprised of 276 ezRA .txt data files, each covering a 24-hour period. Individual data points are the result of integration of data in Easy Radio Astronomy over 15 seconds which, on this particular telescope, equates to integration 31,000 in ezRA (number of samples in given time period varies depending on the computer speed/RAM/hard disc type/etc.)

A new script in Easy Radio Astronomy Suite (ezRA) to enable 3D plotting of interpolated velocity against galactic longitude.

Ted Cline's free Easy Radio Astronomy Suite (ezRA, <https://github.com/tedcline/ezRA>) is a popular option for collecting a processing Milky Way hydrogen line data. Many of us have large data sets available which will benefit from a new method of presenting this data. Rinearn 3D is another free software package, which can be used to present the data in a more accessible picture form.

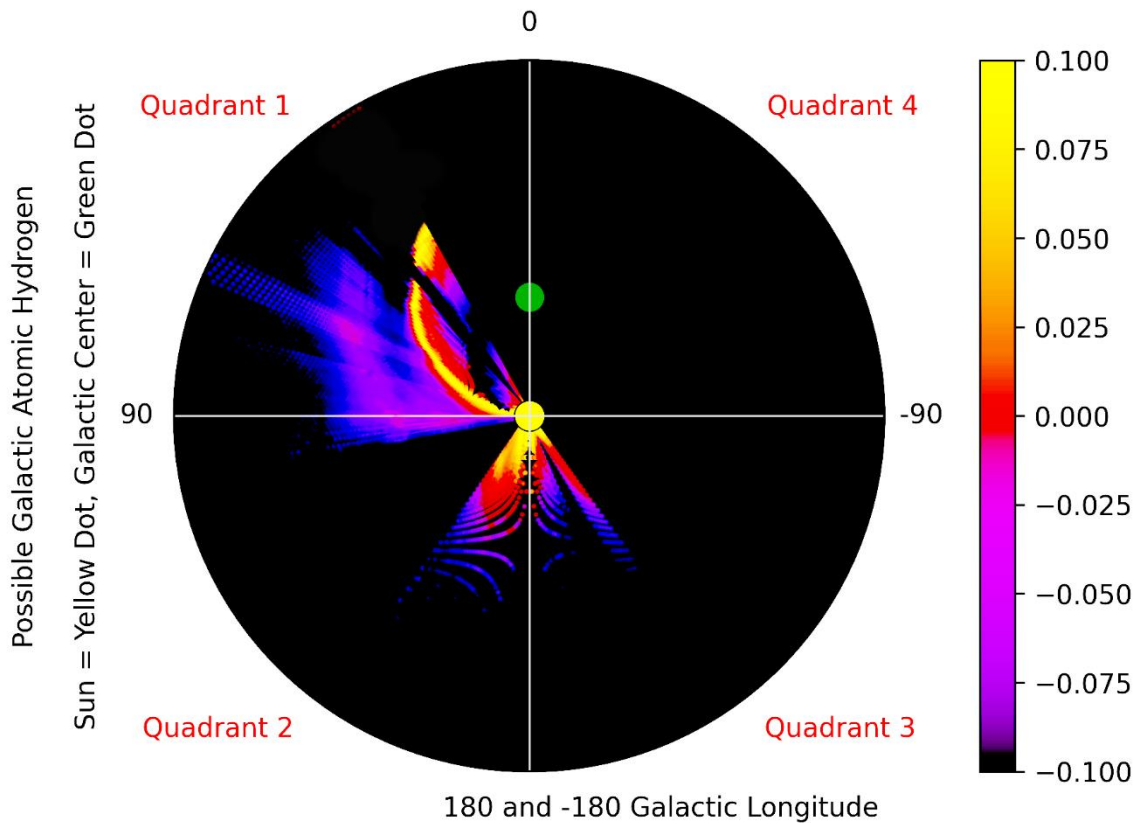
The plot produced by ezCon.py called ezCon510velGLon.png presents in two dimensions interpolated velocity against galactic longitude.

There is now a new ezRA script available for ezRA (**ezGal250118e.py**) which will process NPZ/EZB files created via the ezCon.py script to produce a CSV file, ezGal510velGLonMsh.csv, capable of being processed in Rinearn 3D. These 3 dimensions plotted in Rinearn3D as a result of this process include galactic longitude, interpolated velocity, intensity reading for each interpolated velocity point.

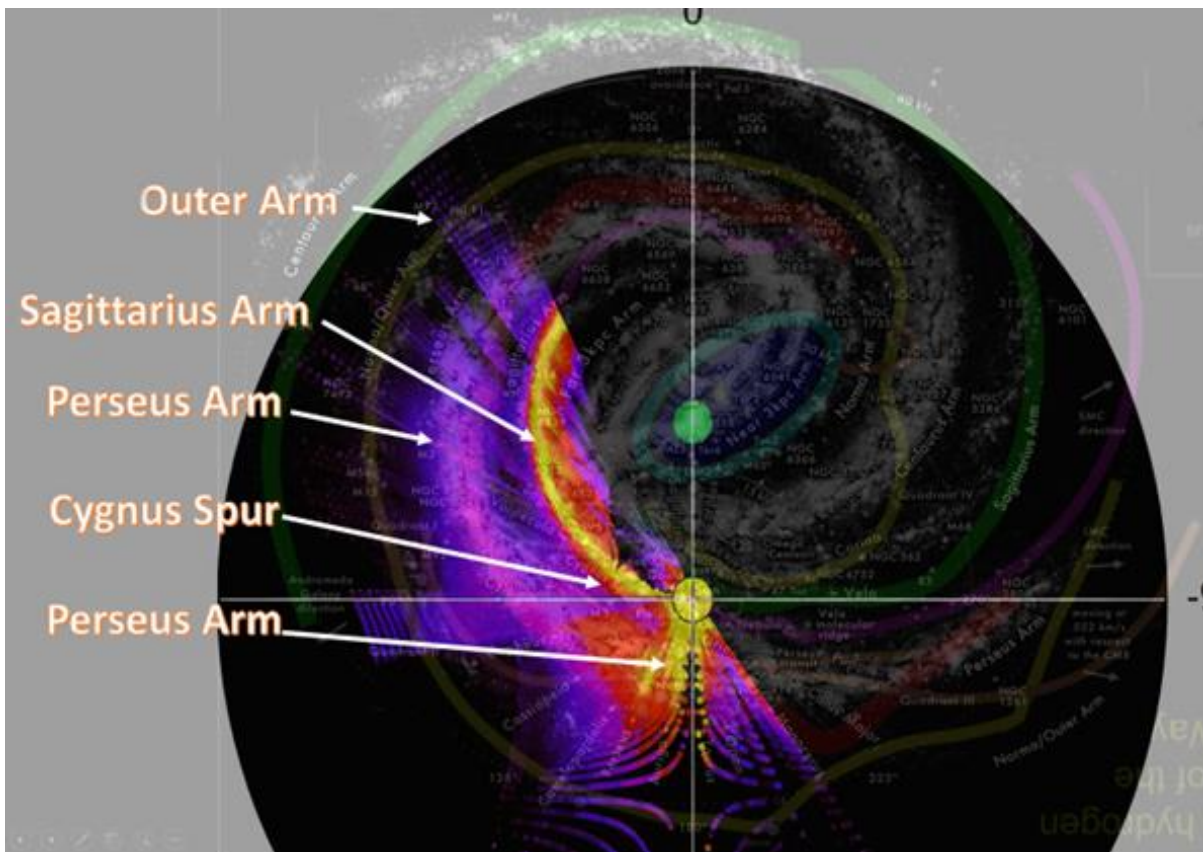
Results

The results from this new script and plotting within Rinearn3D are presented below. The 3D plots of interpolated velocity give a more accessible method of visualizing the difference in velocity at different parts of the Milky Way. Understanding this plot is inherently difficult as the concepts it embodies are alien to many people who have little experience in radio astronomy, even if they have considerable experience in other aspects of astronomy such as visual observing or astrophotography. Any method of improving access to the data is valuable to us as we explain our findings in talks, articles and outreach to these communities.

2D map in ezRA ezCon.py of Milky Way from the same data set for comparison with the 3D plots from Rinearn3D:

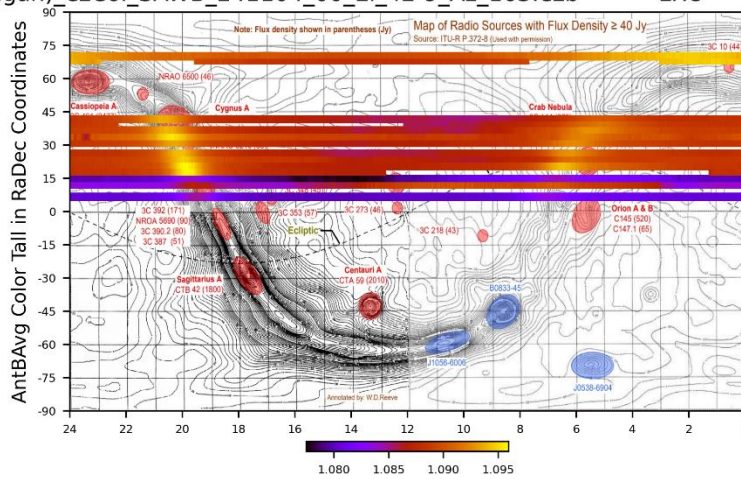


Features of the structure of the galactic arms of the Milky Way above labelled in plot below:

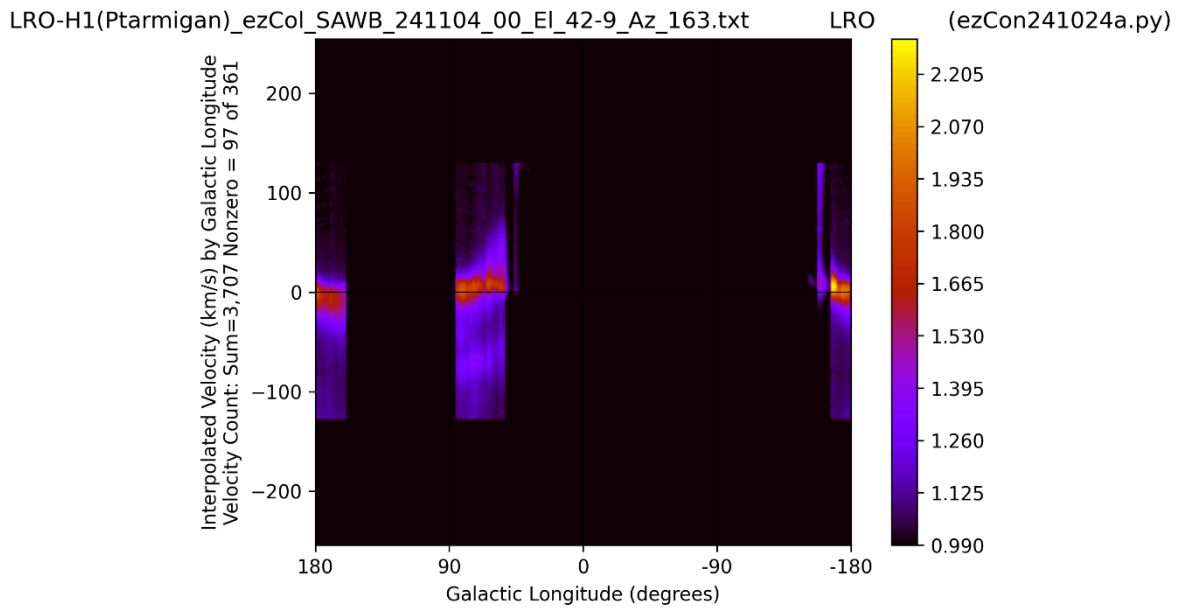


Parts of Milky Way covered in drift scans making up this data set:

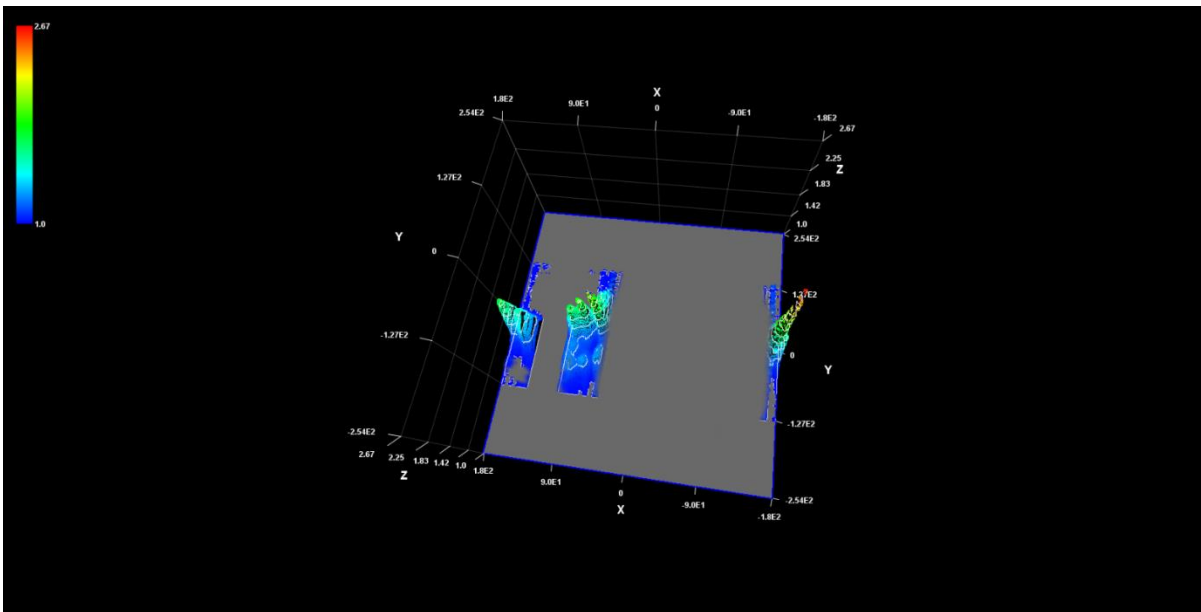
LRO-H1(Ptarmigan) ezCol_SAWB_241104_00_El_42-9_Az_163.ezb LRO (ezSky241201a.py)

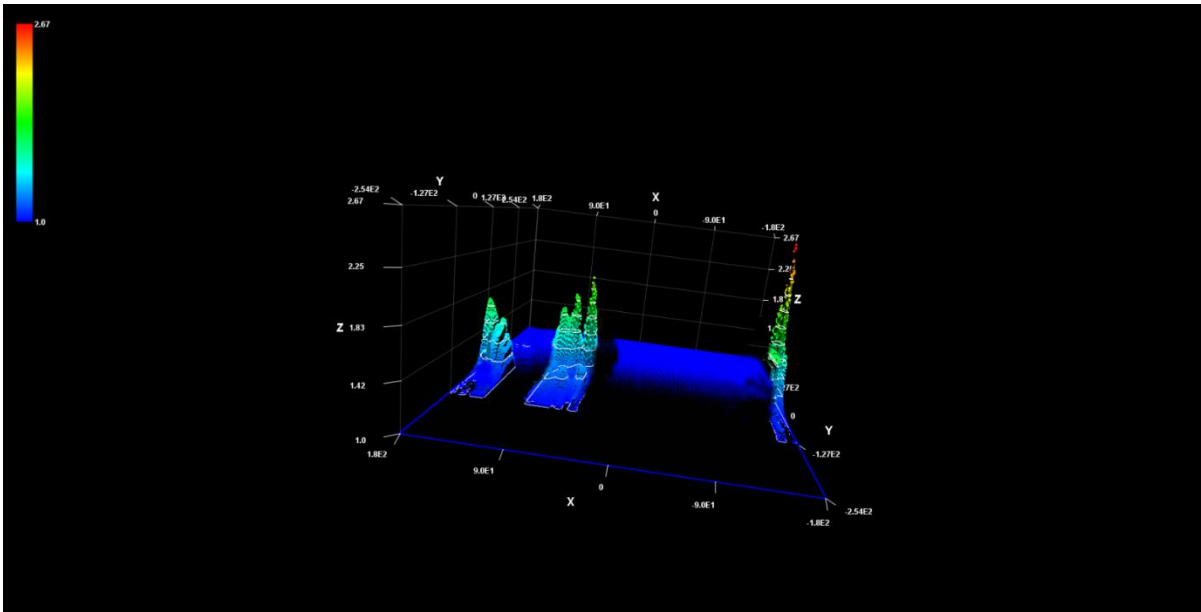


2D representation of interpolated velocity against galactic longitude in this data set:



Plotting 3D images with Rinearn3D using Ted Cline's new ezGal250218e.py script to generate Rinearn3D mesh CSV data file from all viable ezRA NPZ and EZB data files 6 January 2024-1 November 2024:





Further information.

Further information about this project is available on the www.astronomy.me.uk website or by contacting me using the “contact us” page on that website.

The 6.7 GHz maser telescope parameters by solar measurements

by Dmitry Fedorov UA3AVR

Introductory notes and a problem description

This paper is about how to extract characteristics of the telescope for methanol maser observations from the Sun radiation measurements. It is assumed the telescope uses a parabolic dish. The System Equivalent Flux Density (SEFD) is the most important maser telescope parameter. This flux density gives the same antenna temperature T_a as the System Temperature T_{sys} . SEFD is usually measured in Jy and can be expressed via the System Temperature and the telescope Forward Gain (dish sensitivity) Γ

$$SEFD = \frac{T_{sys}}{\Gamma}, \quad \Gamma = \eta_A \frac{\pi D^2}{8k}, \quad (1)$$

where k – the Boltzmann constant $\approx 1.38 \cdot 10^{-23}$ J/K, D – the parabolic reflector diameter, η_A – the Aperture Efficiency. The Forward Gain Γ is usually measured in K/Jy and allows to calculate what antenna temperature T_a would be induced by received radiation with known flux density. For more details about Γ see eq. (7.25) in [1] and text comments there.

SEFD defines the maser telescope performance and allows converting maser observation results to Jy in post-processing. Its knowledge allows calculating the minimal detectable peak flux density from the radiometer equation [2]

$$F_{peak} = \frac{K SEFD}{\sqrt{\Delta t RBW}} \quad (2)$$

especially adapted for maser lines. Here $K \approx 3$ – is the peak factor of the background noise, Δt – is the integration time, RBW – the Resolution Bandwidth of the receiver. When a maser line has F_{peak} from (2), its peak is about the background noise peaks. A maser line would become higher over the noise on the spectrum picture if the integration time Δt increases.

The solar measurements allow extracting SEFD immediately without knowledge the System Temperature T_{sys} ; this will be shown in further consideration. A number of solar observatories measures the radio flux of the Sun radiation, and data for microwave frequencies are available online. I usually use the data from Learmonth observatory in Australia [3]. The Antenna Temperature T_a induced by the solar radio flux S_{SUN} can be obtained by

$$T_a = \frac{A_{geom} \eta_A S_{SUN}}{2}, \quad A_{geom} = \frac{\pi D^2}{4}, \quad (3)$$

where A_{geom} is the geometric area of parabolic reflector aperture.

Formula (3) is correct when the angular size of the Sun is much smaller the antenna beamwidth, i.e. when the Sun is considered point-like. Even for small dishes like used by me now at 6.7 GHz (see Figure 1) applying (3) would be not quite correct. The dish size $D = 2.4$ m, Half Power Beam Width $\delta_{HPBW} \approx 70^\circ D/\lambda \approx 1.3^\circ$, where λ – the wavelength. The solar angular size $\delta_{sun} = 0.53^\circ$ is comparable with the dish size; therefore, correction



Figure 1. 2.4 m dish mounted on the roof of apartment building ([55°46'00.5"N 37°49'25.8"E](#)) with 6.7 GHz RX downconverter at the focus. The dish was designed by Sergei Zhutyayev RW3BP for mm-waves initially.

of the formula (3) have to take into account the beamwidth and the Sun angular size. This situation is illustrated in Figure 2.

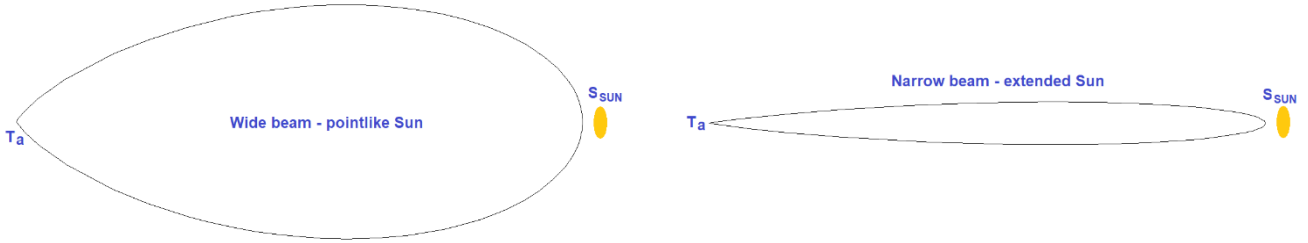


Figure 2. Illustration to receiving the Sun radiation by wide and narrow beams: right – the Sun fills the beam tip only, left – the beam filling is obviously higher.

For a wide beam the solar flux is received by the beam tip only, and the Sun can be considered as point-like. The narrow beam means an extended Sun, and the Sun fills the antenna beam for more than tip only. So, we can introduce the Beam Filling Factor f_{BEAM} to describe the case of extended sources [4]. For point-like Sun f_{BEAM} is very small (but not 0), for narrower beam or extended Sun $0 < f_{BEAM} < 1$, and $f_{BEAM} = 1$ when the beam fits completely in the Sun size or even narrower. The Antenna Temperature T_a for extended source can be expressed as (see ch. 8.2.3 in [1])

$$T_a = \eta_B T_B f_{BEAM} , \quad (4)$$

where η_B – is the Main Beam Efficiency (for Gaussian beams $\eta_B \approx \eta_A/0.75$ [5]), T_B – the brightness temperature of observed source (the Sun in our case). The formula (4) assumes the Sun has a uniform brightness across its disk. The value of product $\eta_B T_B$ can be considered as a constant, which not depends on the Sun size; therefore, a correct formula for the Antenna Temperature T_a from the solar radio flux is

$$T_a = \frac{1}{2} \frac{f_{BEAM}(\text{extended Sun})}{f_{BEAM}(\text{pointlike Sun})} A_{geom} \eta_A S_{SUN} \quad (5)$$

instead of (3). Common expression for the Beam Filling Factor f_{BEAM} is [4,5]

$$f_{BEAM} = 1 - 2^{-\left(\frac{\delta_{sun}}{\delta_{HPBW}}\right)^2} . \quad (6)$$

Derivation of (6) assumes that the beam is Gaussian, and the brightness temperature is uniformly distributed over seen solar disk. For the extended Sun (6) can be used without changes,

$$f_{BEAM}(\text{extended Sun}) = f_{BEAM} = 1 - 2^{-\left(\frac{\delta_{sun}}{\delta_{HPBW}}\right)^2} . \quad (7)$$

For the point-like Sun $\delta_{sun} \ll \delta_{HPBW}$, and one can get from (6)

$$f_{BEAM}(\text{pointlike Sun}) \approx \ln 2 \left(\frac{\delta_{sun}}{\delta_{HPBW}}\right)^2 . \quad (8)$$

With (7) and (8) the common formula (5) for T_a from the solar radio flux turns into (3) when $\delta_{sun} \ll \delta_{HPBW}$, i.e. when the Sun is point-like.

Formula (5) does not work for very narrow beams when the antenna main beam sees a part of the solar disk only. In this case, an approach based on the brightness temperature T_B and T_a from (4) can be applied. The common form of Beam Filling Factor f_{BEAM} from (6) is not perfectly accurate for very narrow beams but can give reasonable results in this case too.

Processing the solar radio flux data

I would demonstrate how to obtain needed flux density value on example of Learmonth observatory data [3]. Solar radio flux values are available for frequencies 4995 MHz and 8800 MHz; they are presented in Solar Flux Units (SFU), $1 \text{ SFU} = 10^4 \text{ Jy} = 10^{-22} \text{ W}/(\text{Hz m}^2)$.

Actual SFU value for 6700 MHz can be obtained by linear interpolation

$$SFU_{6700} = \frac{SFU_{8800} - SFU_{4995}}{8800 - 4995} (6700 - 4995) + SFU_{4995} \quad (9)$$

or by log-log interpolation

$$SFU_{6700} = SFU_{4995} \left(\frac{6700}{4995} \right)^{\frac{\ln \frac{SFU_{8800}}{SFU_{4995}}}{\ln \frac{8800}{4995}}} \quad (9a)$$

For typical values $SFU_{4995} = 232$ and $SFU_{8800} = 292$ we have $SFU_{6700} = 259$ by linear interpolation (9) and $SFU_{6700} = 261$ by log-log interpolation (9a).

The solar flux near the ground is slightly weaker at 6.7 GHz due to the atmosphere attenuation; S_{SUN} received by the telescope with the atmosphere correction is

$$S_{SUN} = 10^4 \frac{SFU}{L_{atm}} [Jy] = 10^{-22} \frac{SFU}{L_{atm}} \left[\frac{W}{Hz m^2} \right]. \quad (10)$$

Attenuation ratio here is $L_{atm} > 1$; as expected for 6.7 GHz value of L_{atm} does not exceed 1.02–1.04, and one can set $L_{atm} = 1$ in first approximation.

The solar flux values can change from day to day and even during the day; it is preferable to pick out SFU_{4995} , SFU_{8800} values maximally close to the time of measurements.

Measurements of the solar radiation, a practical formula for SEFD

The antenna temperature T_a can be calculated from the solar flux data by (5). On other hand, the antenna temperature can be obtained from measurements the Sun's radiation. If Y is a ratio (Y-factor) of receiver outputs when the beam sees the Sun and outside in the Cold Sky, then

$$T_a = T_{sys} (Y - 1), \quad (11)$$

If a measurement result $Y(\text{dB})$ is expressed in dB, it should be recalculated to the ratio $Y = 10^{Y(\text{dB})/10}$. Here Y is understood as a ratio of values in power units.

Antenna temperatures from (5) and (11) must coincide; therefore, we have for the Aperture Efficiency

$$\eta_A = \frac{\ln 2}{\pi} 8 \times 10^{22} k T_{sys} (Y - 1) \left(\frac{SFU}{L_{atm}} \right)^{-1} D^{-2} f_{BEAM}^{-1} \left(\frac{\delta_{sun}}{\delta_{HPBW}} \right)^2. \quad (12)$$

For the Forward Gain (dish sensitivity) $\Gamma = \eta_A \frac{\pi D^2}{8 k}$ according eq. (1), and we have in K/Jy

$$\Gamma = \ln 2 \times 10^{-4} T_{sys} (Y - 1) \left(\frac{SFU}{L_{atm}} \right)^{-1} f_{BEAM}^{-1} \left(\frac{\delta_{sun}}{\delta_{HPBW}} \right)^2, \text{ K/Jy}. \quad (13)$$

The System Equivalent Flux Density, $SEFD = T_{sys} / \Gamma$ does not depend on T_{sys} explicitly and will be in Jy

$$SEFD = \frac{10^4}{\ln 2} (Y - 1)^{-1} \frac{SFU}{L_{atm}} f_{BEAM} \left(\frac{\delta_{sun}}{\delta_{HPBW}} \right)^{-2}, \text{ Jy}. \quad (14)$$

This formula can be used for calculation of SEFD immediately having known the beam size, SFU at 6.7 GHz (SFU_{6700} from above described solar flux data processing), and the measurement result for Y-factor. The System Temperature T_{sys} is not needed for SEFD calculations, and T_{sys} uncertainty does not affect SEFD results.

Formulas (11), (13), (14) do not work for very narrow beams when antenna beam sees a part of the solar disk only.

The small single dish telescope parameters

Here are results for the maser telescope 6.7 GHz used by me now, see Figure 1. By measurements 2024-07-27 for Y-factor I have obtained $Y(\text{dB}) = 13.2$ dB, $Y = 20.9$. The solar fluxes $SFU_{4995} = 232$, $SFU_{8800} = 292$ from Learmonth observatory data, and $SFU_{6700} = 259$ by the linear interpolation (9). The dish size $D = 2.4$ m, Half Power Beam Width $\delta_{HPBW} \approx 70^\circ D/\lambda \approx 1.3^\circ$, the solar angular size $\delta_{sun} = 0.53^\circ$, $f_{BEAM} = 0.11$ by (6), $L_{atm} = 1.03$.

System Temperature values were obtained separately:

$T_{\text{sys}} = 110 \text{ K}$ – from Y-factor Moon measurements [6], $T_{\text{sys}} = 125 \text{ K}$, obtained predictively from known receiver Noise Figure and estimated spillover.

Resulting values for telescope parameters are:

η_A in range 0.61 – 0.66 for the Aperture Efficiency by (12) with T_{sys} in range of uncertainty 120 – 130 K;

$\Gamma = 0.001 \text{ K/Jy}$ – for the Forward Gain (dish sensitivity) by (13) with $T_{\text{sys}} = 125 \text{ K}$;

SEFD = $1.2 \cdot 10^5 \text{ Jy}$ – for System Equivalent Flux Density by formula (14).

Minimal detectable peak flux density $F_{\text{peak}} = 80 \text{ Jy}$ was calculated from the radiometer equation for maser lines (2) with $K = 3$, $\Delta t = 1 \text{ hour}$, $\text{RBW} = 5 \text{ kHz}$.

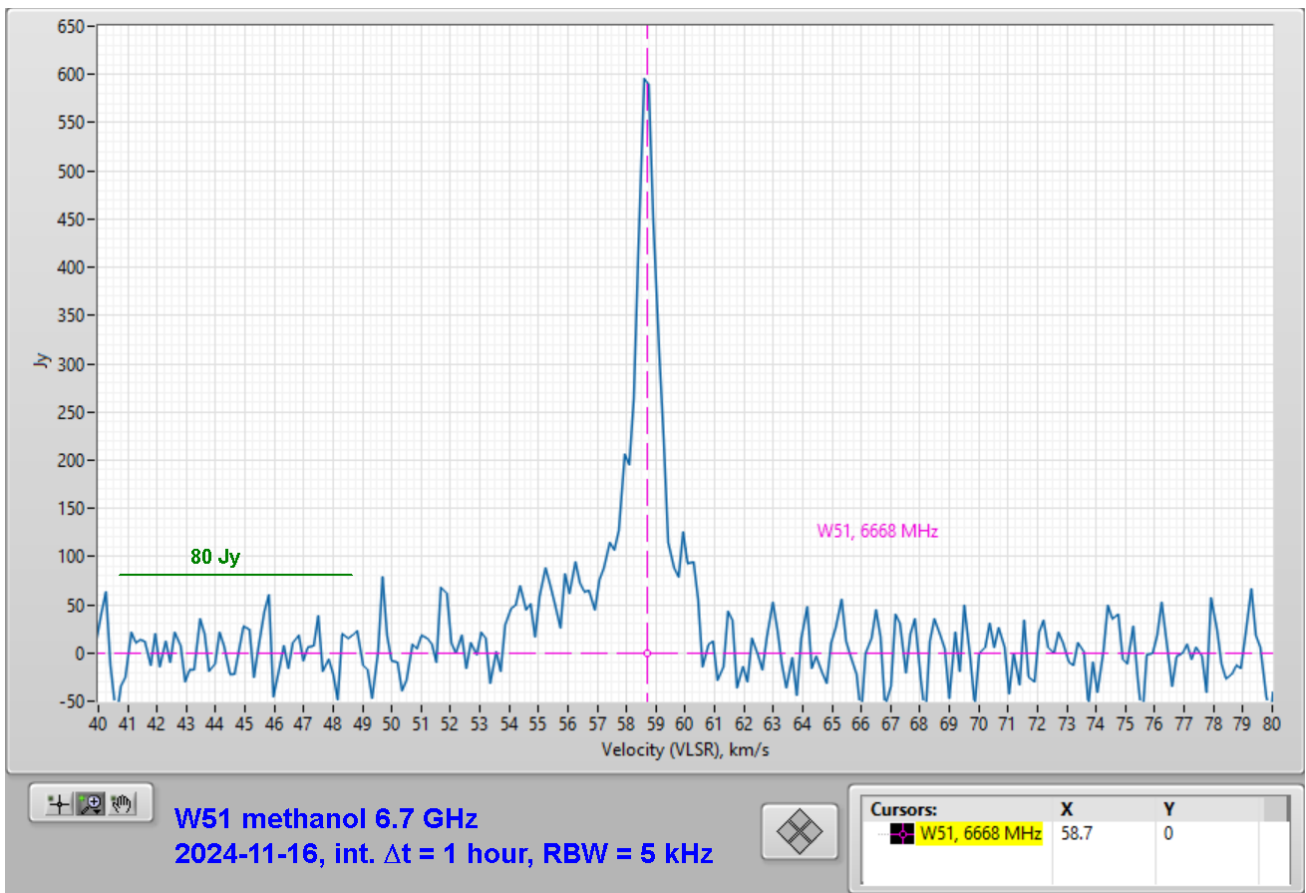


Figure 3. W51 methanol spectrum from real observations 2024-11-16 with marked level 80 Jy (green) corresponding to the background noise peaks. The telescope from Figure 1 was used in observations.

A methanol spectrum from real observation of W51 star forming region is shown on Figure 3. As one can see, highest background noise peaks are testing a level about $F_{\text{peak}} = 80 \text{ Jy}$ calculated above.

Discussion and concluding notes

System Equivalent Flux Density is the most important parameter for maser telescopes. Its knowledge makes possible estimating the telescope performance (minimal detectable peak flux density of maser lines); known SEFD value also allows presenting observed maser levels in Jy [2]. Formula (14) works well when the Sun angular size becomes comparable with antenna beamwidth (except very narrow beams) and can be applied in practice. It gives SEFD immediately from solar measurements without knowledge the System Temperature T_{sys} . The System Temperature may depend on the dish elevation and may have its own uncertainty, but it is

not impact on SEFD results. SEFD from (14) do not depend on T_{sys} explicitly, although the Y-factor in solar measurements is sensitive to the noise background, which conditions T_{sys} .

Surely, the described approach to SEFD measurements can be generalized and extended to other frequencies and dish sizes.

References

- [1] T.L. Wilson, K. Rohlfs, S. Hüttemeister, *Tools of Radio Astronomy*, 6th ed, Springer, 2013.
- [2] D. Fedorov UA3AVR, *Notes on building a maser receiver*, Radio Astronomy, Journal of the Society of Amateur Radio Astronomers, March – April 2024, p. 71; D. Fedorov UA3AVR, Low Signal-to-Noise observations of masers, Proceedings of Annual Eastern Conference and Global Symposium on Amateur Radio Astronomy, Green Bank, West Virginia, August 4-7, 2024, p. 232.
- [3] Learmonth solar observatory, radio flux, <https://www.sws.bom.gov.au/Solar/3/4>.
- [4] Joachim Köppen DF3GJ, *A Closer Look at Filling Factors*, DUBUS 4/2021, v 50, p 15.
- [5] D. Fedorov UA3AVR, *Solar Flux and Temperature at Millimetre Wavelengths*, DUBUS 3/2016, p. 41; <http://dx.doi.org/10.13140/RG.2.1.1656.9361>.
- [6] D. Fedorov UA3AVR, *System temperature T_{sys} by measurements the Moon radiation*, Radio Astronomy, Journal of the Society of Amateur Radio Astronomers, January – February 2024, p. 62.

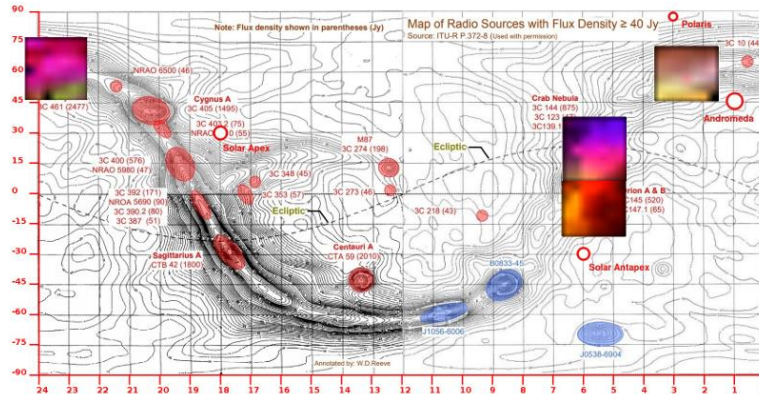
About the author



Dimitry Fedorov, UA3AVR was first licensed as a radio amateur in 1982. In 1990 Dmitry graduated with an MS in electronics from Moscow Power Engineering University. Now he works as research and development engineer in the wireless industry, developing RF and microwave modules for LTE/5G NR and SAT communications. He also has previous scientific experience in nuclear and particle physics, while working at Moscow State University, Institute of Nuclear Physics and Universität Tübingen, Institut für Theoretische Physik, see his profile blog at <https://www.researchgate.net/profile/Dimitry-Fedorov-2>. Radio Astronomy has been a hobby since 2012, mainly in applications for weak signals reception. You can contact Dimitry at ua3avr@yandex.ru.

H1 Mosaic (Raster Scan) Study

by Paul Gochin (KB3PUW)



Study Overview

- The objective of the study was to create an image-like representation of the area surrounding points in space centered on cosmic objects known to have high levels of radio emissions near 1.42 GHz
- The procedure was to sample a matrix of points centered on an object and treat them as they were pixels from an optical image sensor assembled into a 2D image
- The data acquisition was in a scanning pattern reminiscent of a raster scan
- By mapping integrals of frequency ranges to pseudo colors an image could be created analogous to constructing optical images from a set of narrowly filtered monochromatic captures
- Note that the data were collected in a uniformly spaced matrix in RA/DEC coordinates (5 degree spacing) which makes the presentation appear linear when plotted on a linear RA/DEC map
- The distortion relative to what would be seen with a linear image sensor is provided in this report
- Again analogous to amateur optical astronomy, computational processing was applied to the data to reduce various forms of noise in order to extract a "clarified" image of the target area
- This RA data is not necessarily directly related to the centered deep-sky object
- Drift experiments were also conducted, and tools built, to validate the utilized computations by comparison against existing data and tools
- The physical experimental apparatus was based on relatively inexpensive, off-the-shelf, amateur optical astronomy and radio components
- Data analysis was done using a purpose built application

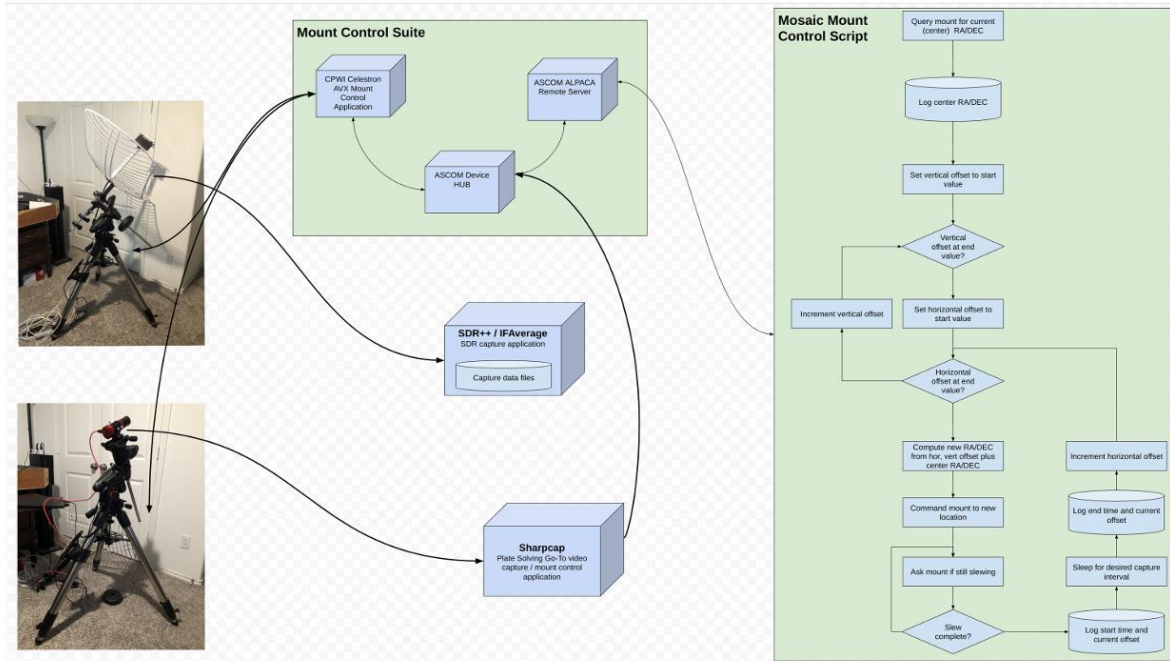
Hardware

- The hardware used for all experiments was a “Scope-in-a-box” type setup
- Nooelec Satellite Mesh Antenna (1.42 GHz, 21dBi gain)
- Nooelec SAWbird+ H1 (LNA- Low Noise Amplifier – gain 40 dB)
- White 5D-FB coax (8.2db loss/100ft = 0.8 dB loss for 10ft Mosaic study, 50ft 4.1dB loss for Drift)
- Nooelec NESDR SMARTEE v2 SDR (SDR- Software Defined Radio Dongle which powers the LNA)
- The SDR was cooled with an open-loop Peltier cooling unit
- Celestron AVX computer controlled equatorial mount for mosaic and a fixed tripod for drift studies
- Custom built Vixen rail mount, with counterweight for the Mesh antenna
- SVBony SV165 120mm F4 guide scope
- ZWO ASI678MC camera

Mosaic Data Collection Methodology

- A Guide scope/camera was initially mounted on the computer controlled equatorial mount
- A laptop computer was configured to run ASCOM Device Hub, Alpaca Remote Server, Celestron CPWI mount control, Sharpcap Pro for video acquisition and mount targeting and SDR++/IFAverage for RA data collection
- Sharpcap Pro was used to Polar align the mount using the guide scope/camera
- Sharpcap Pro plate solving was used to accurately “Go-To” the desired target using the guide scope/camera
- Sharpcap was then shut down
- The guide scope was then replaced with the Mesh antenna assembly
- The assembly is designed so that the antenna boom is very close to the center axis of the guide scope and therefore the antenna is centered where the guide scope was pointing
- The mount very accurately maintains the Go-To location to within seconds of arc, far more precise than required for Radio Astronomy
- A baseline recording was saved of a 50 ohm dummy load resistor replacing the antenna on the LNA, using IFAverage
- This configuration was also saved and used as the background baseline for IFAverage
- The antenna was then reconnect and SDR++/IFAverage was started recording spectra in 15 second intervals
- A custom written set of utility programs (nodejs) that communicate with ASCOM/Alpaca and a control script (Linux bash) were written for the project
- This software package was used to control sampling a set of points surrounding the center point that was set using the described optical techniques
- In most experiments a 7x7 matrix was used with spacing of 5 degrees between sample points and collecting about 3 minutes of spectra data per point, therefore covering about a 30x30 degree area taking about 150 minutes (including mount movement and settling time)
- The control script performed the following:
 - Interrogated the mount and recorded, in a file, the center RA/DEC
 - Sent a command to go to the first specified offset RA/DEC coordinate
 - The mount was then interrogated to determine when slewing was complete
 - The offset in degrees and the start and stop time were recorded in the file
 - The process continued until all points of the matrix were covered
- The data from IFAverage and the control script are utilized together by RAISE to organize the mosaic data
- Some experiments were also done using ezCol: good results were obtained for drift data, but we were unable to obtain satisfactory results for mosaic data because it was not possible to consistently “flatten” the baseline
- Both Explore Scientific iEXOS-100 and Celestron AVX mounts were tested – the iEXOS-100 produced too much RFI (probably due to its WiFi), the AVX worked well

Data Collection Software Control Framework



Data Analysis Using RAISE (Radio Astronomy Interactive Study Environment)

RAISE Overview

- The RAISE (Radio Astronomy Interactive Study Environment) application was developed primarily to facilitate analysis of Mosaic (Raster Scan) RA data
- Features were added to handle Drift data as well, primarily for validation of the computations
- The approach was to compare data processed with RAISE to the same data processed with EzRA and other applications
- RAISE is capable of utilizing both EzRA/EZCol and SDR#/IFAverage drift data sets
- Data sets may be one or more drift elevations
- Data may also be from EZCol or IFAverage mosaic sets (specific data organization and metadata are required)
- Data sets, plot types and processing options can be selected from the RAISE UI and immediately rendered with the various display options
- RAISE may work to a limited degree on a Windows platform but is intended for use on a LINUX operating system and requires a screen with a resolution of at least 3000 by 2000 pixels (it is not resizable)
- RAISE is written in Java but automates external processes leveraging Python3 (for access to the Astropy library) and GNUPlot (for 3D surface plotting)

Data Preparation Methods

- A variety of optionally selectable features were created to handle various types of RFI:
 - Selective suppression of specified spectra (to remove spectra overwhelmed by RFI)
 - Linear interpolation suppression of specified frequency ranges (to remove obvious noise spikes in spectra)
 - Normalization (scaling) of each spectrum relative to a specified point's value in that spectrum (to remove offsets and match magnitudes with the reference spectrum)
 - Smoothing ("Boxcar" smoothing: convolution with a window of specified width)
 - Chunking (averaging successive power spectra)
 - Trimming (elimination of leading and trailing portions of the power spectra outside the H1 range)
- Spectrum flattening;
 - Both EZCol and IFAverage spectra displayed curvature not related to the H1 signals
 - Subtraction of a reference spectrum is required to "flatten" the spectra, if possible, only leaving peaks for H1 signals
 - For EzCol data, choosing a reference spectrum of "cold sky" was necessary
 - For IFAverage, either cold sky or a reference resistor load (instead of an antenna signal) was successful when applied in post processing of the data
 - For IFAverage it was also possible to use the reference load as the IFAverage "background" to get flat baselines in real-time
 - Two-point flattening was also often used (linear flattening of "slanted" spectra using 2 specified reference points)
- Additional RAISE features were also created for the studies:
 - VLSR adjustment
 - Peak finding and marking
 - Integration range selection

Data Presentation Methods

- RAISE options for displaying time series data:
 - Time series waterfall
 - RA/Dec galactic map overlay plot of power spectrum integrals
 - Doppler spectrum heat maps (2 & 3D versions)
- RAISE options to evaluate mosaic data.
 - Waterfall Grid
 - Description matrix
 - Pseudo color images
 - 3D mosaic heat maps
 - Mosaic sample point RA/DEC and Alt/Az maps
 - Mosaic Galactic span

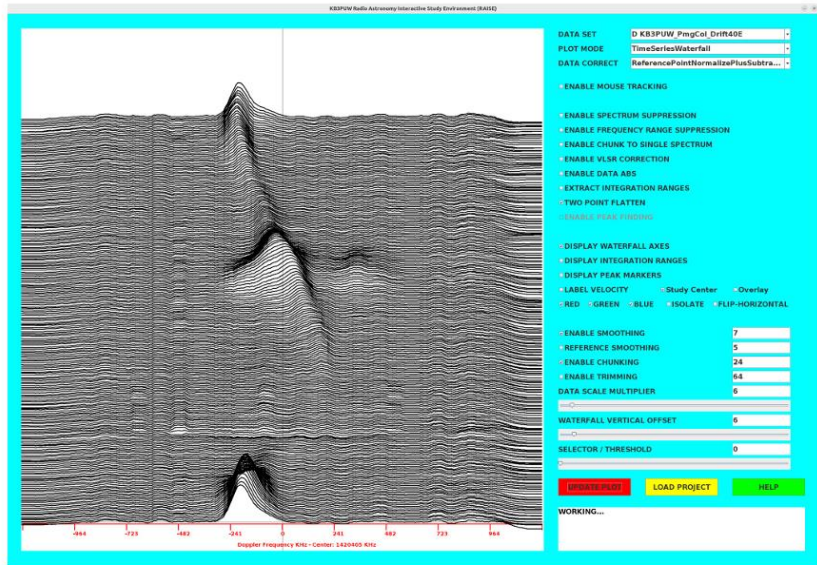
Drift Study Results

Example ezCol / RAISE Waterfall Plot

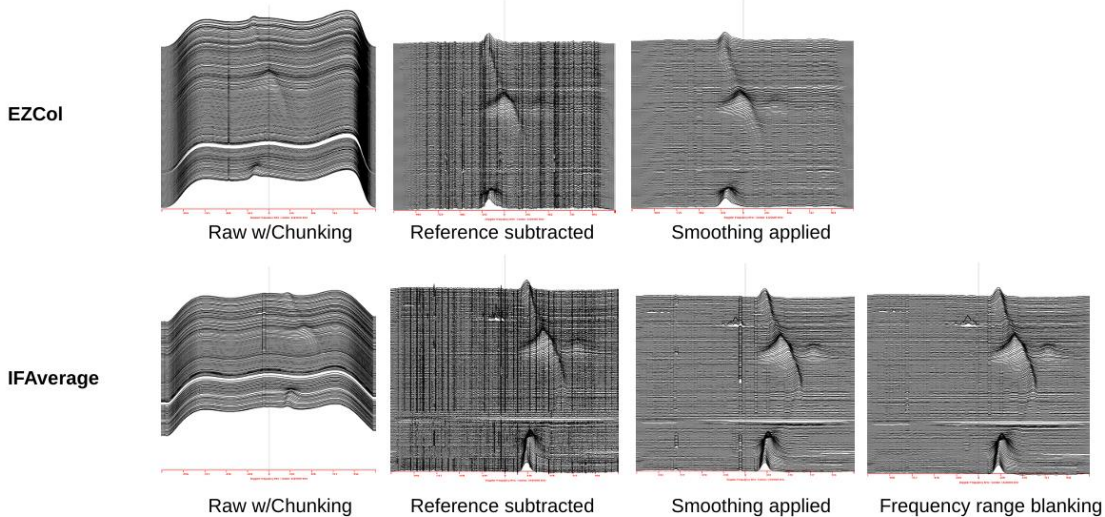
RAISE plot option "TimeSeriesWaterfall"

Example:

- EZCol collected power spectra
- Single drift scan for 24 hours
- Antenna pointed East (90deg)
- 40 deg elevation
- 5629 captures
- 15 sec averaged per spectrum
- 2.4MHz bandwidth
- 256 bins
- 24 spectra "chunking" (successive averaging)
- "Cold Sky" reference sample was subtracted from each spectrum
- Reference was selected from a quiet period about 1/4 up from the bottom
- Reference and samples were all divided by the value of their own 64th bin for scale normalization
- Subtraction utilized scaled spectra
- Spectra were then smooth with a 7 element boxcar filter
- Next the spectra were adjusted with a 2 point flattening procedure using the points 64 and 192



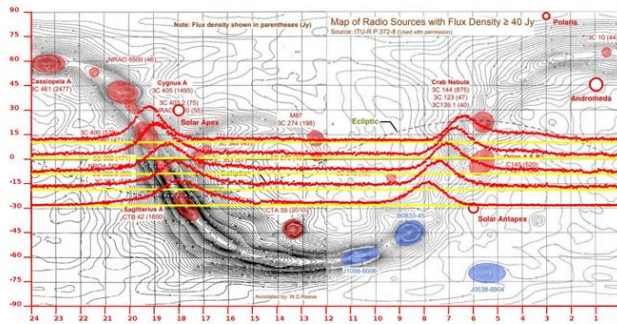
RFI noise reduction processing examples with IFAverage and EzCol Data



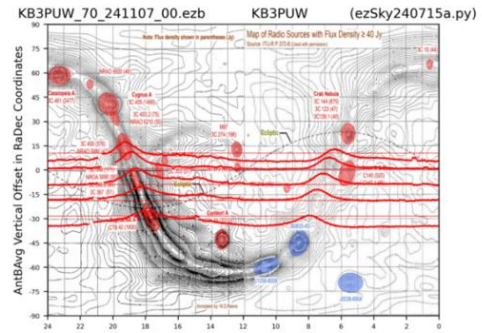
Drift Scan Integration Displays

- Both plots are from the same 5 sets of drift scan data
- Each scan was collected with ezCol
- Antenna was fixed at Azimuth 165 degrees and the Elevation varied as 30, 40, 50, 60 and 70 degrees
- Each scan was about 24 hours sampled at 15 seconds, bandwidth 2.4MHz, 256 bin power spectra
- The points on the red curves are the integral of the power spectra values (which are relative units, not calibrated to any absolute scale) – baselines are also shown
- The two plots (the first RAISE, the second ezRA: ezCon) vary due to differences in the processing of the spectra prior to integration

RAISE



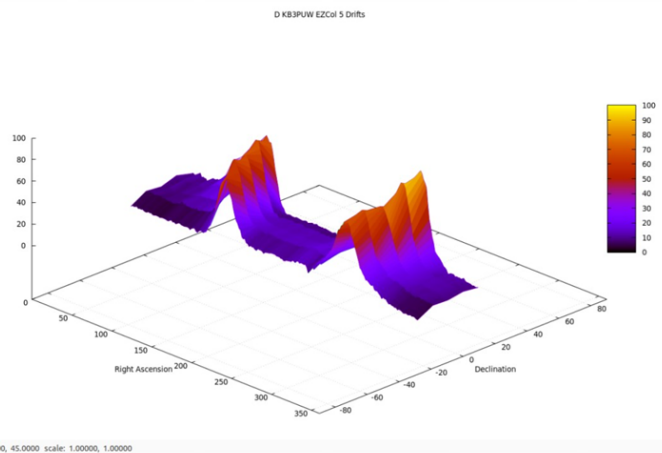
ezCon/ezSky



Integration 3D Heatmap Display

RAISE plot option for multiple drift scan sets

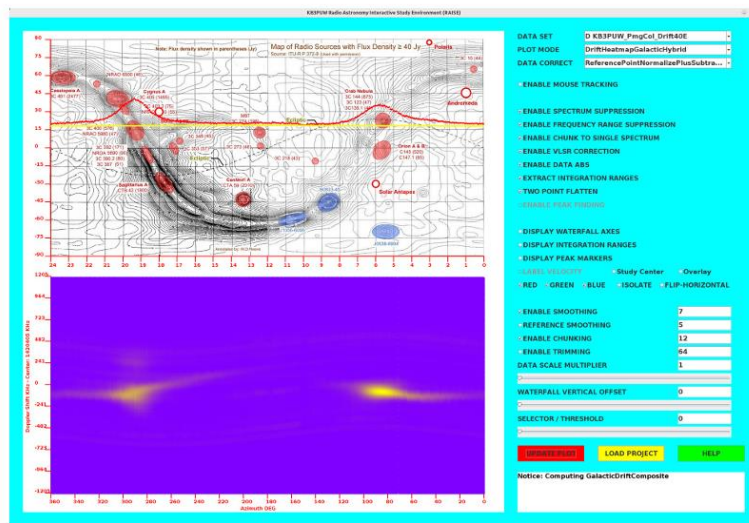
- The plot renderings are done using GNUPlot – an open source, primarily LINUX based, general purpose plotting application which supports surface plotting
- RAISE does all the data preparations and stores the results as a matrix file
- RAISE also generates the script file in GNUPlot language to specify the plot characteristics
- RAISE then remotely executes GNUPlot
- All of these operations are done automatically by RAISE by selecting the "DriftCompositeSurface" option
- A GNUPlot window is launched which can be dynamically manipulated to change size and 3D perspective on the plot
- This is the same data as the maps shown previously



Combined Integration and Frequency Heatmap Display

RAISE hybrid display of integration and frequency spectrum for the same drift data set

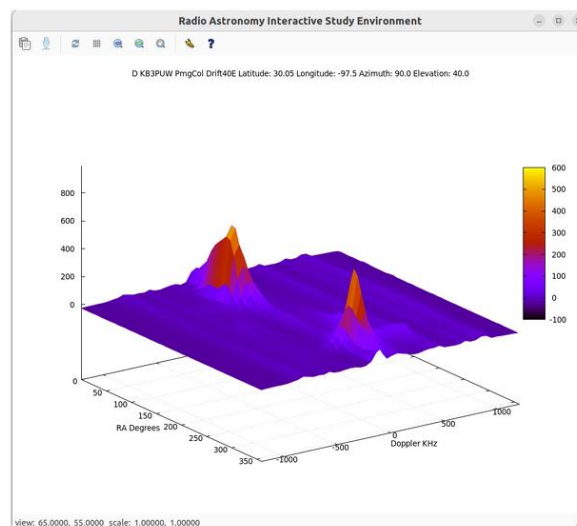
- This plot simultaneously presents the same data set in two ways, time aligned
- The consisted of multiple sets of spectra (the 5 drift elevations)
- Moving the "SELECTOR" slide bar, followed by the "UPDATE PLOT" button, allowed viewing of other members of the data set



3D Doppler Frequency Heatmap Display

RAISE plot option for 3D heatmap frequency spectrum for the same data set

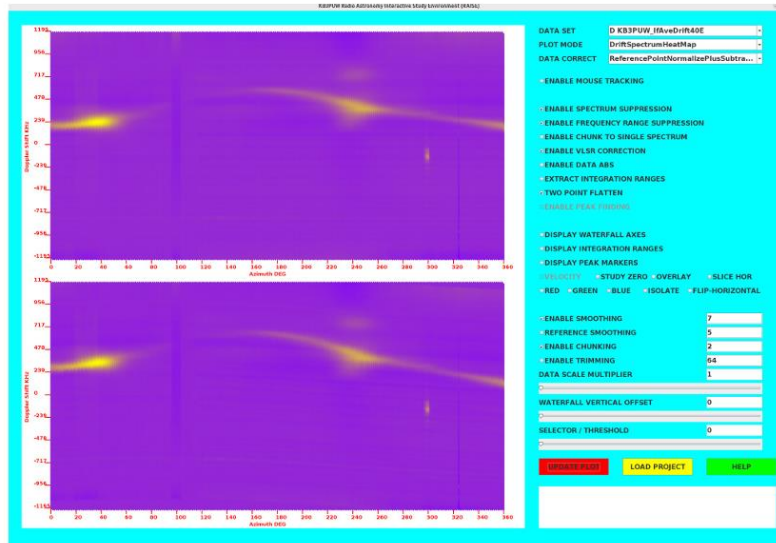
- This function launches a GNUplot window which is resizable and rotatable
- If the data set consists of multiple spectra the selector slide bar followed by the "UPDATE PLOT" button will display another member of the data set



VLSR Adjustment Comparison

RAW

VLSR
Adjusted



- This plot facilitated comparison of the effect of applying VLSR adjustment to the
- This plot currently only supports axes in frequency – other plots have the option to display velocity

Mosaic (Raster) Data Results

Mosaic Data Description

Keys

Element ID	RA, Dec (offset in degrees)	RA (deg), Dec (deg)	Longitude (km), latitude (km)	Sample point VLSR, doppler shift (km/s) - VLSR (km/s)	Telescope (MHz) (degrees)
1	10:00:00.000	10:00:00.000	10:00:00.000	10:00:00.000	10:00:00.000
2	10:00:00.000	10:00:00.000	10:00:00.000	10:00:00.000	10:00:00.000
3	10:00:00.000	10:00:00.000	10:00:00.000	10:00:00.000	10:00:00.000
4	10:00:00.000	10:00:00.000	10:00:00.000	10:00:00.000	10:00:00.000
5	10:00:00.000	10:00:00.000	10:00:00.000	10:00:00.000	10:00:00.000
6	10:00:00.000	10:00:00.000	10:00:00.000	10:00:00.000	10:00:00.000
7	10:00:00.000	10:00:00.000	10:00:00.000	10:00:00.000	10:00:00.000
8	10:00:00.000	10:00:00.000	10:00:00.000	10:00:00.000	10:00:00.000
9	10:00:00.000	10:00:00.000	10:00:00.000	10:00:00.000	10:00:00.000
10	10:00:00.000	10:00:00.000	10:00:00.000	10:00:00.000	10:00:00.000
11	10:00:00.000	10:00:00.000	10:00:00.000	10:00:00.000	10:00:00.000
12	10:00:00.000	10:00:00.000	10:00:00.000	10:00:00.000	10:00:00.000
13	10:00:00.000	10:00:00.000	10:00:00.000	10:00:00.000	10:00:00.000
14	10:00:00.000	10:00:00.000	10:00:00.000	10:00:00.000	10:00:00.000
15	10:00:00.000	10:00:00.000	10:00:00.000	10:00:00.000	10:00:00.000
16	10:00:00.000	10:00:00.000	10:00:00.000	10:00:00.000	10:00:00.000
17	10:00:00.000	10:00:00.000	10:00:00.000	10:00:00.000	10:00:00.000
18	10:00:00.000	10:00:00.000	10:00:00.000	10:00:00.000	10:00:00.000
19	10:00:00.000	10:00:00.000	10:00:00.000	10:00:00.000	10:00:00.000
20	10:00:00.000	10:00:00.000	10:00:00.000	10:00:00.000	10:00:00.000
21	10:00:00.000	10:00:00.000	10:00:00.000	10:00:00.000	10:00:00.000
22	10:00:00.000	10:00:00.000	10:00:00.000	10:00:00.000	10:00:00.000
23	10:00:00.000	10:00:00.000	10:00:00.000	10:00:00.000	10:00:00.000
24	10:00:00.000	10:00:00.000	10:00:00.000	10:00:00.000	10:00:00.000
25	10:00:00.000	10:00:00.000	10:00:00.000	10:00:00.000	10:00:00.000
26	10:00:00.000	10:00:00.000	10:00:00.000	10:00:00.000	10:00:00.000
27	10:00:00.000	10:00:00.000	10:00:00.000	10:00:00.000	10:00:00.000
28	10:00:00.000	10:00:00.000	10:00:00.000	10:00:00.000	10:00:00.000
29	10:00:00.000	10:00:00.000	10:00:00.000	10:00:00.000	10:00:00.000
30	10:00:00.000	10:00:00.000	10:00:00.000	10:00:00.000	10:00:00.000
31	10:00:00.000	10:00:00.000	10:00:00.000	10:00:00.000	10:00:00.000
32	10:00:00.000	10:00:00.000	10:00:00.000	10:00:00.000	10:00:00.000
33	10:00:00.000	10:00:00.000	10:00:00.000	10:00:00.000	10:00:00.000
34	10:00:00.000	10:00:00.000	10:00:00.000	10:00:00.000	10:00:00.000
35	10:00:00.000	10:00:00.000	10:00:00.000	10:00:00.000	10:00:00.000
36	10:00:00.000	10:00:00.000	10:00:00.000	10:00:00.000	10:00:00.000
37	10:00:00.000	10:00:00.000	10:00:00.000	10:00:00.000	10:00:00.000
38	10:00:00.000	10:00:00.000	10:00:00.000	10:00:00.000	10:00:00.000
39	10:00:00.000	10:00:00.000	10:00:00.000	10:00:00.000	10:00:00.000
40	10:00:00.000	10:00:00.000	10:00:00.000	10:00:00.000	10:00:00.000
41	10:00:00.000	10:00:00.000	10:00:00.000	10:00:00.000	10:00:00.000
42	10:00:00.000	10:00:00.000	10:00:00.000	10:00:00.000	10:00:00.000
43	10:00:00.000	10:00:00.000	10:00:00.000	10:00:00.000	10:00:00.000
44	10:00:00.000	10:00:00.000	10:00:00.000	10:00:00.000	10:00:00.000
45	10:00:00.000	10:00:00.000	10:00:00.000	10:00:00.000	10:00:00.000
46	10:00:00.000	10:00:00.000	10:00:00.000	10:00:00.000	10:00:00.000
47	10:00:00.000	10:00:00.000	10:00:00.000	10:00:00.000	10:00:00.000
48	10:00:00.000	10:00:00.000	10:00:00.000	10:00:00.000	10:00:00.000
49	10:00:00.000	10:00:00.000	10:00:00.000	10:00:00.000	10:00:00.000
50	10:00:00.000	10:00:00.000	10:00:00.000	10:00:00.000	10:00:00.000
51	10:00:00.000	10:00:00.000	10:00:00.000	10:00:00.000	10:00:00.000
52	10:00:00.000	10:00:00.000	10:00:00.000	10:00:00.000	10:00:00.000
53	10:00:00.000	10:00:00.000	10:00:00.000	10:00:00.000	10:00:00.000
54	10:00:00.000	10:00:00.000	10:00:00.000	10:00:00.000	10:00:00.000
55	10:00:00.000	10:00:00.000	10:00:00.000	10:00:00.000	10:00:00.000
56	10:00:00.000	10:00:00.000	10:00:00.000	10:00:00.000	10:00:00.000
57	10:00:00.000	10:00:00.000	10:00:00.000	10:00:00.000	10:00:00.000
58	10:00:00.000	10:00:00.000	10:00:00.000	10:00:00.000	10:00:00.000
59	10:00:00.000	10:00:00.000	10:00:00.000	10:00:00.000	10:00:00.000
60	10:00:00.000	10:00:00.000	10:00:00.000	10:00:00.000	10:00:00.000
61	10:00:00.000	10:00:00.000	10:00:00.000	10:00:00.000	10:00:00.000
62	10:00:00.000	10:00:00.000	10:00:00.000	10:00:00.000	10:00:00.000
63	10:00:00.000	10:00:00.000	10:00:00.000	10:00:00.000	10:00:00.000
64	10:00:00.000	10:00:00.000	10:00:00.000	10:00:00.000	10:00:00.000
65	10:00:00.000	10:00:00.000	10:00:00.000	10:00:00.000	10:00:00.000
66	10:00:00.000	10:00:00.000	10:00:00.000	10:00:00.000	10:00:00.000
67	10:00:00.000	10:00:00.000	10:00:00.000	10:00:00.000	10:00:00.000
68	10:00:00.000	10:00:00.000	10:00:00.000	10:00:00.000	10:00:00.000
69	10:00:00.000	10:00:00.000	10:00:00.000	10:00:00.000	10:00:00.000
70	10:00:00.000	10:00:00.000	10:00:00.000	10:00:00.000	10:00:00.000
71	10:00:00.000	10:00:00.000	10:00:00.000	10:00:00.000	10:00:00.000
72	10:00:00.000	10:00:00.000	10:00:00.000	10:00:00.000	10:00:00.000
73	10:00:00.000	10:00:00.000	10:00:00.000	10:00:00.000	10:00:00.000
74	10:00:00.000	10:00:00.000	10:00:00.000	10:00:00.000	10:00:00.000
75	10:00:00.000	10:00:00.000	10:00:00.000	10:00:00.000	10:00:00.000
76	10:00:00.000	10:00:00.000	10:00:00.000	10:00:00.000	10:00:00.000
77	10:00:00.000	10:00:00.000	10:00:00.000	10:00:00.000	10:00:00.000
78	10:00:00.000	10:00:00.000	10:00:00.000	10:00:00.000	10:00:00.000
79	10:00:00.000	10:00:00.000	10:00:00.000	10:00:00.000	10:00:00.000
80	10:00:00.000	10:00:00.000	10:00:00.000	10:00:00.000	10:00:00.000
81	10:00:00.000	10:00:00.000	10:00:00.000	10:00:00.000	10:00:00.000
82	10:00:00.000	10:00:00.000	10:00:00.000	10:00:00.000	10:00:00.000
83	10:00:00.000	10:00:00.000	10:00:00.000	10:00:00.000	10:00:00.000
84	10:00:00.000	10:00:00.000	10:00:00.000	10:00:00.000	10:00:00.000
85	10:00:00.000	10:00:00.000	10:00:00.000	10:00:00.000	10:00:00.000
86	10:00:00.000	10:00:00.000	10:00:00.000	10:00:00.000	10:00:00.000
87	10:00:00.000	10:00:00.000	10:00:00.000	10:00:00.000	10:00:00.000
88	10:00:00.000	10:00:00.000	10:00:00.000	10:00:00.000	10:00:00.000
89	10:00:00.000	10:00:00.000	10:00:00.000	10:00:00.000	10:00:00.000
90	10:00:00.000	10:00:00.000	10:00:00.000	10:00:00.000	10:00:00.000
91	10:00:00.000	10:00:00.000	10:00:00.000	10:00:00.000	10:00:00.000
92	10:00:00.000	10:00:00.000	10:00:00.000	10:00:00.000	10:00:00.000
93	10:00:00.000	10:00:00.000	10:00:00.000	10:00:00.000	10:00:00.000
94	10:00:00.000	10:00:00.000	10:00:00.000	10:00:00.000	10:00:00.000
95	10:00:00.000	10:00:00.000	10:00:00.000	10:00:00.000	10:00:00.000
96	10:00:00.000	10:00:00.000	10:00:00.000	10:00:00.000	10:00:00.000
97	10:00:00.000	10:00:00.000	10:00:00.000	10:00:00.000	10:00:00.000
98	10:00:00.000	10:00:00.000	10:00:00.000	10:00:00.000	10:00:00.000
99	10:00:00.000	10:00:00.000	10:00:00.000	10:00:00.000	10:00:00.000
100	10:00:00.000	10:00:00.000	10:00:00.000	10:00:00.000	10:00:00.000

DATA SET M KB3PUW JFave Orion3
PLOT MODE MosaicDescription
DATA CORRECT ReferencePointNormalize
ENABLE MOUSE TRACKING X: 159 Y: 99
 KHz: 858 KMs: 181
ENABLE SPECTRUM SUPPRESSION
ENABLE FREQUENCY RANGE SUPPRESSION
ENABLE CHUNK TO SINGLE SPECTRUM
ENABLE VLSR CORRECTION
ENABLE DATA ABS
EXTRACT INTEGRATION RANGES
TWO POINT FLATTEN
ENABLE PEAK FINDING
DISPLAY WATERFALL AXES
DISPLAY INTEGRATION RANGES
DISPLAY PEAK MARKERS
VELOCITY STUDY ZERO OVERLAY SLICE HOR
RED GREEN BLUE ISOLATE FLIP-HORIZONTAL
ENABLE SMOOTHING 11
REFERENCE SMOOTHING 5
ENABLE CHUNKING 6
ENABLE TRIMMING 64
DATA SCALE MULTIPLIER 24
WATERFALL VERTICAL OFFSET 17
SELECTOR / THRESHOLD 4
UPDATE PLOT **LOAD PROJECT** **HELP**

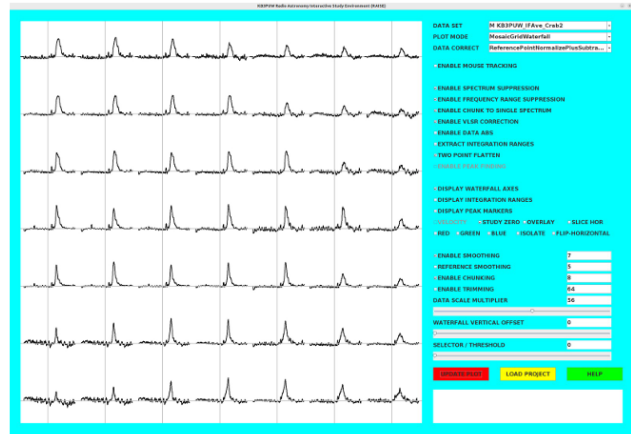
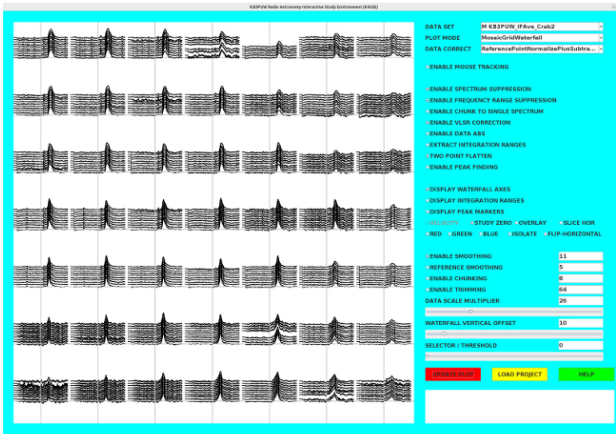
MosaicDescription:

- This plot mode provided a description of the data in each cell of the Mosaic facilitating verification of sampling layout
- Included are coordinates, sample order, VLSR, etc.

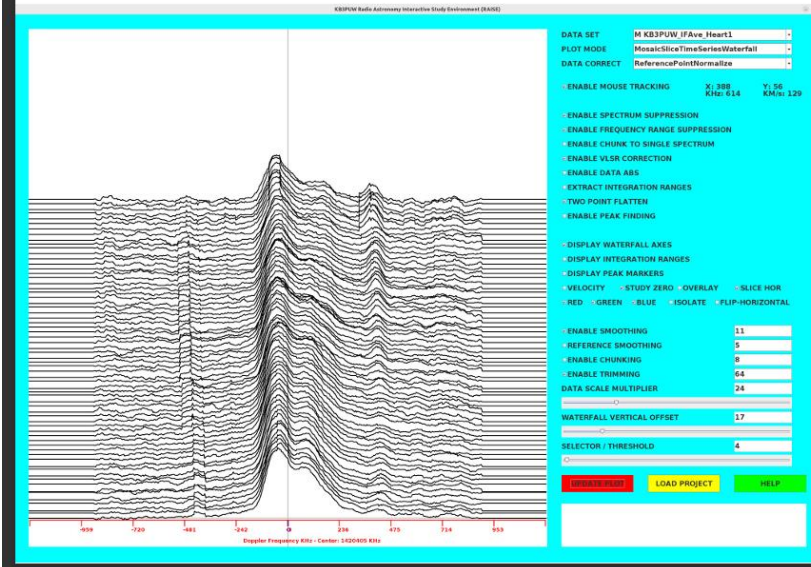
Mosaic Spectra Display

Waterfall

Averaged



Slice Presentation

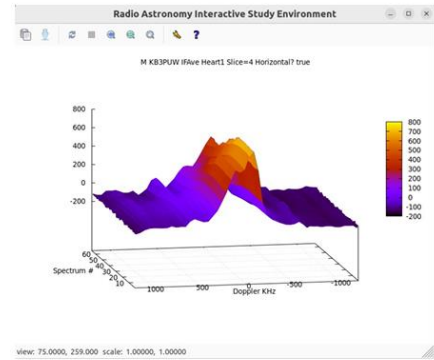


MosaicSliceTimeSeriesWaterfall (left):

- "Slices" were plotted from Mosaic data matrices
- The slices are a waterfall of all of the spectra in a slice
- Slices may be either horizontal or vertical
- The selector slide is used to select the slice and "SLICE HOR" when checked makes horizontal slices, otherwise the slices are vertical
- These plots allowed more detailed evaluation of time and shape features than the small waterfall grid plots
- Also, there is the option to view the data as Velocity or Doppler frequency

MosaicSliceTimeSeriesSpectrumSurface (below):

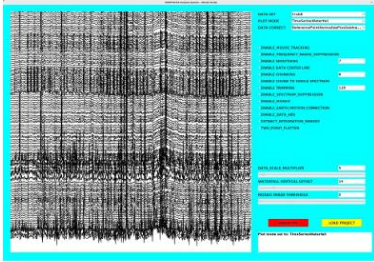
- Alternatively the waterfall may be displayed in 3D and rotated for studying curve time/shape characteristics



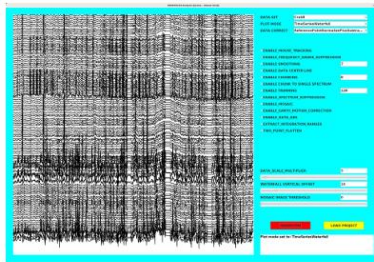
Mosaic RFI Reduction Methodologies

Noise Reduction: Time Series Display (Crab Nebula Example)

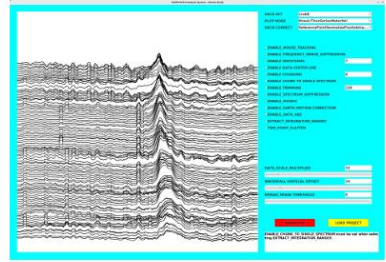
Raw



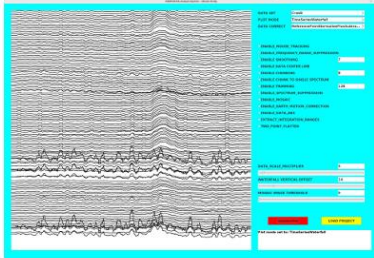
Frequency Range Suppression



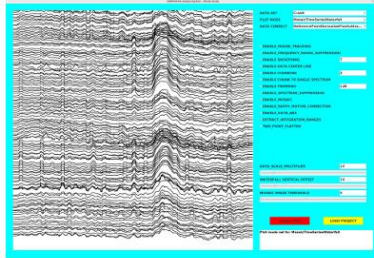
Chunking (successive averaging)



Boxcar Smoothing

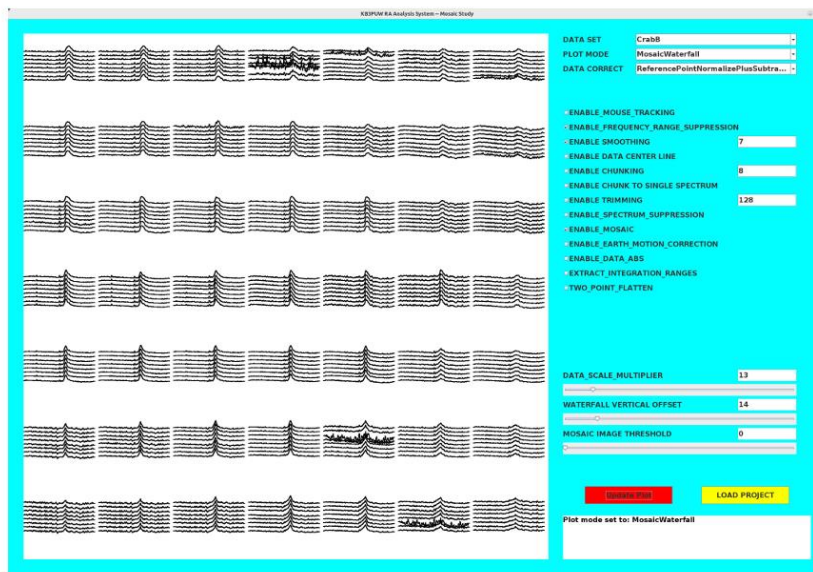


Selective Spectrum Removal



- The mosaic data tended to have more RFI than the drift data
- This may in part be due to the proximity of the antenna to the laptop (10 feet vs 50 ft)
- I also suspected the motorized equatorial mount, but with testing (i.e. turning off the mount power), the AVX mount did not seem to be a significant noise source (the iEXOS had too much RFI to be usable)
- It was clear that the pointing direction of the antenna mattered (this was also the case for my drift studies – but for this study I did not have the option to avoid bad directions)
- I also noticed that environmental RFI sources would come and go (e.g. neighbor devices, passing aircraft, perhaps satellites) – this was possibly worse for the mosaic studies because the time period of data collection was short exaggerating the effect
- The techniques noise reduction techniques shown here brought the data into a usable range

Mosaic Waterfall: with strong RFI traces included

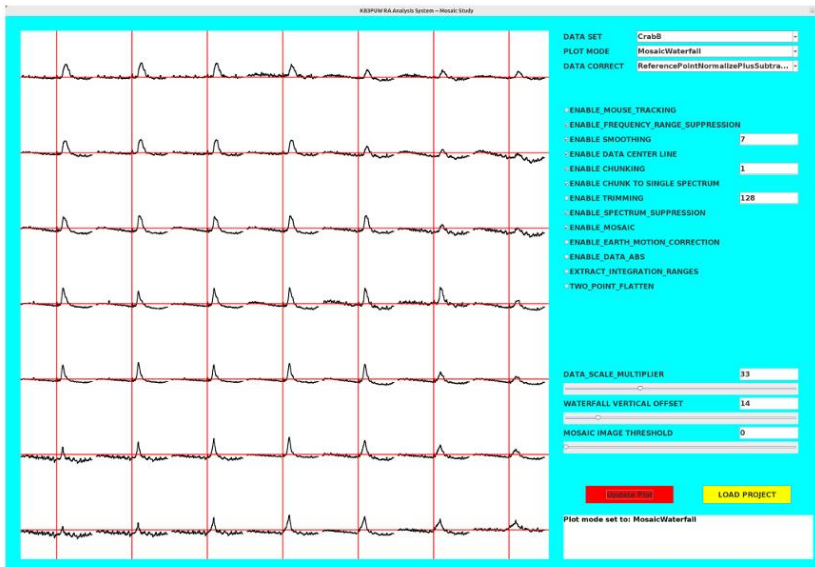


Selective Spectrum Elimination: Strong RFI traces spectra removed



- This plot shows the remaining samples after unusable data was removed
- Note that within a cell the data generally look quite consistent
- Each trace was about 15 seconds of averaged data (done by IFAverage)
- The H1 signal to baseline noise looks quite reasonable in each trace and therefore significant additional averaging was of little value (4 trace averaging reduces Gaussian random noise by a factor of 2 – it would take 16 samples to reduce noise by a factor of 4 and 64 to reduce by 8 etc.)
- Inspection of the data suggested that the noise was largely RFI and was synchronous- not random photon shot noise – and thus averaging would enhance this noise as well as the signal

Mosaic with RFI reduction and Averaged



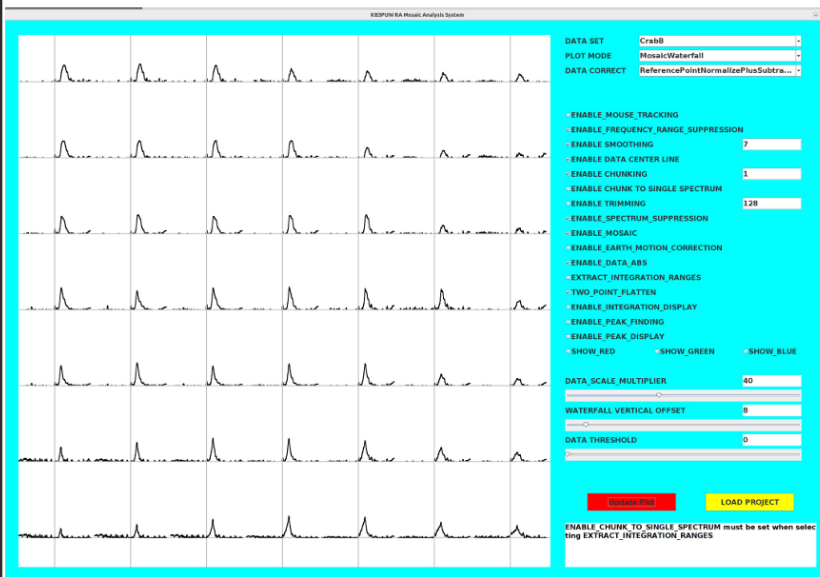
- This plot shows the results after averaging the processed data
- The spectra look reasonable but still had some "slant" and offset

2-point Baseline Flattening



- This plot shows the results after 2-point flattening
- Two points (one near the beginning the other the end) of the spectra were chosen
- The same point locations were used for all spectra, but the values were taken from the corresponding spectrum
- A linear interpolation was computed between the points and subtracted from the spectra

Negative Data Set to Zero

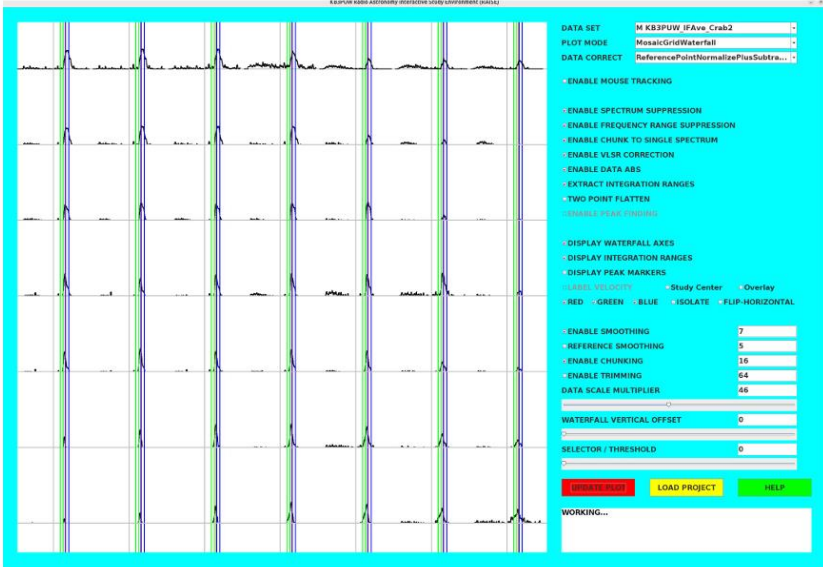


- This plot shows the results after setting all negative values to zero
- This was done before integrals were computed

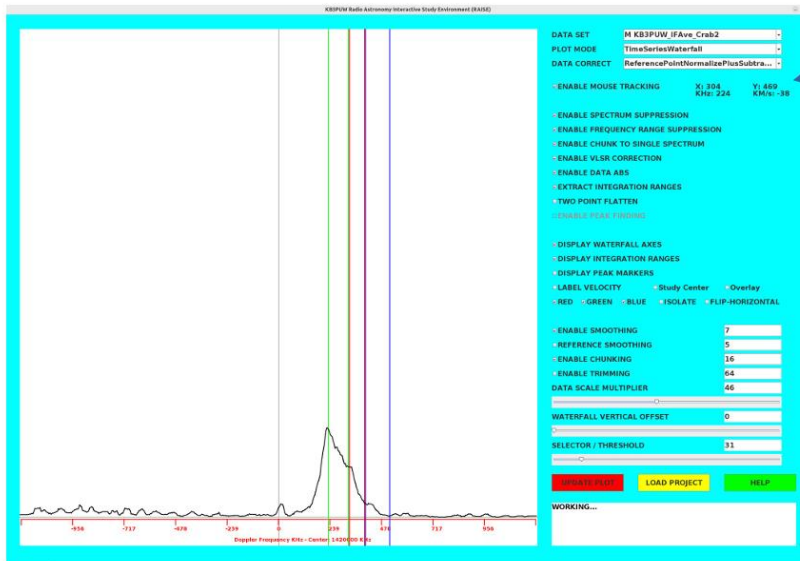
3D Pseudocolor Imagery Results

Pseudocolor Integration Range Specification

- Spectra integrated magnitude was measured for each mosaic sample point
- Up to 3 frequency ranges were evaluated
- The integrated frequency ranges were then be mapped to pseudocolors in order to create image-like representations of the data
- Each integral area was mapped to a color (Red, Green or Blue)



Integration Range Specification



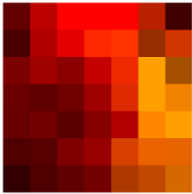
Shows position of the mouse in multiple coordinate systems

Filter range selection:

- A mouse tracking feature was used to identify the start and end bin for desired frequency ranges
- The ranges and associated pseudocolor for the range is entered in a text file
- The ranges can be shown in the waterfall displays, as seen here
- The ranges are used for computing integrals which are then used in image displays

Orion Nebula Centered Mosaic Results

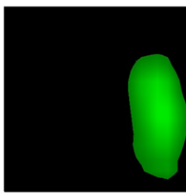
Raw Pseudocolor



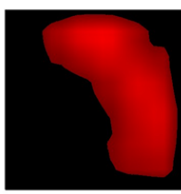
Smoothed Pseudocolor



Green band only

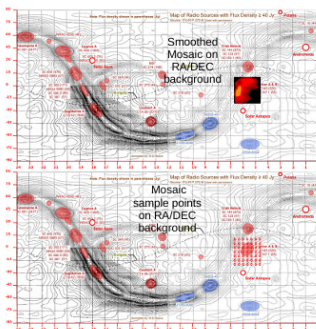


Red band only



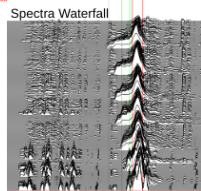
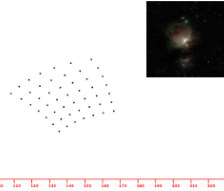
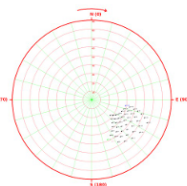
Results:

- Bottom right is the mosaic grid
- Left of the grid is a waterfall showing integration ranges
- Across the top are various versions of pseudocolor images of the integration data
- Lower left shows position of the samples and data on a RA/DEC map
- Mid right is a 3D heatmap of summed integration
- Mid center plot shows actual linearity of the images
- Mid lower plot shows actual raster Alt/Az points

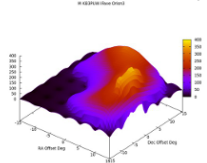


Theoretical Alt/Az mapping of sample points if all data were captured simultaneously with the center point - Shows non-linearity of RA data as compared to an optical photograph - NOTE: NOT TO SCALE - RA data is 30x30 degrees, optical image is about 3x3 degrees

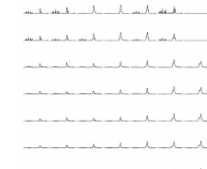
Actual Alt/Az position of sample points during data collection



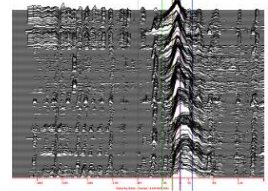
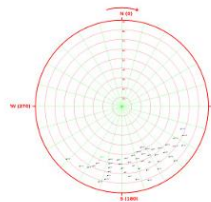
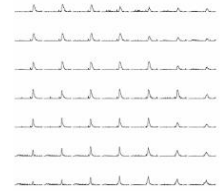
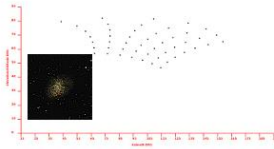
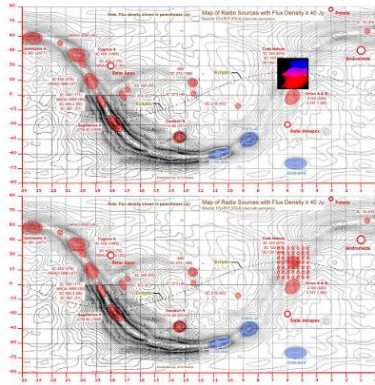
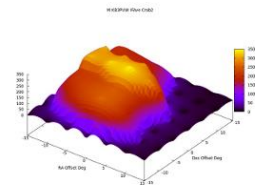
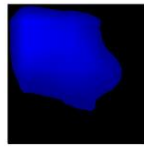
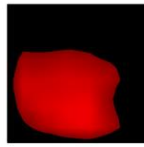
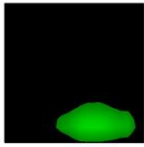
Mosaic All Band 3D Heatmap



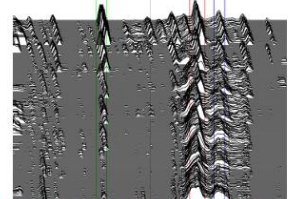
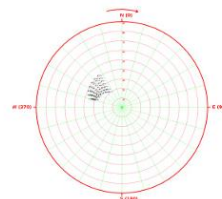
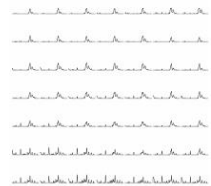
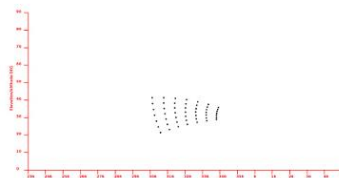
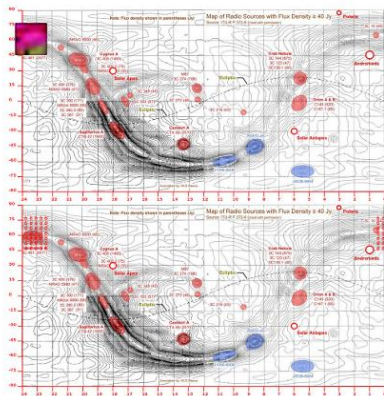
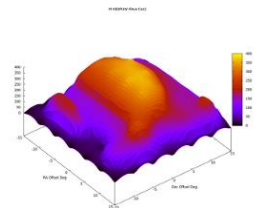
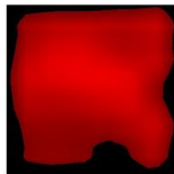
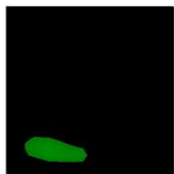
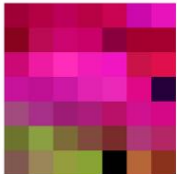
Spectra Mosaic



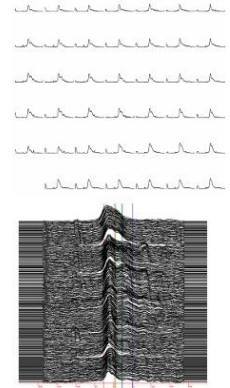
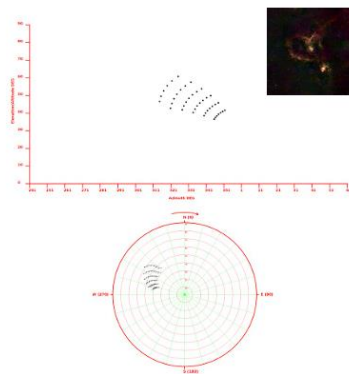
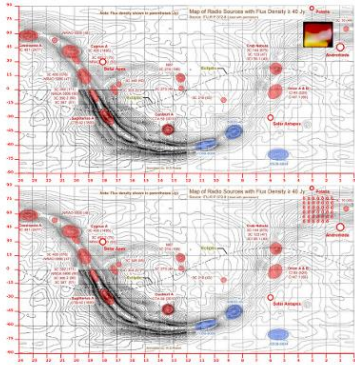
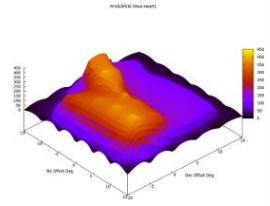
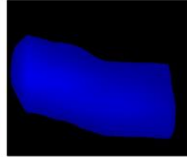
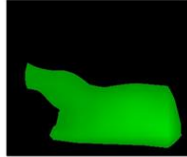
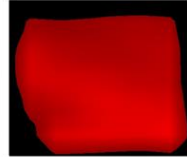
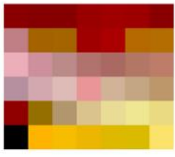
Crab Nebula Centered Mosaic



Cassiopeia A Centered Mosaic

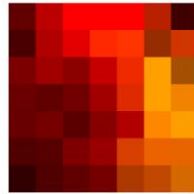
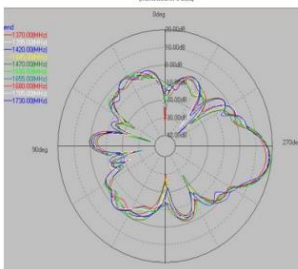


Heart Nebula Centered Mosaic

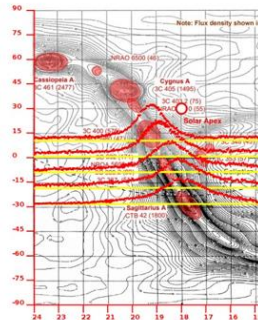
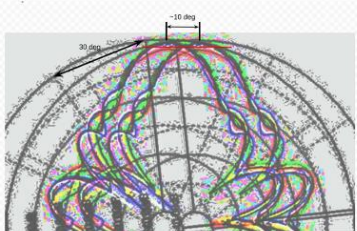


Mosaic Resolution

Nooelec Mesh Antenna Gain Profile



Resolution Extrapolation



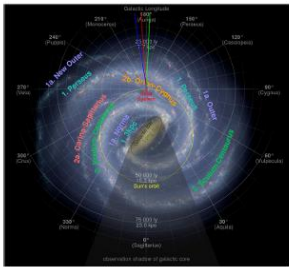
What is the spatial resolution of the antenna when used in creating a mosaic?

- Empirical observation of the mosaic data suggests 5 degrees was resolvable
- Similarly, in drift data, curve shape and width is quite evident within a 15 degree window, thus suggesting the spatial resolution of the antenna is better than 15 degrees
- Analogous to contrast adjustment in an optical image, thresholding of power spectra data appears to improve spatial resolution

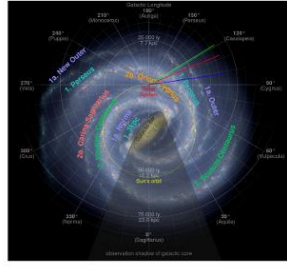
Galactic Sampling

(Galactic Mosaic Sampling Ranges using RAISE
"MosaicGalacticCoordinates" feature)

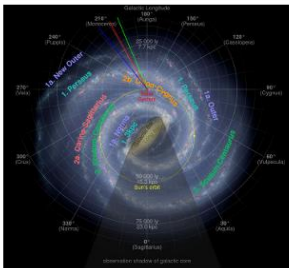
Crab



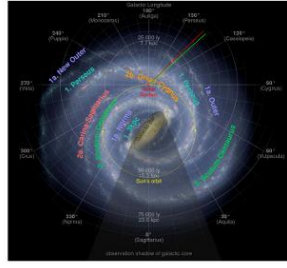
Cas A



Orion



Heart



The red, green and blue lines indicate the center and range of Galactic longitude

Next Steps: Data Evaluation

- Check spectra shapes against other studies to identify RFI artifacts
- Evaluation of velocity profiles against other studies for validation and interpretation
- Interpretation of spatial structure: correlation with galactic arm location established from other studies
- Determination if any of the data is consistent with detection of extragalactic signals (i.e. from the nebula)

Journal Archives and Other Promotions

The rich and diverse legacy of member contributed content is available in the SARA Journal Archives. Table of contents for journals is available online at: [SARA-Journal-Master-Index.xlsx \(live.com\)](#)

The entire set of The Journal of The Society of Amateur Radio Astronomers is available by online download. It goes from the beginning of 1981 to the present (over 6000 pages of SARA history!)

All SARA journals and conference proceedings are available through the previous calendar year.

SARA Store (radio-astronomy.org/store.)

SARA Online Discussion Group

SARA members participate in the online forum at <http://groups.google.com/group/sara-list>. This is an invaluable resource for any amateur radio astronomer.

SARA Conferences

SARA organizes multiple conferences each year. Participants give talks, share ideas, attend seminars, and get hands-on experience. For more information, visit <http://www.radio-astronomy.org/meetings>.

What is Radio Astronomy?

Radio Astronomy is just what the name implies.... Astronomy observed at radio wavelengths instead of optical. But why do radio astronomy? Radio astronomy has expanded the knowledge of the universe about as much since its discovery in 1932 as optical has since humans first looked up at the sky. (The sky in the different frequencies or colors of radio are as different and varied as all of the flowers on Earth. Each frequency has its own information about what is happening in the universe.) This knowledge has been gained by both professional astronomers as well as amateurs, with amateurs contributing to this day.

Do I need a big dish and expensive equipment?

No. Complete beginner projects are available at the [SARA store](#) at very reasonable prices. You can monitor the Sun's effects upon our planet with [SuperSID](#). This information is gathered for Stanford for research into our ionosphere and radio signal propagation. Another project is the detection the hydrogen line just like Dr. Ewen had done in 1951 for a fraction of the cost using the [Scope in a Box](#) kit.

That said, radio astronomy is like optical astronomy in that you can spend as much as you want to. Many amateurs push the lower boundaries of cost by using very low-cost receivers and low-noise low-cost amplifiers that were not available even a few years ago. (See the [Scope in a Box](#) kit in the store for examples of both.)

Is everything 'plug and play' and boring?

The kits mentioned above are a starting point which are mostly plug-and-play... that gets you started. After you have mastered the basics, where you go from there depends upon your interests. Monitoring pulsars is done by amateurs. (One even noticed a [pulsar glitch](#) before the professionals!) These amateurs are pushing the boundaries of what can be done. Papers are being published and discussions had about pulsar detection as well detection of a MASER with a 50-inch dish. Techniques on new detection methods are posted in the [SARA forum](#) and elsewhere. You are free to build your own equipment to receive the signals as well as software to collect and analyze the data.

What is SETI?

SETI is the Search for Extra-Terrestrial Intelligence. Some amateurs scan the sky and search for signals that might be from aliens. To date no one has received a definitive alien signal (professional or amateur), but the search continues. The search has resulted not just in better receiving equipment but also wide and lively discussions about how aliens might communicate and how they might be trying to contact us. Some of these techniques have interesting ideas for our own communication techniques here on Earth!

What should I do to get started?

You should start with reading our [Introduction to Radio Astronomy](#) and joining our online [SARA Forum](#). Look at the [SARA store](#) to get a project to get your feet wet without much expense and minimal risk. We will work with you so you can succeed.

Administrative

Officers, directors, and additional SARA contacts

The Society of Amateur Radio Astronomers is an all-volunteer organization. The best way to reach people on this page is by email with SARA in the subject line SARA Officers.

President: Dr. Rich Russel, AC0UB, <https://www.radio-astronomy.org/contact/President>

Vice President: Marcus Fisher, <https://www.radio-astronomy.org/contact/Vicepresident>

Secretary: Bruce Randall, NT4RT, <https://www.radio-astronomy.org/contact/Secretary>

Treasurer: Tom Jacobs, <https://www.radio-astronomy.org/contact/Treasurer>

Asst. Treasurer: Donna Hallin, <https://www.radio-astronomy.org/contact/Treasurer>

Past President: Dennis Farr

Founder Emeritus and Director: Jeffrey M. Lichtman, KI4GIY, jeff@radioastronomysupplies.com

Board of Directors

Name	Term expires	Email
Dennis Farr	2026	dennisfarr@verizon.net
Dr. Wolfgang Herrmann	2025	messbetrieb@astropeiler.de
Paul Butler	2025	paul.butler.melbourne@gmail.com
Charles Osborne	2025	k4cso@twc.com
Don Latham	2026	djl@montana.com
Steve Tzikas	2026	Tzikas@alum.rpi.edu
Ted Cline	2025	TedClineGit@gmail.com
Jay Wilson	2026	jwilson@radio-astronomy.org

Other SARA Contacts

All Officers	http://www.radio-astronomy.org/contact-sara	
All Directors and Officers	http://www.radio-astronomy.org/contact/All-Directors-and-Officers	
Eastern Conference Coordinator	http://www.radio-astronomy.org/contact/Annual-Meeting	
All Radio Astronomy Editors	http://www.radio-astronomy.org/contact/Newsletter-Editor	
Radio Astronomy Editor	Dr. Richard A. Russel	drrichrussel@radio-astronomy.org
Contributing Editor	Bogdan Vacaliuc	bvacaliuc@iee.org
Educational Co-Chairs	Ken Redcap, Tom Hagen: http://www.radio-astronomy.org/contact/Educational-Outreach	
Grant Committee	Tom Crowley	grants@radio-astronomy.org
Membership Chair	http://www.radio-astronomy.org/contact/Membership-Chair	
Technical Queries (David Westman)	http://www.radio-astronomy.org/contact/Technical-Queries	
Webmaster	Ciprian (Chip) Sufitchi, N2YO	webmaster@radio-astronomy.org

Resources

Great Projects to Get Started in Radio Astronomy

Radio Observing Program

The Astronomical League (AL) is starting a radio astronomy observing program. If you observe one category, you get a Bronze certificate. Silver pin is two categories with one being personally built. Gold pin level is at least four categories. (Silver and Gold level require AL membership which many clubs have membership. For the bronze level, you need not be a member of AL.)

Categories include.

- 1) SID
- 2) Sun (aka IBT)
- 3) Jupiter (aka Radio Jove)
- 4) Meteor back-scatter
- 5) Galactic radio sources

This program is a collaboration between NRAO and AL. Steve Boerner is the Lead Coordinator and a SARA member.

For more information:

Steve Boerner

2017 Lake Clay Drive

Chesterfield, MO 63017

Email: sboerner@charter.net

Phone: 636-537-2495

<http://www.astroleague.org/programs/radio-astronomy-observing-program>

Radio Jove



The Radio Jove Project monitors the storms of Jupiter, solar activity and the galactic background. The radio telescope can be purchased as a kit, or you can order it assembled. They have a terrific user group you can join. <http://radiojove.gsfc.nasa.gov/>

INSPIRE Program



The INSPIRE program uses build-it-yourself radio telescope kits to measure and record VLF emissions such as tweeks, whistlers, sferics, and chorus along with man-made emissions. This is a very portable unit that can be easily transported to remote sites for observations.

<http://theinspireproject.org/default.asp?contentID=27>

SARA/Stanford SuperSID



Stanford Solar Center and the Society of Amateur Radio Astronomers have teamed up to produce and distribute the SuperSID (Sudden Ionospheric Disturbance) monitor. The monitor utilizes a simple pre-amp to magnify the VLF radio signals which are then fed into a high-definition sound card. This design allows the user to monitor and record multiple frequencies simultaneously. The unit uses a compact 1-meter loop antenna that can be used indoors or outside. This is an ideal project for the radio astronomer that has limited space.

To request a unit, send an e-mail to supersid@radio-astronomy.org

Radio Astronomy Online Resources

SARA YouTube Videos: https://www.youtube.com/@radio-astronomy	Pisgah Astronomical Research Institute: www.pari.edu
AJ4CO Observatory – Radio Astronomy Website: http://www.aj4co.org/	A New Radio Telescope for Mexico - ORION 2021 01 20. Dr. Stan Kurtz https://www.youtube.com/watch?v=Q9aBWr1aBVc
Radio Astronomy calculators https://www.aj4co.org/Calculators/Calculators.html	National Radio Astronomy Observatory http://www.nrao.edu
Introduction to Amateur Radio Astronomy (presentation) http://www.aj4co.org/Publications/Intro%20to%20Amateur%20Radio%20Astronomy,%20Typinski%20(AAC,%202016)%20v2.pdf	NRAO Essential Radio Astronomy Course http://www.cv.nrao.edu/course/astr534/ERA.shtml
RF Associates Richard Flagg, rf@hawaii.rr.com 1721-1 Young Street, Honolulu, HI 96826	Exotic Ions and Molecules in Interstellar Space -- ORION 2020 10 21. Dr. Bob Compton https://www.youtube.com/watch?v=r6cKhp23SUo&t=5s
RFSpace, Inc. http://www.rfspace.com	The Radio JOVE Project & NASA Citizen Science – ORION 2020.6.17. Dr. Chuck Higgins https://www.youtube.com/watch?v=s6eWAXjywp8&t=5s
CALLISTO Receiver & e-CALLISTO http://www.reeve.com/Solar/e-CALLISTO/e-callisto.htm	UK Radio Astronomy Association http://www.ukraa.com/
Deep Space Exploration Society http://DSES.science	CALLISTO software and data archive: www.e-callisto.org
Deep Space Object Astrophotography Part 1 -- ORION 2021 02 17. George Sradnov https://www.youtube.com/watch?v=Pm_Rs17KlyQ	Radio Jove Spectrograph Users Group http://www.radiojove.net/SUG/
European Radio Astronomy Club http://www.era.net	Radio Sky Publishing http://radiosky.com
British Astronomical Association – Radio Astronomy Group http://www.britastro.org/baa/	The Arecibo Radio Telescope; It's History, Collapse, and Future - ORION 2020.12.16. Dr. Stan Kurtz, Dr. David Fields https://www.youtube.com/watch?v=rBZIPOLNX9E
Forum and Discussion Group http://groups.google.com/group/sara-list	Shirleys Bay Radio Astronomy Consortium marcus@propulsionpolymers.com
GNU Radio https://www.gnuradio.org/	SARA Twitter feed https://twitter.com/RadioAstronomy1
SETI League http://www.setileague.org	SARA Web Site http://radio-astronomy.org
NRAO Essential Radio Astronomy Course http://www.cv.nrao.edu/course/astr534/ERA.shtml	Simple Aurora Monitor: Magnetometer http://www.reeve.com/SAMDescription.htm
NASA Radio JOVE Project http://radiojove.gsfc.nasa.gov Archive: http://radiojove.net/archive.html https://groups.io/g/radio-jove	Stanford Solar Center http://solar-center.stanford.edu/SID/
Green Bank Observatory https://greenbankobservatory.org/	https://www.csiro.au/ There's a wealth of info on this site of the Australian National Science Agency. It's much more than just radio astronomy. Looking under "Research" opens a real family tree of interesting pages of things they are involved with.

Found an interesting Grote Reber link: <https://www.utas.edu.au/groterebmuseum> Their gallery is interesting, but sure wish they had some captions to indicate who and what some of it is about. I can guess, knowing some of Grote's stories, but others might need more info. Several pictures show the University of Tasmania 26m dish that

was once one of the NASA worldwide Satellite Tracking and Data Network (STDN) dishes like the ones at the Pisgah Astronomical Research Institute (www.pari.edu). PARI's dishes were the first qualification units for that network.

For Sale, Trade and Wanted

At the SARA online store: radio-astronomy.org/store.

New on-demand store for SARA SWAG! <https://saragifts.org/>

Scope in a Box

radio-astronomy.org/store.

Kit of parts and software to build a working Radio Telescope to detect Hydrogen Line emissions. Available to USA addresses only at this time.

SuperSID Complete Kit

radio-astronomy.org/store.



SARA Publication, Journals and Conference Proceedings (various prices)

radio-astronomy.org/store.

SARA Journal Online Download

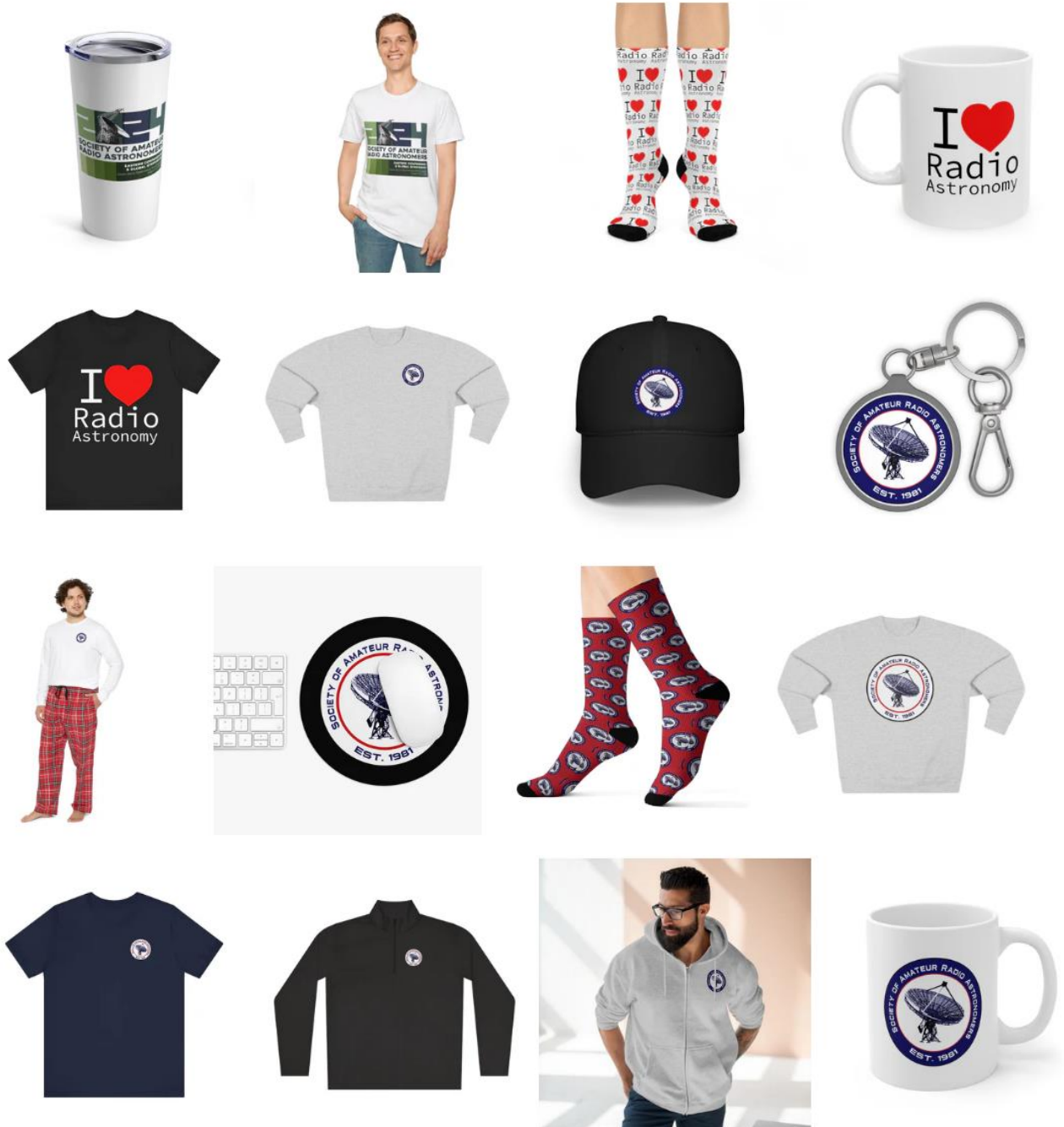
radio-astronomy.org/store.

The Journal archive covers the society journal "Radio Astronomy" from the founding of the organization in 1981 through the present. Articles cover a wide range of topics including cosmic radiation, pulsars, quasars, meteor detection, solar observing, Jupiter, Radio Jove, gamma ray bursts, the Itty Bitty Telescope (IBT), dark matter, black holes, the Jansky antenna, methanol masers, mapping at 408 MHz and more.

New! SARA On-Demand Store: <https://saragifts.org>

These are the current items – more to come in the future!

(Note: No returns or refunds possible because of the on-demand production approach)





SARA Brochure

Membership Information

Annual SARA dues individual \$20, Classroom \$20, Student \$5 (US funds) anywhere in the world. Membership includes a subscription to Radio Astronomy, the bimonthly Journal of The Society of Amateur Radio Astronomers, delivered electronically (via a secure web link, emailed to you as each new issue is posted). We regret that printing and postage costs prevent SARA from providing hardcopy subscriptions to our Journal.

We would appreciate the following information included with your check or money order, made payable to SARA:

Name: _____
 Email Address: _____
(required for electronic Journal delivery)
 Ham call sign: _____ (if applicable)
 Address: _____
 City: _____
 State: _____
 Zip: _____
 Country: _____
 Phone: _____

Please include a note of your interests. Send your application for membership, along with your remittance, to our Treasurer.

For further information, see our website at:

<http://radio-astronomy.org/membership>

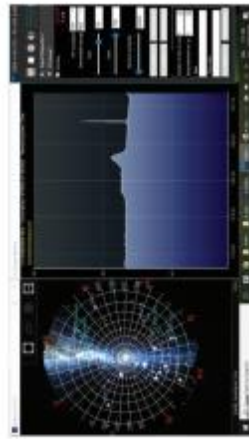


Society of Amateur Radio Astronomers, Inc.
 Founded 1981

Membership supported, nonprofit [501(c) (3)]
 Educational and Radio Astronomy Organization
**Knowledge through Common Research,
 Education and Mentoring**

How to get started?

SARA has a made a kit of software and parts to detect the Hydrogen line signal from space. This is an excellent method to get started in radio astronomy. It teaches the principles of antenna design, signal detection, and signal processing. Read more about this and other projects on our web site.



SARA members have been privileged to use this forty foot diameter drift-scan hydrogen line radio telescope every year at their annual meeting in Green Bank.

Why Radio Astronomy?

Because about sixty five percent of our current knowledge of the universe has stemmed from radio astronomy alone. The discovery of quasars, pulsars, black holes, the 3K background from the "Big Bang" and the discovery of biochemical hydrogen/carbon molecules are all the result of professional radio astronomy.



<http://radio-astronomy.org>

The Society of Amateur Radio Astronomers

SARA was founded in 1981, with the purpose of educating those interested in pursuing amateur radio astronomy.

The society is open to all, wishing to participate with others, worldwide.

SARA members have many interests, some are as follows:

SARA Areas of Study and Research:

- ✔ Solar Radio Astronomy
- ✔ Galactic Radio Astronomy
- ✔ Meteor Detection
- ✔ Jupiter
- ✔ SETI
- ✔ Gamma Ray/High Energy Pulse
- ✔ Detection
- ✔ Antennas
- ✔ Design of Hardware / Software

The members of the society offer a friendly mentor atmosphere. All questions and inquiries are answered in a constructive manner. No question is silly!

SARA offers its members an electronic bi-monthly journal entitled Radio Astronomy. Within the journal, members report on their research and observations. In addition, members receive updates on the professional radio astronomy community and, society news.



The Reber Telescope at NRAO. Constructed by Grote Reber in 1937 in his back yard in Wheaton, Illinois

Once a year SARA meets for a three-day conference at the Green Bank Observatory in Green Bank West Va.

There is also a spring conference held at various cities in the Western USA. Previous meetings have been at the VLA in Socorro, NM and at Stanford University.



How do I get started?

Just as a long journey begins with the first step, the project you elect must start with a clear idea of your objectives. Do you wish to study the sun? Jupiter? Make meteor counts? Do you wish to engage in imaging radio astronomy? What you decide will not only determine the type of equipment you will need, but also the local radio spectrum.

How do amateurs do radio astronomy?

Radio astronomy by amateurs is conducted using antennas of various shapes and sizes, from smaller parabolic dishes to simple wire antennas. These antennas are connected to receivers and most of these receivers are software defined radios these days. Data from the receivers are collected by computers, and the received signals will be displayed as charts, graphs or maybe even sky maps. As diverse as the observed objects, so is are the instruments and tools used. SARA members will always be supportive to find good solutions for what one wishes to observe.

Is amateur radio astronomy instrumentation expensive?

Technical information freely circulated in our monthly journal helps amateurs to obtain good low noise equipment from off the shelf assemblies, or to build their own units. The actual cash investment in radio astronomy equipment need not exceed that of any other hobby.

What are amateurs actually looking for in the received data?

The aim of the radio amateur is to find something new and unusual. Just as an amateur optical observer hopes to notice a supernova or a new comet, so does an amateur radio observer hope to notice a new radio source, or one whose radiation has changed appreciably.



SARA Members discussing the IBT (Itty Bitty Telescope)